AEDC-TDR-63-127

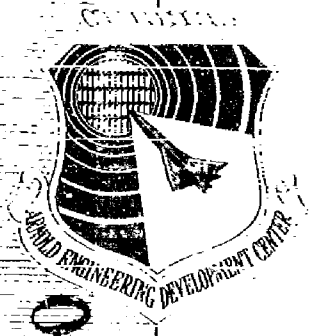

RESEARCH STUDY OF THE CRYOTRAPPING OF HELIUM AND HYDROGEN DURING 20°K CONDENSATION OF GASES PHASES I AND II

By

R.A. Hemstreet, D.J. Webster, D.M. Ruttenbur,
W.J. Wirth, and J.R. Hamilton

Linde Company, Research Laboratories,
a division of Union Carbide Corporation

TECHNICAL DOCUMENTARY REPORT NO. AEDC-TDR-63-127

May 1963

AFSC Program Area 850E, Project 7778, Task 777801

(Prepared under Contract No. AF 40(600)-945 by Linde Company, Research Laboratories, a division of Union Carbide Corporation, Tonawanda, New York.)

ARNOLD ENGINEERING DEVELOPMENT CENTER

AIR FORCE SYSTEMS COMMAND

UNITED STATES AIR FORCE

NOTICES

RESEARCH STUDY OF THE CRYOTRAPPING OF HELIUM AND HYDROGEN DURING 20°K CONDENSATION OF GASES PHASES I AND II

By

R. A. Hemstreet, D. J. Webster, D. M. Ruttenbur, W. J. Wirth, and J. R. Hamilton

Linde Company, Research Laboratories,

a division of Union Carbide Corporation

(The reproducible copy supplied by the authors was used in the reproduction of this report.)

May 1963

AF - AEDC
Arnold AFS Tenn

ABSTRACT

Phase I:

A study of the variables affecting cryotrapping of helium and hydrogen during 20°K condensation of oxygen and nitrogen is presented. The mechanism of helium trapping appears to involve burying helium atoms in the solid oxygen or nitrogen. The process is most efficient at high condensation rates, but is not likely to find application for the removal of helium in a large space chamber.

Experimental results indicate that hydrogen trapping occurs by adsorption of hydrogen molecules on the surface of the solid oxygen or nitrogen and is most efficient at low condensation rates and low heat flux to the solid surface. These conditions indicate that hydrogen trapping may be applicable for hydrogen removal in a large space chamber.

Attempts to improve helium trapping by ionizing the atoms and collecting them on a charged 20°K surface were unsuccessful.

Phase II:

The trapping of hydrogen by nitrogen condensed on a 20°K surface has been studied under conditions where the surface was shielded from ambient temperature radiation. The process is shown to be an inefficient means for hydrogen pumping and is likely to have value only as a bonus in the operation of a large space chamber.

Hydrogen trapping by methane, some simple fluorocarbons, and carbon dioxide condensed on a 20°K surface not shielded from ambient temperature radiation has been studied. CCl_2F_2 and carbon dioxide show rather large capacities for hydrogen and may be useful for the pumping of hydrogen in a space chamber and in special applications.

PUBLICATION REVIEW

This report has been reviewed and publication is approved.

Ross G. Roepke
Chief, Special Projects Branch
Engineering Division
Space Systems Office

Donald D. Carlson
Lt Col, USAF
Chief, Space Systems Office

TABLE OF CONTENTS

PHASE I

ILLUSTRATIONS

Figure

PHASE II

TABLES

ILLUSTRATIONS

Figure

NOMENCLATURE

The following symbols are arranged in the order of their appearance in the text. The number in parenthesis following the symbols refers to the equation where the symbol is first used.

P_R (1)	Gas pressure in the room temperature portions of the apparatus.
P_c (1)	Gas pressure over the solid nitrogen or oxygen surface.
T_R (1)	Room temperature.
T_c (1)	Temperature of the cold portion of the apparatus.
N (2)	Number of gaseous helium atoms in the apparatus.
A (2)	Surface area of the solid nitrogen or oxygen condensates.
f (2)	Fraction of helium atoms in the gaseous nitrogen source.
R (2)	Condensation rate.
t (2)	Time.
γ (2)	Rate constant for helium trapping.
N_S (4)	Number of gaseous helium atoms in the apparatus, under steady state conditions.
V (6)	Volume of the apparatus.
k (6)	Boltzmann constant.
T (6)	Temperature.
M (6)	Atomic mass of the helium atom.
F(R) (7)	Helium trapping probability.
C (12)	γ/A.
P_S (13)	Steady state helium pressure.
d (14)	Density of solid nitrogen.
ℓ (14)	Thickness of solid nitrogen or oxygen deposits.
D (15)	Diffusion constant.
D_o' (15)	Constant in the expression giving the temperature dependence of the diffusion constant.
E (15)	Energy of activation for diffusion.

E_o (16) Energy of activation for diffusion thru a disordered, porous solid.

E_d Energy of activation for diffusion thru a dense, crystalline solid.

ϵ (16) A constant relating E_d and E_o.

$\exp \alpha = e^{\alpha}$.

Λ (16) A constant in the expression for the time dependence of the activation energy for diffusion.

D_o (19) $D_o' \exp\left[-\frac{E_o}{kT}\right]$.

β (19) $\frac{\epsilon\Lambda}{kT}$

L (20) Rate of leakage of helium out of solid nitrogen.

B (23) AfR, Rate of admission of helium into the apparatus.

G (23) $\alpha - \beta R$.

t_{max} (29) Time for occurrence of the maximum in the helium pressure curves.

φ (30) A number between 1 and 2.

N_{max} Maximum number of helium atoms in the apparatus.

H (34) $\gamma + D$.

m (37,38) A constant relating the helium trapping probability and the condensation rate.

$\dot{Q}$ (45) Total heat flux to a solid nitrogen or oxygen surface.

$\mu(T)$ (45) Temperature dependent thermal conductivity.

T_b (46) Substrate temperature.

T_s (46) Condensate surface temperature.

T_o (47) Ordering temperature.

ℓ_o (47) Thickness of solid nitrogen or oxygen at which ordering commences.

K (48) A constant. The integral of $\mu(T)$ between the limits T_b and T_o.

K' (48) $\ell_o \dot{Q}$, AK .

t_o (49) Time required for the condensate surface temperature to reach t_o. Also called the hydrogen pumping time.

$\dot{Q}_c$ (50) Heat flux to the solid nitrogen or oxygen surface due to gas condensation.

$\dot{Q}_r$ (50) Heat flux to the solid nitrogen or oxygen surface to radiation.

b (52) A constant relating $\dot{Q}_c$ to the condensation rate.

σ (54) Stefan-Boltzmann constant.

ϵ_1, ϵ_2 (54) Emissivities of two surfaces.

$F(\epsilon)$ (55) $\dfrac{\epsilon_1 \epsilon_2}{\epsilon_1 + \epsilon_2 - \epsilon_1 \epsilon_2}$.

ΔH^p (56) Change of heat content due to a phase change.

C_p^s (56) Heat capacity of the solid.

C_p (56) Heat capacity of the liquid.

C_p^g (56) Heat capacity of the gas.

T_m (56) Melting (triple point) temperature.

T_v (56) Boiling point.

T_g (56) Gas temperature.

n (57) Avogadro number.

μ (58) A thermal conductivity.

C_v (62) Heat capacity at constant volume.

v (62) Velocity of phonon or lattice waves.

S (62) Phonon mean free path.

Δ (62) A constant relating μ to v, S, and C_v.

RESEARCH STUDY OF THE CRYOTRAPPING OF HELIUM AND HYDROGEN BY OXYGEN AND NITROGEN CONDENSED AT 20°K (PHASE I)

By

R. A. Hemstreet, D. J. Webster,
W. J. Wirth, and J. R. Hamilton

Research Laboratories, Linde Company
a division of Union Carbide Corporation

1.0 INTRODUCTION

The environmental conditions dictated for space simulation chambers require pumping systems capable of removing large volumes of gas under high vacuum conditions. A system of mechanical and diffusion pumps does not meet this requirement when very large chambers are considered, particularly from the standpoint of economics. Present-day getter-ion pumps fare no better. The unique requirement of high vacuum and high load, however, make the possibilities of cryopumping look attractive.(Ref. 1).

Cryopumping customarily means the pumping of gases by freezing them on cold surfaces. The ultimate pressure is limited by the vapor pressure of the solidified gas at the temperature of the surface. As the gas increases in thickness its surface temperature will increase and it is this surface temperature which will determine the ultimate pressure. At 20°K the vapor pressure of solid nitrogen is about 10^{-11} torr (Ref. 2).

Although cryopumping can be an efficient and rapid pumping technique, it is limited by the vapor pressure of the solidified gases. A condensing temperature of 20°K is most commonly chosen because this is adequate for low pressure pumping of nitrogen, oxygen, carbon dioxide, water, etc. However, hydrogen, neon, and helium will not be pumped. The vapor pressures of hydrogen and neon are 1 atm. and 33 torr (Ref. 3) respectively at 20°K. The critical temperature of helium is 5.2°K. With respect to 20°K cryopumping, hydrogen, neon, and helium are referred to as non-condensables.* All the other gases are called condensables because their solid vapor pressures are 10^{-11} torr or less at 20°K.

Even though hydrogen, neon, and helium are non-condensables at 20°K, in actual practice it has been established that there is a secondary pumping phenomenon of these gases associated with condensable cryopumping (Ref. 4). This phenomenon is the physical trapping of non-condensable gases (cryotrapping) in the solid matrix of condensables formed during conventional cryopumping. This trapping has not been studied extensively. It is the objective of this research to study this phenomenon to elucidate its mechanism and to determine whether non-condensable trapping will have an application in a large space chamber.

2.0 APPARATUS

There are two techniques which could be employed to study non-condensable trapping during the cryopumping of condensables:

a) A mixture of condensable and non-condensable could be continuously frozen on a cold surface and the non-condensable pressure monitored as a function of time. Deviations from a linear non-condensable pressure-time curve would be evidence for cryotrapping. This is a dynamic type experiment.

---

* Although neon is solid at 20°K, its vapor pressure is high enough to be considered a non-condensable.

b) The experimental apparatus could be filled to a certain non-condensable pressure and then the freezing of a pure condensable started. A reduction of the non-condensable pressure would be evidence of non-condensable trapping. This is referred to as a static type of experiment.

In all the work reported here the condensable gases were nitrogen, oxygen, and air while the non-condensables were hydrogen, helium, and neon. The dynamic type experiment was chosen for two reasons. First, all available sources of nitrogen, oxygen, and of course air, contain helium so that, even if the static type experiment was desired, in reality a dynamic experiment would result. The importance of small amounts of helium impurities will become evident in the section concerning experimental results. Secondly, the dynamic type experiments more nearly represent the operating conditions likely to be encountered in the practical application of cryotrapping.

2.1 CRYOTRAPPING APPARATUS DESIGN

The cryotrapping apparatus consisted of three sections. The central section was an ultra-high vacuum system where gases were introduced to a refrigerated surface. To this section was fitted an ion gauge and mass spectrometer for pressure measurements and variable leaks for controlling gas flow rates. The second section was a simple gas handling system for admitting gases to the cryopump. The third section was a diffusion pump with trap to evacuate the cryopump to pressures of the order of 10^{-7} torr. These sections will be described separately.

2.1.1 Cryopump. Figure 1 is a schematic diagram of the cryopump with the cryostat omitted. With the exception of the ion gauge and gas inlet tube, it was constructed entirely of 304 stainless steel. Wherever possible the joints were heliarc welded using argon backing. Granville-Phillips 6400 series flanges with copper gaskets were used for demountable couplings. The main cut-off valve, isolating the cryopump from the diffusion pump, was a 1" - 6403 Granville-Phillips valve. The line running from the 6403 valve to the diffusion pump was a 1" O.D. flexible stainless steel tube. Gas flow rates were controlled by Granville-Phillips variable leaks.

Gases were admitted to the refrigerated surface by means of a central copper inlet tube. Copper was used because of its high thermal conductivity. Calculations show that at gas pressures $< 10^{-5}$ torr, this inlet tube remains around 273°K at its lower end when the outer wall of the cryopump is 20°K. Consequently no condensation would occur in the inlet tube. The inlet tube was jointed to the vacuum system by means of a "hermaphrodite" flange. This fitting was male on one side and female on the other and fits between a conventional Granville-Phillips flange combination. Figure 2 shows a detailed drawing of this arrangement. X-ray photographs were used to be sure that the inlet tube was centered.

Three separate heaters were used for bake-out of the cryopump and it is convenient to divide the cryopump into three parts to describe them (see Figure 1). The upper part, containing the valves, flanges, and pressure

measuring devices was heated in an oven. This oven was an insulated box constructed of Marinite having Chromalox heaters attached to the inside walls. The box was hinged so it could be opened. The heaters were capable of baking the upper portion to 500°C. The middle and lower section (in the cryostat) were wrapped with tape heaters rated to 500°C. Chromel-alumel thermocouples were used for temperature measurements along the sections wrapped with the heater tapes.

It was not necessary to remove the cryopump from the cryostat for bake-out. During bake-out the inside of the cryostat was evacuated to reduce the heat flow to the glass walls.

The Consolidated Vacuum Corporation GIC-011 Bayard-Alpert ion gauge and Consolidated Electrodynamics Corporation Residual Gas Analyzer (Mass Spectrometer) were used for pressure measurements.

The cryostat was of conventional design and is shown in Figure 3. It consisted of a vacuum jacketed glass container for holding liquid hydrogen (hydrogen dewar). The hydrogen dewar was immersed in another vacuum jacketed glass container holding liquid nitrogen (nitrogen dewar). Both the hydrogen and nitrogen dewars were mounted in a metal frame to eliminate strains on the glass. The top of the hydrogen dewar was closed with a stainless steel cap. The cryopump tube extended down, thru this cap, into the liquid hydrogen bath. Electrical leads from the lower portion of the cryopump tube were led out thru the side walls of the cap by means of Conax fittings. There were ports for evacuating the hydrogen dewar, liquid hydrogen filling, hydrogen exhaust during filling, and pressure measurements. Figure 4 is a photograph of the cryopump tube with the dewar cap in place, and Figure 5 is a photograph of the entire apparatus.

2.1.2 Gas-Handling System. The gas-handling system was constructed of glass and had a volume of one liter. The volume was calibrated to ± 0.5 c.c. It was used for feeding gas to the cryopump and measuring condensation rates. A schematic diagram is shown in Figure 6. The connections between the gas-handling system and the cryopump were 3/8" I.D. flexible stainless tubing.

2.1.3 Diffusion Pump System. The diffusion pump system is shown schematically in Figure 7. A Consolidated GF-25 pump was used with a liquid nitrogen trap. The pumping system contained a Consolidated Vacuum Corporation GM-110 McLeod gauge (4×10^{-3} to 10^{-7} torr.). The McLeod gauge was used to calibrate the ion gauge and Residual Gas Analyzer. Note that the McLeod gauge could be used independently on either the cryopump or the diffusion pump system. The diffusion pump was only used to evacuate the cryopump during bake-out.

3.0 PROCEDURES

3.1 CRYOPUMP

With few exceptions the cryopump was baked-out prior to each experiment. The bake-out temperatures were 420°C for the upper section in the oven and 350°C for the parts wrapped with the tape heaters. During the bake-out the

cryopump was evacuated with the diffusion pump. The normal bake-out time was 12 hours. After bake-out the apparatus was cooled and the ion gauge outgassed until the GM-110 McLeod gauge indicated a pressure < 10^{-6} torr. After the ion gauge outgassing the cut-off valve was closed and the ion gauge turned to pressure reading operation. The ion gauge pumped the cryopump to about 1×10^{-9} torr and, once this pressure was reached, the ion gauge could be turned off and the cryopump remained at constant pressure.

Following the pump-down with the ion gauge, the cryopump was cooled by introducing liquid hydrogen intc the hydrogen dewar. At this point, an experiment could be started.

Prior to each bake-out the cryopump was purged 10 times or more with high purity nitrogen. This served to flush-out contamination left by the previous experiment.

All the cryotrapping experiments were conducted with the condensing surface cooled to 20°K.

3.2 ION GAUGE CALIBRATION

The Bayard-Alpert ion gauge was calibrated against nitrogen using the GM-110 McLeod gauge. The ion gauge was found to read nitrogen pressures correctly to 5×10^{-7} torr. Pressures below 5×10^{-7} torr were obtained by assuming that the ion gauge output current was linear with the pressure. When gases other than nitrogen were read, the factors quoted by Alpert (Ref. 5) were used.

During an experiment, the ion gauge was operated intermittently because of its pumping action. This was done by switching the filament on only long enough to get a constant pressure reading. The filament switch, which controls the emission current, was marked so that the emission current could be fixed in about one second. Each pressure measurement took about five seconds and was recorded on a Leeds and Northrup milli-volt recorder. The frequency of pressure measurement varied with the experiment, but usually a reading was taken every five minutes.

3.3 RESIDUAL GAS ANALYZER (MASS SPECTROMETER) CALIBRATION

The mass spectrometer was operated continuously during an experiment and its output was recorded. Experience showed that the spectrometer did not interfere with the experimental results. The mass spectrometer was calibrated against the ion gauge at the end of each experiment by deliberately introducing the particular gas of interest and noting the corresponding increase of ion gauge and spectrometer readings. In most of the experiments hydrogen and helium were the only components of interest. As an added check on the calibration procedure, the ratio of the sensitivity factors for hydrogen and helium were determined for each experiment. Although the absolute sensitivity of the mass spectrometer varied from one run to the next, the ratio of sensitivity factors remained constant.

All the pressures quoted in this report were read from the mass spectrometer.

3.4 PRESSURE CORRECTIONS

The ion gauge and mass spectrometer measured pressures in a part of the apparatus which was at room temperature. The pressure above the condensate is given by

$$\frac{P_R}{P_C} = \left[\frac{T_R}{T_C}\right]^{1/2} \tag{1}$$

where the subscripts R and C refer to room temperature and the gas temperature over the condensate. Exact specification of T_C is difficult. The low temperature portion of the apparatus consisted of an outer wall at 20°K and a central gas inlet tube which does not touch the 20°K wall. Calculations showed that the temperature of the lower end of the inlet tube was near 273°K. At the pressures encountered experimentally, gas molecules or atoms had a much larger probability of colliding with the metal walls than with each other. It was assumed that the probability of collision with the relatively warm inlet tube was the same as with the 20°K wall. Therefore, the gas temperature was taken to be an average of these temperatures and a round number of T_C = 145°K was used. All pressure readings were corrected using this value.

4.0 RESULTS

4.1 HELIUM TRAPPING BY SOLID NITROGEN

4.1.1 Experimental. These studies were conducted with a single cylinder of pure nitrogen containing 0.11 p.p.m. helium. The helium concentration was determined from the results of the trapping experiments.

The trapping experiments consisted of freezing the nitrogen-helium mixture in the cryopump and reading the helium pressure as a function of time during the condensation. The nitrogen leak rates were varied between 6.8×10^{16} sec^{-1} and 9.9×10^{20} sec^{-1}. The results are shown in Figure 8. With the exception of the slowest leak rates, the pressure curves went thru a maximum then assumed a form where the pressure remained constant with time. When the pressure became constant the trapping rate equaled the rate of admission of helium to the cryopump. For nitrogen leak rates up to 10^{19} sec^{-1} the initial slope of the helium pressure curve was proportional to the nitrogen leak rate as shown in Figure 9. This behavior indicated that there was little or no helium trapping at the beginning of each condensation. The helium pressure curves at 6.8×10^{16} sec^{-1} and 1.3×10^{17} sec^{-1} are perfectly linear and show no evidence of helium trapping. The values of the maximum pressures showed no obvious dependence on the experimental conditions. However, Figure 10 shows that the time at which the maximum occurs is inversely proportional to the nitrogen condensation rate. The maximum in the helium pressure curves represents the onset of helium trapping and this occurred more

rapidly as the condensation rate was increased. None of the experiments showed any evidence of helium leaking out of the solid nitrogen after the condensation was terminated. In all cases the helium pressure remained constant after the end of the condensation.

4.1.2 Theory of Helium Trapping. We will start with a very simple model of helium trapping. Assume that diffusion of trapped helium atoms out of the solid nitrogen can be ignored. The increase in the number N of helium atoms in the gas space above the solid nitrogen during a condensation can be expressed by

$$\frac{dN}{dt} = AfR - \gamma N. \tag{2}$$

AfR is the rate of introduction of helium atoms into the cryopump. R is the condensation rate (cm^{-2} sec^{-1}), A the condensation surface area, and f the ratio of helium to nitrogen. In the present case $f = 1.1 \times 10^{-7}$. The term γN is the trapping rate which is assumed proportional to the number of helium atoms in the gas phase, i.e. the trapping rate is first order in the helium pressure. Equation 2 assumes nothing about the trapping mechanism other than that it is a first order process. It states that the change in the number of gaseous helium atoms is equal to the rate of their introduction minus the rate of removal by trapping. If $N = 0$ at $t = 0$, the solution of Equation 2 is

$$N = \frac{AfR}{\gamma}\left(1 - e^{-\gamma t}\right) \tag{3}$$

After long periods of time

$$N_S = \frac{AfR}{\gamma} \tag{4}$$

where the subscript S refers to a steady state. The initial slope of Equation 3 ($t = 0$) is

$$\left[\frac{dN}{dt}\right]_{t=0} = AfR. \tag{5}$$

A plot of N (or pressure P) has the following appearance:

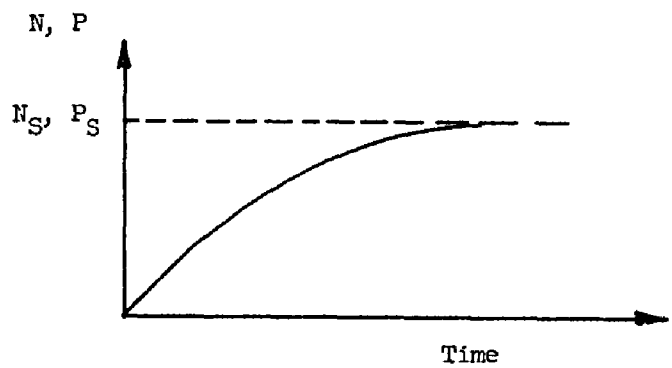

The initial slope of the curve should be equal to the rate of admission of helium to the cryopump. With the exception of the maximum, the simple theory is in rough qualitative agreement with the experimental results.

It is doubtful whether adsorption plays a significant role in helium trapping because the condensation surface (20°K) is well above the helium critical temperature of about 5°K. However, assume that every helium atom impinging on the solid nitrogen surface will remain at a particular site for a short but finite length of time, i.e. the collision time is greater than zero. If the helium atom is not trapped during its collision time, then it will leave the surface returning to the gas phase. Some of the helium atoms may move (or jump) to other surface sites, but the result is no different than if they arrived at the new site directly from the gas phase. A helium atom will not be trapped unless it remains localized long enough for it to be buried by a layer of solid nitrogen, i.e. become incorporated into the solid nitrogen lattice.

The rate at which helium atoms strike the solid nitrogen surface is

$$\frac{A}{V}\left[\frac{kT}{2\pi M}\right]^{1/2} N \text{ (Ref. 6)} \tag{6}$$

where V is the cryopump volume, k the Boltzmann constant, T the absolute temperature of the gas, and M the atomic mass of helium. The trapping rate is

$$F(R)\,\frac{A}{V}\left[\frac{kT}{2\pi M}\right]^{1/2} N \tag{7}$$

where F(R) is the probability that any helium atom striking the solid nitrogen surface will be trapped. F(R) may be a function of the condensation rate. The expression given by (7) replaces γN in Equation (4). The solution is

$$N = \frac{fR}{C}\left(1-e^{-\gamma t}\right), \tag{8}$$

$$N_S = \frac{fR}{C}, \tag{9}$$

$$\left[\frac{dN}{dt}\right]_{t=0} = AfR, \tag{10}$$

where

$$\gamma = F(R)\frac{A}{V}\left[\frac{kT}{2\pi M}\right]^{1/2} \tag{11}$$

and

$$C = \frac{F(R)}{V}\left[\frac{kT}{2\pi M}\right]^{1/2} \tag{12}$$

In pressure terms Equation (9) becomes

$$P_S = 5.73 \times 10^{-22}\,\frac{fRT^{1/2}}{F(R)} \text{ torr.} \tag{13}$$

The constant steady state pressure is not dependent on the apparatus geometry or condensing surface area. However, the rate at which the steady state pressure is achieved is dependent on the ratio of the condensing surface area to the apparatus volume.

The existence of a maximum in the helium pressure curves is not contained in the simple helium trapping model. At first it might be presumed that the time up to the maximum represents the formation of the first layer of solid nitrogen on the 20°K substrate, and there is no trapping during this time. Karamcheti (Ref. 7) gives the density of solid nitrogen formed by direct condensation of the gas at 20°K as

$$d = 1 \text{ gm/cm}^3 = 2.14 \times 10^{22} \text{ molecules/cm}^3.$$

The thickness of the condensate at any time is

$$\ell = \frac{Rt}{d} \tag{14}$$

From curve D of Figure 8 the maximum occurs at about 8 minutes and the corresponding thickness is 1 mm. This is much greater than many monolayers of solid and a different explanation of the maximum must be sought.

The simple trapping model assumes that trapped helium atoms do not escape from the solid nitrogen. This is based on the observation that the helium pressure remains constant after the termination of a condensation. However, this assumption is not necessarily true at all times during a condensation. The linear pressure increase at the beginning of a condensation indicates that very little of the helium is being trapped and that trapping commences only after some change takes place in the solid nitrogen.

Normally the diffusion constant of a substance depends only on the activation energy E and the temperature T (Ref. 8), i.e.

$$D = D_0' e^{-E/kT}. \tag{15}$$

However, the activation energy may depend on the density of the solid nitrogen. If a low density, porous solid is formed, it would be expected that the helium diffusion constant would be larger than in the case of a well ordered, closely packed structure. The activation energy for diffusion would be smaller in the more open structure. At a given temperature the activation energy may vary between E_o (porous solid) and E_d (dense solid); $E_d > E_o$. Furthermore, due to the low thermal conductivity of the solid nitrogen, the surface temperature will be somewhat higher than the metal surface where it is first formed and the surface temperature will increase with the solid thickness. In addition, it might be expected that the solid would become more dense as its surface temperature increases, because each impinging nitrogen molecule finds it easier to migrate on the surface to a minimum energy lattice position. Consequently, it is postulated that the activation energy for helium diffusion depends on the solid nitrogen thickness. However, the activation energy cannot increase without limit because the upper limit will be for diffusion in a perfectly crystalline solid. Beyond this, any further changes in the diffusion constant will be determined by the temperature alone.

A precise description of helium trapping would require detailed knowledge of thermal conductivities, temperature gradients, diffusion constants, solid nitrogen structures and densities, etc. Such data are not available. Therefore, assumptions will be used which permit the problem to be treated in its simplest and most easily handled form. The best that can be hoped for is a qualitative treatment which will give a demonstration of the plausibility of the concepts concerning helium trapping.

Assume a function for the diffusion activation energy which causes it to vary between E_o and E_d as the solid thickness increases. Let $E_d = E_o + \epsilon$ where ϵ is a constant. A convenient form is

$$E = E_o + \epsilon(1-e^{-\Lambda Rt}) \tag{16}$$

where Λ is a constant. The diffusion constant (Equation 15) becomes

$$D = D_o' \exp\left\{-\left[\frac{E_o + \epsilon(1-e^{-\Lambda Rt})}{kT}\right]\right\} \tag{17}$$

Equation 15 can be simplified if ΛR is assumed to be small and discussion is restricted to small values of t. What constitutes a small t depnds on the magnitude of ΛR. Since $\exp(-\alpha) \approx 1-\alpha$ for small values of α,

$$D = D_o' \exp\left[\frac{-E}{kT}\right] \exp\left[\frac{-\epsilon\Lambda Rt}{kT}\right] \tag{18}$$

This is simplified further to read

$$D = D_o e^{-\beta Rt} \tag{19}$$

where

$$\beta = \frac{\epsilon\Lambda}{kT} \text{ and } D_o = D_o' \exp\left[\frac{-E_o}{kT}\right]$$

Equation 19 ignores the time dependence of the temperature and implies that the dominant factor is the dependence of the diffusion activation energy on the solid nitrogen thickness. The differential equation for helium trapping is

$$\frac{dN}{dt} = AfR-\gamma N+L \tag{20}$$

where L is the rate of leakage of helium out of the solid nitrogen. L is proportional to the number of helium atoms in the solid and has the form

$$L = (AfRt-N)D.$$

Substituting Equations 21 and 19 into 20:

$$\frac{dN}{dt} + (\gamma + D_o e^{-\beta Rt}) N = AfR(1 + D_o t e^{-\beta Rt}). \tag{22}$$

For purposes of simplicity let $D_0 << \gamma$ and $B = AfR$;

$$\frac{dN}{dt} + \gamma N = B(1 + D_0 t\, e^{-\beta R t}) \tag{23}$$

If $N = 0$ at $t = 0$ and $G = \gamma - \beta R$;

$$N = \frac{B}{\gamma} + D_0 B \left\{ \frac{t}{G} - \frac{1}{G^2} \right\} e^{-\beta R t} + \left\{ \frac{D_0 B}{G^2} - \frac{B}{\gamma} \right\} e^{-\gamma t}. \tag{24}$$

The term βR cannot be a very large number, or Equation 17 would reduce to

$$D = D_0' \exp\left[-\frac{(E_0 + \epsilon)}{kT} \right]$$

in a few seconds and the densely packed state would be achieved very soon after the condensation is started. Assume $\gamma >> \beta R$ and let $G = \gamma$.

$$N = \frac{B}{\gamma} + D_0 B \left\{ \frac{t}{\gamma} - \frac{1}{\gamma^2} \right\} e^{-\beta R t} + \left\{ \frac{D_0 B}{\gamma^2} - \frac{B}{\gamma} \right\} e^{-\gamma t}. \tag{25}$$

If $t >> \frac{1}{\gamma}$ and $B >> \frac{D_0 B}{\gamma}$, then Equation 25 can be simplified to

$$N = \frac{B}{\gamma} + \frac{D_0 B t e^{-\beta R t}}{\gamma} - \frac{B}{\gamma} e^{-\gamma t} \tag{26}$$

The first and second derivatives of Equation 26 are

$$\frac{dN}{dt} = \frac{D_0 B e^{-\beta R t} (1 - \beta R t)}{\gamma} + B e^{-\gamma t} \tag{27}$$

and

$$\frac{d^2 N}{dt^2} = \frac{D_0 B \beta R (\beta R t - 2)\, e^{-\beta R t}}{\gamma} \tag{28}$$

The second derivative is negative and the pressure curve has a maximum as long as $\beta R t < 2$. The time, t_{max}, at which the pressure maximum occurs is obtained by setting Equation 27 equal to zero. However, it is readily seen that a real solution for t_{max} can only exist if $\beta R t_{max} > 1$. Thus, there are two conditions on $\beta R t_{max}$, i.e.

$$1 < \beta R t_{max} < 2. \tag{29}$$

Because the range of values of $\beta R t_{max}$ is very limited, $\beta R t_{max}$ is assumed approximately equal to a constant φ. Then

$$R t_{max} = \frac{\varphi}{\beta} \tag{30}$$

A plot of log R vs. log t_{max} should be linear with a slope of -1. Figure 10 shows this is the case. The maximum in the helium pressure curves represents the point where the solid nitrogen density increases so that the trapped helium atoms are held by the solid and do not rapidly diffuse back out.

The discussion does not account for the apparently random variation in the values of the maximum pressures. From Equation 26 and 30 the maximum value of N is

$$N_{max} = \frac{fR}{C}\left(1 - e^{\frac{-\gamma\varphi}{\beta R}}\right) + \frac{D_o\varphi f}{\beta C}\, e^{-\varphi} \tag{31}$$

where $C = \frac{\gamma}{A}$. The exponential term in R and γ may make N_{max} more sensitive to experimental errors in R and A than the t_{max} relation (Equation 30). Also, the fact that φ may not absolutely be a constant could cause further variations in N_{max}. The log-log plot (Figure 10) used to display the t_{max} relation will smooth out much of the scatter.

The initial slope of the helium pressure curve is approximated from Equation 23. When t is very small this becomes

$$\frac{dN}{dt} = B - \gamma N$$

which is the same as Equation 2. The initial slope is equal to the helium leak rate.

When t is large, Equation 17 becomes

$$D = D_o' \exp\left\{-\left[\frac{E + \epsilon}{kT}\right]\right\} \tag{32}$$

which is independent of the time. Combining Equations 20 and 21

$$\frac{dN}{dt} = AfR - \gamma N + (AfRt - N)D \tag{33}$$

If N = 0 at t = 0, the solution is

$$N = \frac{B}{H} + \frac{BDt}{H} - \frac{BD}{H^2} - \left[\frac{B}{H} - \frac{BD}{H^2}\right] e^{-Ht} \tag{34}$$

where $H = \gamma + D$. If $D \ll \gamma$ (experimentally no helium leaks out of the solid nitrogen after the termination of the condensations),

$$N_s = \frac{B}{\gamma}\left(1 - \frac{D}{\gamma}\right) + \frac{BDt}{\gamma}. \tag{35}$$

N_s is the steady state value of N, but note that a time dependence is indicated. If $D/\gamma \ll 1$,

$$N_s = \frac{B}{\gamma} + \frac{BDt}{\gamma} \tag{36}$$

For the experimental conditions $B = AfR \approx 10^9$ and $\gamma \approx 70$ if $F(R) = 1$. Except at very long periods of time, far longer than the duration of the experiments,

$$N_S \approx \frac{B}{\gamma} ,$$

which is the same result obtained from the simple model (see Equations 11 and 15).

From the data of runs F and A of Figure 8 and Equation 13, the following helium trapping probabilities are obtained.

Helium Trapping Probabilities with Solid Nitrogen

Run Number	Condensation Rate	Trapping Probability, F(R)
F	1.53×10^{18} cm^{-2} sec^{-1}	3.3×10^{-5}
A	5.63×10^{20} cm^{-2} sec^{-1}	4.2×10^{-2}

The data indicates that the trapping probability increases with the condensation rate, but the data are not sufficient to determine the type of dependence. However, at the most rapid condensation rate a helium atom strikes the solid nitrogen surface about 400 times before it is trapped. This condensation rate is equivalent to 3.3 pounds of nitrogen per square foot per minute.

According to Equation (13), the steady state pressure should increase with the condensation rate if F(R) is constant. Such a behavior is not observed in Figure 8. Although a regular pattern of behavior was not obtained, the results suggest that P_S decreases with increasing R, but in no case was a final pressure obtained less than 10^{-6} torr. The inverse relation would be expected if F(R) increases faster than R. However, a minimum value of P_S is also expected because F(R), being a probability, cannot be larger than unity while the condensation rate can increase without limit. This can be shown by assuming two forms for F(R). They are

$$F(R) = 1-e^{-mR} \quad \text{or} \tag{37}$$

$$F(R) = e^{-m/R} . \tag{38}$$

These functions are chosen so that F(R) varies between 0 and 1 as R goes from 0 to infinity. m is a constant. Substituting 37 and 38 into 9,

$$N_S = \frac{fR}{C\,(1-e^{mR})} \tag{39}$$

and

$$N_S = \frac{fR}{C}\, e^{m/R}; \quad C = \frac{1}{V} \left[\frac{kT}{2\pi M}\right]^{1/2} \tag{40}$$

The first and second derivatives of 39 and 40 are

$$\frac{dN_S}{dR} = \frac{f}{C}\left[\frac{1}{1-e^{-mR}} - \frac{mRe^{-mR}}{(1-e^{-mR})^2}\right] \tag{41}$$

$$\frac{dN_S}{dR} = \frac{f}{C} e^{m/R}\left(1 - \frac{m}{R}\right), \tag{42}$$

$$\frac{d^2N_S}{dR^2} = \frac{fme^{-mR}}{C(1-e^{-mR})^2}\left[\frac{2mRe^{-mR}}{1-e^{-mR}} + mR - 2\right], \tag{43}$$

$$\frac{d^2N_S}{dR^2} = \frac{fm^2e^{m/R}}{C\,R^3}. \tag{44}$$

Both second derivatives are positive as long as $mR > 2$ so a minimum value of N_S or P_S is expected. If 38 is correct, the minimum occurs at $R = m$. Thus, at a constant rate of helium in-leakage, it is likely that there will be a certain minimum helium pressure regardless of the nitrogen condensation rate.

The results of the hydrogen trapping study will show that oxygen behaves like nitrogen with respect to helium trapping.

4.2 HYDROGEN TRAPPING BY SOLID NITROGEN AND OXYGEN

4.2.1 Experimental. The procedure used was the same as employed in the helium trapping studies. Cylinders of nitrogen and oxygen were prepared containing known amounts of hydrogen ranging from 10 p.p.m. to 1,000 p.p.m. All the samples of nitrogen and oxygen contained small amounts of helium impurities (0.1 to 0.4 p.p.m.). The helium always appeared during the condensations and served as a very useful indication of the nitrogen or oxygen flow rate. Also, the presence of helium permitted a direct comparison of the trapping behaviors of hydrogen and helium.

Figures 11, 12, and 13 show the hydrogen and helium pressures during condensations of nitrogen containing 10 p.p.m. hydrogen. In each case the helium appeared at the start of the condensation and, as the condensation proceeded, the pressure approached a constant, steady state value in a manner very similar to the results of the previous section. When the nitrogen condensation rate was low (Figure 13), the helium pressure curve was perfectly linear indicating no trapping.

The behavior of hydrogen was entirely different from helium. Following the beginning of a condensation there was a period where the hydrogen pressure remained constant or undetectable. When the hydrogen pressure did begin to rise, it did so rather abruptly. This is clearly shown with the log scale for the hydrogen pressure. It appears as though the slope of the hydrogen pressure curve approached the theoretical leak rate, i.e. the leak rate calculated on the assumption that the hydrogen was simply leaking into the cryopump in the absence of any pumping. This approach to the theoretical leak rate could not be conclusively demonstrated because the pressures could be run no higher for fear of damaging the spectrometer.

The hydrogen and helium pressure curves had exactly the opposite behavior. In the beginning no helium was pumped while all the hydrogen was removed. After a period of time, the helium was pumped as fast as it is admitted while the hydrogen appeared to approach a condition where there was no pumping. In Figure 13 there was no evidence of helium pumping and no trace of hydrogen was found. Furthermore, the commencement of helium pumping and cessation of hydrogen pumping were very nearly simultaneous. With decreasing condensation rate, the induction time for the onset of helium pumping increased, while the hydrogen pumping time correspondingly increased. At the end of the experiments, the final hydrogen pressure expected in the absence of pumping is indicated. It is obvious that most of the hydrogen introduced into the apparatus was pumped and that the mechanism controlling helium pumping works in the opposite way with respect to hydrogen pumping.

Helium and hydrogen pumping by solid oxygen was very similar to nitrogen as shown in Figures 14 and 15. Figure 14 clearly shows the correspondence between the times for the beginning and end of helium and hydrogen pumping respectively. Figure 15 shows that it was not absolutely necessary that helium pumping commence before hydrogen pumping breaks down. Figure 16 compares the hydrogen pressure curves from a series of oxygen condensations. The dotted line shows the times at which the same amount of hydrogen had been introduced into the apparatus. The amount of hydrogen pumped increased with decreasing oxygen condensation rate. In Figure 17 a plot of the log of the hydrogen pumping time (time for first detectable increase of the hydrogen pressure) against the log of the oxygen leak rate shows a linear relation with a slope of -1. This is the same type of relation found for the time of occurrence of the maximum in the helium pressure curves (see Figure 10).

Figure 18 shows the effect of increasing the hydrogen concentration in the nitrogen. The condensation rates were comparable but the pumping time was shortened as the initial hydrogen concentration increased. When the nitrogen contained a significant amount of an impurity (krypton), the pumping time was shortened as shown in Figure 19 even though the condensation rates and hydrogen concentrations were nearly equal for both runs. In addition to shortening the pumping time, the presence of the krypton impurity slightly increased the slope of the hydrogen pressure curve.

In all the experiments the hydrogen pressure remained constant after the condensations were stopped. No hydrogen leaked out of the solids.

The experimental results show that hydrogen was being pumped in a manner related to, but entirely different from, helium pumping. The first question needing an answer is whether the hydrogen pumping was due to adsorption on the metal walls of the apparatus. The close correspondence between the beginning of helium and end of hydrogen pumping suggests that wall adsorption was not a significant factor and that the pumping was related to the behavior or properties of the solid oxygen or nitrogen. This is particularly evident when the effect of the krypton impurity is considered (Figure 19). The behavior shown with solid oxygen in Figure 16 is not consistent with wall adsorption of hydrogen being the dominant pumping process. Otherwise the final hydrogen pressure in each experiment should have been the same since the curves as shown represent the same amount of hydrogen introduced into the apparatus. The initial conditions with respect to bake-out and apparatus preparation were the same. Figure 20 shows an experiment where nitrogen containing 10 p.p.m. hydrogen was condensed in the pump with the initial hydrogen pressure $\sim 3.5 \times 10^{-8}$ torr, well above the limit of detectability and well up on the hydrogen pressure curve as in Figure 11. In this case most of the hydrogen in the apparatus before the experiment was pumped and all of the hydrogen admitted during the condensation also was pumped. If wall adsorption were important, the pressure should have risen immediately.

Figure 21 compares hydrogen pressure curves during nitrogen and oxygen cryotrapping with the pressure curves for admission of pure hydrogen to a 20°K charcoal adsorbent (Ref. 9). The trapping curves are characterized by a period of constant pressure followed by a rather abrupt increase. Over the charcoal the pressure rises smoothly from the origin as the surface is loaded. If the constant pressure pumping period was due to wall adsorption, then it should have been observed with the charcoal since the surface area of the charcoal greatly exceeded that of the walls of the apparatus. Finally, consider Figure 22. Here is compared the hydrogen pressures during an oxygen trapping experiment with an experiment where pure hydrogen was admitted into the empty pump. In the latter case the hydrogen leak rate was 30 times faster than the trapping run, but the hydrogen appeared much sooner. The slight curvature of the pure hydrogen run suggests some wall adsorption. We cannot tell whether the curve extends back smoothly to the origin, but the dotted line is taken as an extrapolation which assumes a behavior similar to that observed during cryotrapping. From this extrapolation an upper limit of 1×10^{14} hydrogen molecules adsorbed on the walls ($< 2.5 \times 10^{11}$ cm^{-2}) is calculated before a sharp pressure rise occurs. This point is indicated by a small arrow on the cryotrapping data of Figure 22. It is apparent that wall adsorption did not significantly affect the present cryotrapping results, but could be significant at extremely low hydrogen leak rates.

4.2.2 Theory of Hydrogen Trapping. At first, the inverse relation between hydrogen and helium pumping would seem to contradict the model of helium cryotrapping. However, the model developed for helium did not consider adsorption of the non-condensable on the surface of solid oxygen or nitrogen. At 20°K helium adsorption is not significant and helium trapping will occur only if the helium atoms are literally buried during their collision time with the surface. Although it probably is correct to

ignore helium adsorption, it is not true that hydrogen adsorption can be ignored. The trapping process is being carried out at the normal condensation temperature of hydrogen. Consequently, it is postulated that hydrogen adsorption is more important than brute force burying as in the case of helium.

If adsorption is the dominant process in hydrogen trapping, then the amount of hydrogen that can be trapped will be proportional to the effective surface area of the solid oxygen or nitrogen and the heat of adsorption. Diffusion of trapped hydrogen out of the solid is regarded as unimportant because it was not observed experimentally. Once adsorption is accepted as accounting for hydrogen trapping, the inverse relation between hydrogen and helium pumping becomes obvious. Early in a condensation, the porous, disordered form of solid oxygen or nitrogen will not hold helium, but, by virtue of having a relatively high effective surface area, will adsorb considerable amounts of hydrogen. As the condensation proceeds, a point is reached where the solid begins to pack densely and helium trapping commences. However, the formation of a densely packed solid reduces the surface available for hydrogen adsorption and hydrogen pumping breaks down. Since the beginning of dense packing is associated with an increased surface temperature, the increased temperature will reduce the adsorptive capacity of the surface for hydrogen and contribute to the breakdown of hydrogen pumping.

Although not clearly shown by the figures in this report, experience showed that the hydrogen pumping time of oxygen was somewhat shorter than with nitrogen under conditions of equivalent condensation rates. The reason for this probably is due to oxygen molecules having a greater surface mobility than nitrogen. Oxygen has a lower freezing point (triple point = 54°K) than nitrogen (triple point 6 64°K) and, in addition, solid oxygen has a solid phase change at 21-23°K, (Ref. 10), while nitrogen has a solid phase change at 35°K (Ref. 10). On this basis we would expect it to be easier for oxygen to form a densely packed solid than nitrogen under conditions of the same surface temperature. At equal condensation rates, this would happen faster with oxygen. The thermal conductivities of the solid are important, but unfortunately no values for solid oxygen in the 20°K region are available.

Previously it was noted that at low condensation rates, hydrogen pumping can breakdown when there is no evidence of the beginning of helium pumping (Figure 15). There are two criteria for helium pumping: the solid must be densely packed and the condensation rate must be large enough to give a reasonable probability of burying the helium atoms during their collision time with the solid oxygen or nitrogen. No matter how slow the condensation rate, eventually the surface temperature must increase to the point where dense packing occurs. Thus, hydrogen pumping will eventually breakdown even though the condensation rate is too low for helium atoms to be trapped, i.e. to be buried during their collision time.

The temperature gradient dT across an infinitesimal slice $d\ell$ of the solid oxygen or nitrogen normal to the direction of the gas flow is

$$dT = \frac{\dot{Q}}{A\mu(T)} \, d\ell , \qquad (45)$$

where $\mu(T)$ is the temperature-dependent thermal conductivity, A the condensate surface area, and $\dot{Q}$ the heat flux to the condensate surface (Cal/sec). If $\dot{Q}$ is independent of the surface temperature,

$$\mathcal{L} = \frac{A}{\dot{Q}} \int_{T_b}^{T_s} \mu(T)dT. \tag{46}$$

T_s and T_b are the condensate surface temperature and the temperature of the substrate respectively. Ordering or dense packing will occur over a temperature range. Nevertheless, a temperature T_o (called the ordering temperature) will be used which will correspond roughly to the temperature where dense packing becomes rapid enough to permit helium trapping and reduce hydrogen trapping. Equation 46 becomes

$$\mathcal{L}_o = \frac{A}{\dot{Q}} \int_{T_b}^{T_o} \mu(T)dT. \tag{47}$$

For a particular condensate, the integral is a constant, K. Then

$$\mathcal{L}_o\dot{Q} = K, \; K = AK. \tag{48}$$

The condensate thickness is Rt/d (Equation 14) and if the time required to reach the ordering temperature T_o is t_o,

$$Rt_o\dot{Q} = Kd. \tag{49}$$

The heat flux consists of two terms:

$$\dot{Q} = \dot{Q}_c + \dot{Q}_r \, , \tag{50}$$

where $\dot{Q}_c$ is the heat flux due to gas condensation and Q_r is the heat flux due to radiation. The heat flux due to gas condensation is proportional to the condensation rate, $\dot{Q}_c = bR$, and

$$Rt_o(bR + \dot{Q}_r) = Kd. \tag{51}$$

If the gas condensation is the most important contributor to the total heat flux, $Q_c \gg Q_r$,

$$R^2t_o = \frac{Kd}{b} \, , \tag{52}$$

and a log-log plot of R vs. t_o should be linear with a slope of - 1/2. If the principal contributor to the total heat flux is radiation, then

$$Rt_o = \frac{Kd}{\dot{Q}_r} \, , \tag{53}$$

and a log-log plot of R vs. t_o should also be linear, but with a slope of -1 (Q_r should not be dependent on the condensation rate). Figure 17 shows for oxygen that Equation 53 is obeyed when the time for the first increase of the hydrogen pressure is taken as t_o, also called the pumping time. This immediately suggests that radiation is the dominant factor controlling the surface temperatures of the solid oxygen and nitrogen in the experiments reported here.

In the theory of helium trapping and expression similar to Equation 55 was derived (see Equation 30). In the case of helium the time is that required for the helium pressure curve to reach its maximum which indicates that the condensate had packed densely enough to hold most of the trapped helium. Although the condensate packing density is assumed related to the thickness, no expression for the surface temperature was used and there was no indication of which factors were most important in controlling the surface temperature. The treatment in this section gives direct statements concerning the factors controlling surface temperatures, but, not being a rate analysis, does not predict the shape of the pressure curves. The two approaches compliment each other nicely.

The radiant heat flux between two surfaces of area A is (Ref. 11)

$$\dot{Q}_r = \sigma A(T_1^4 - T_2^4) \frac{\epsilon_1 \epsilon_2}{\epsilon_1 + \epsilon_2 - \epsilon_1 \epsilon_2} \tag{54}$$

σ has the value 5.67×10^{-12} watt/cm^2 deg^4 and ϵ_1 and ϵ_2 are the emissivities of the surfaces at temperatures T_1 and T_2 respectively. For convenience let

$$\dot{Q}_r = \sigma A(T_1^4 - T_2^4) F(\epsilon) \tag{55}$$

where $F(\epsilon)$ is simply that part of Equation 54 involving the emissivities. The geometry of the experimental apparatus is complicated, but assume that the solid condensable surface "looks" directly up the gas inlet tube at a 300°K surface and that the condensable surface temperature is 20°K. $\dot{Q}_r$ is plotted as a function of $F(\epsilon)$ in Figure 23. Other curves are included for T_1 = 77, 90, 100, 150, and 400°K.

The heat dissipated by gas condensation is

$$Q_c = \Sigma \Delta H^p + \int_{T_1}^{T_m} C_p^s dT + \int_{T_m}^{T_v} C_p dT + \int_{T_v}^{T_g} C_p^g dT. \tag{56}$$

$\dot{Q}_c$ has the units cal/mole. The first term is the sum of the heats of all the phase changes between 20°K (T), and the gas temperature T_g. The last three terms are the integrated heat capacities for the solid, liquid, and gas. T_m and T_v are the melting and vaporization temperatures. If there is a solid-solid phase change, the first integration must be done separately for the

heat capacities of the solid forms above and below the temperature of the phase change.* Oxygen has solid-solid phase changes at 23°K, and 43°K while nitrogen has one at 35°K. The heat capacity of the gas is taken as 7/2 R which includes only the translational and rotational contributions. The heat flux due to condensation is

$$\dot{Q}_c = \frac{Q_c R}{n}, \tag{57}$$

n = Avogadro number. On Figure 23 $\dot{Q}_c$ is plotted as a function of condensation rate for oxygen and nitrogen assuming gas temperatures of 100°K, and 273°K.

A direct comparison of the radiant and condensation heat load in the experimental apparatus is difficult due to uncertainty about the value of $F(\epsilon)$. However, if it is assumed that the emissivities of the 300°K surface and the 20°K condensate are each 1.0, then the radiant heat load is 1.05×10^{-2} cal/cm^2 sec. This is equal to the condensation heat load for nitrogen at 2×10^{18} cm^{-2} sec^{-1} and oxygen at 1.7×10^{18} cm^{-2} sec^{-1}. If the emissivities of each surface are as low as 10^{-2} (which is unlikely) then the radiant heat load is 1.05×10^{-4} cal/cm^2 sec. which corresponds to the condensation heat load from nitrogen at less than 10^{16} cm^{-2} sec^{-1}. It would be expected that radiation is the principal factor affecting the condensate surface temperature at all condensation rates less than 10^{17} cm^{-2} sec^{-1} and, because the emissivities are probably much larger than 10^{-2}, for all but the most rapid condensation rates used in the experiments reported here.

If the thermal conductivity is independent of temperature, Equation 47 becomes

$$T_o = \frac{\ell \dot{q}}{\mu} + T_b \tag{58}$$

where $\dot{Q}$ has the units cal/cm^2 sec. Substituting $\ell = \frac{Rt_o}{d}$ (Equation 14),

$$T_o = \frac{Rt_o}{d} \cdot \frac{\dot{Q}}{\mu} + T_b \tag{59}$$

Karamcheti (Ref. 7) gives $\mu = 2.455 \times 10^{-4}$ cal/sec. cm°K and d = 1 gm/cm^3 (2.14×10^{22} molecules/cm^3) for solid nitrogen. If a radiant heat flux of $\dot{Q}_r = 10^{-2}$ cal/cm^2 sec. [corresponding to $F(\epsilon) \approx 1.0$] is assumed, T_b = 20°K, and a nitrogen condensation rate of 7×10^{17} cm^{-2} sec^{-1} is assumed (Figure 12),

$$T_o = 1.33 \times 10^{-3} t + T_b. \tag{60}$$

---

* See Scott (Ref. 10) for heat capacity data.

T_o is unknown, but it is arbitrarily assumed that $T_o = 23°K$.* This surface temperature will occur 35.9 minutes after the condensation is started at a solid nitrogen thickness of 0.070 cm. Experimentally the pumping time is about 40 minutes corresponding to a thickness of 0.078 cm. The times are very close but the agreement may be fortuitous to some extent because of the uncertainty in the values of T_o, μ, d, and $\dot{Q}r$. If the heat from gas condensation is the dominant factor, the time required to reach 23°K is 99.3 minutes ($\dot{Q}c = 3.8 \times 10^{-2}$ cal/cm^2 sec.) which is considerably longer than the experimental value and there is justification for ruling out the heat load due to gas condensation as an important factor in determining the condensate surface temperature.

From Equation 59, the time required for breakdown of hydrogen pumping is

$$t_o = \frac{\mu d}{R\dot{Q}} (T_o - T_b). \tag{61}$$

The thermal conductivity of a solid may be written as (Ref. 12)

$$\mu = \Delta C_V v S \tag{62}$$

where Δ is a constant, C_V the heat capacity at constant volume, v the velocity of phonon or lattice waves, and S the phonon mean free path. Combining Equations 61 and 62

$$t_o = \frac{\Delta C_V v d S}{R\dot{Q}} (T_o - T_b). \tag{63}$$

Generally, lattice imperfections and impurities cause phonon scattering (reduce S, the phonon mean free path) and consequently reduce the thermal conductivity of the solid. Since the hydrogen pumping time varies directly with the thermal conductivity (and S), it is expected that impurities will reduce the pumping time. This is clearly demonstrated in Figure 19 where the presence of krypton impurity greatly shortens the pumping time. Since adsorbed hydrogen molecules also constitute an impurity in the condensate, it might be expected that the pumping time would be decreased as the amount of hydrogen in the gaseous oxygen or nitrogen is increased. This is shown on Figure 18.

4.3 CRYOTRAPPING WITH MIXED CONDENSABLES AND NON-CONDENSABLES

These are 12 p.p.m. neon, 5.4 p.p.m. helium, and 0.5 p.p.m. hydrogen in air. Several experiments were performed in which ordinary dry air was cryopumped and the hydrogen, helium, and neon pressures monitored. Figure 24 shows the result of a typical run using a rather low condensation rate. Due

---

* Although the calculation concerns solid nitrogen, it should be noted that in the case of oxygen the choice of $T_o = 23°K$ is reasonable. This temperature corresponds to a solid-solid phase change in oxygen and, if the oxygen molecules have sufficient mobility at this temperature to move to new lattice sites, then at temperatures above this they should be mobile enough to form a dense packed or crystalline structure.

to instrumental problems the helium curve did not appear as a straight line, but there is no evidence of helium trapping. This is expected from the previous results on helium trapping by pure oxygen and nitrogen. There was no evidence of hydrogen, and the neon only appeared at the end of the experiment. The dotted lines are the theoretical neon and hydrogen pressure curves (no trapping).

The air pumping experiments were used to calculate the helium concentration in air. The results averaged to 2 p.p.m., somewhat lower than the accepted value of 5.4. This suggests that the pressures given in this report may be low by a factor of 2.7. However, no attempt was made to apply this correction to all the data because it is not certain whether it is due to error in the assumed gauge sensitivities or due to non-linear behavior of the gauges. In addition, the helium concentration measurements were made during a condensation when one part of the apparatus was at 20°K and the other at 300°K. The total amount of helium in the apparatus should be calculated from a pressure measurement with the entire apparatus at a single temperature. Corrections for non-uniform temperatures are difficult and inaccurate in the present case. It is best to leave the data as they stand with the understanding that all pressures quoted may be higher by a factor of as much as 2.7. Probably the error is considerably smaller.

The air pumping experiments were done late in the project after it was recognized that radiant heat transfer was probably the controlling factor in the condensate surface temperature and, as a result, the controlling factor in the hydrogen and helium pumping times. Consequently, no attempt was made to study the detailed conditions for cryotrapping with solid air.

5.0 CONCLUSIONS

The experimental and theoretical results indicate the following conclusions concerning 20°K trapping of helium and hydrogen by solid nitrogen and oxygen:

1. Helium trapping occurs by physical burying of helium atoms in the solid nitrogen or oxygen.

2. Helium atoms will not be trapped until the solid forms in a state dense enough to prevent the helium atoms from rapidly diffusing back to the surface.

3. There is an induction period where no helium trapping occurs. This is the period during which the oxygen or nitrogen forms a porous or disordered solid. When the surface temperature increases to the point where there is appreciable surface mobility of the nitrogen or oxygen molecules, a dense solid forms and helium trapping commences.

4. The helium trapping probability increases with the nitrogen or oxygen condensate rate. No helium trapping was observed at condensation rates less than about 1×10^{18} cm^{-2} sec^{-1} when the helium concentration in the gaseous nitrogen or oxygen was as low as 0.1 p.p.m.

5. At helium concentrations of 0.1 p.p.m., helium pressures could be maintained no lower than about 1×10^{-6} torr regardless of the condensation rate.

6. Helium trapping by solid oxygen or nitrogen is not likely to have a practical application unless very high condensation rates can be tolerated, and the condensable gases contain only very small amounts of helium.

7. Hydrogen trapping appears to occur by adsorption of hydrogen molecules on the surface of the solid oxygen and nitrogen.

8. Hydrogen trapping is most efficient during the initial periods of a condensation when the oxygen or nitrogen is forming a porous, disordered solid.

9. When the solids start to form dense, ordered structures the surface area for adsorption decreases and hydrogen trapping breaks down.

10. The time for breakdown of hydrogen trapping is inversely proportional to the oxygen or nitrogen condensation rate. The presence of krypton impurities in the solid shortens this time.

11. The time for breakdown of hydrogen trapping is dependent on the heat flux to the surface of the solid oxygen or nitrogen. The most important factor in the heat flux appears to be thermal radiation.

12. Hydrogen trapping may find practical application under conditions of low condensation rates and by shielding the solid condensable surface from thermal radiation.

13. Further experimental work on hydrogen trapping using higher hydrogen concentrations and shielded condensing surfaces is desirable. It would be interesting to investigate condensable gases other than oxygen and nitrogen as trapping media.

REFERENCES

1. "Large Space Environments Facility System." (ARDC Project 7776, Task 77794). Feasibility and Facility Requirements, Low Temperature and High Vacuum Simulation.

2. E.S. Borovik, S.F. Grishin, and E. Ya. Grishna, Zhural Tekhnicheskoi Fiziki, Vol. 30, No. 5, pp. 539-545, May, 1960.

3. "Argon, Helium, and the Rare Gases, The Elements of the Helium Group." Ed. by Gerhard A. Cook, Vol. 1, Interscience, 1961.

4. "General Cryopumping Study," E.S.J. Wang, J.A. Collins, and J.D. Haygood. Aero-Space Research, ARO, Inc. Paper presented at 1961 Cryogenic Engineering Conference, Ann Arbor, Michigan, (August 1961).

5. D. Alpert, J. Appl. Phys. 24, 860 (1953).

6. "Kinetic Theory of Gases," Earle H. Kennard, McGraw-Hill, 1938.

7. "A Note on the Thermal Conductivity of Solid Nitrogen and the Direct Condensation of Nitrogen Gas Into a Solid," Karamcheti. AFOSR TN59-183, AD211 323, Engineering Center, University of Southern California, Los Angeles, California, USCEC Report 56-206, January 31, 1959.

8. "Diffusion in Solids, Liquids, Gases," W. Jost, Academic Press, 1952.

9. Stern, S. A., Mullhaupt, J. T., DiPaolo, F. S., and Marasco, L. "The Cryosorption Pumping of Hydrogen and Helium at 20°K." AEDC-TDR-62-200, October 1962.

10. "Cryogenic Engineering," Russell B. Scott, D. Van Nostrand, 1959.

11. "Experimental Techniques in Low Temperature Physics," G.K. White, Oxford, 1959.

12. "Introduction to Solid State Physics," C. Kittel, John Wiley and Sons, 1957.

APPENDIX 1 - CRY-ION PUMP

Part of the cryotrapping research study was an investigation of a technique for improving the cryotrapping of helium. The technique was called the "Cry-ion" pump. Basically, its operation would have been as follows:

If cryotrapping is dependent on the time a helium atom remains on the surface of the condensable, any method whereby this residence time could be increased over the normal collision time should improve the cryotrapping efficiency. If the helium atoms were ionized before they contact the cryopumping surface and, if the 20°K substrate were charged negatively, two effects should be operative.

1. The charged non-condensables would be positive ions, and therefore drawn to the negatively charged condensing surface. However, because of the formation of solid condensables on the charged cryopumping surface, the surface would become covered with an insulating layer. Consequently, a non-condensable ion arriving at the condensable surface could only be neutralized in two ways: (a) by migrating through the solid condensable to the charged metal surface to pick up an electron, or (b) by an electron migrating out through the condensable to the ion on the surface. A combination of these two migrations could occur. Regardless of the mechanism, the time necessary for ion neutralization would increase the residence time of the non-condensable on the condensable surface.

2. A non-condensable ion would be accelerated towards the condensable surface because of the negative charge on substrate, and would impact on the condensable with a velocity larger than in the case where it was a neutral particle. Thus, we might expect the non-condensable to be imbedded rather deeply in the solid condensable. In a sense, the non-condensable would be "self-trapping."

The cryotrapping work indicates that the trapping of helium and hydrogen takes place by different mechanisms. Helium is trapped by a burying mechanism whereby the helium atom is covered by solid condensable during the time the helium atom resides on the surface. Hydrogen is "trapped" by an adsorption mechanism. The number of hydrogen atoms on the condensable surface will be dependent on the surface temperature and surface area. Consequently, we would expect the concept of the cry-ion pump to be more applicable to helium than hydrogen trapping. Our studies with the cry-ion pump were confined to attempts to pump helium with solid nitrogen and, hopefully, the results could be related to the earlier studies of helium trapping by nitrogen.

APPARATUS

The apparatus is shown in Figure 25. The outer vacuum jacket was constructed of stainless steel and glass. The liquid nitrogen and liquid hydrogen containers were constructed of copper. The copper surfaces were cleaned by sandblasting. The liquid nitrogen and hydrogen exhaust and fill tubes were

thin-wall stainless. Flanges were faced flat and sealed with indium gaskets. The manifold containing the residual gas analyzer, ion gauge, McLeod gauge (not shown), and diffusion pump were glass.

Because of the use of indium gaskets, it was not possible to bake the entire apparatus to high temperatures. The apparatus was prepared for a run by warming the outside of the cryostat to 100°C while the ion gauge and residual gas analyzer are baked separately to 300 - 400°C. During the bakeout the apparatus was evacuated to 1×10^{-7} torr. After the bakeout the ion gauge was degassed. When liquid nitrogen and hydrogen were introduced, a pressure of 1×10^{-8} torr was maintained. This pressure was due mainly to helium.

The ion gauge and residual gas analyzer were calibrated as described previously.

A and B were tungsten grids. Ionization of gases was accomplished by electron bombardment. The electron flow, from B to A, was accomplished by field emission. The substrate was at ground potential. The potentials of A and B relative to ground could be varied separately.

PROCEDURE

All experiments were done with a single cylinder of pure nitrogen containing 0.1 p.p.m. He. The procedure was similar to that used in the cryotrapping studies. The nitrogen flow was started and the helium pressure monitored with the gas analyzer. After the trend in the helium pressure curve was established, the grids were charged and the helium pressure curve was examined to see if a pressure drop occurred. Two different electrical conditions were used; i.e., A charged positively and B negatively, and vice versa.* (This merely constitutes a reversal of the electron flow direction between A and B.)

RESULTS

Figures 26, 27, and 28 show some typical helium pressure curves during operation of the cry-ion pump. The arrows indicate when the electrodes were charged. It is readily seen that there was no evidence of helium pumping. All the nitrogen flow rates were set such that helium trapping would not normally be observed. During all the runs the current between electrodes A and B remained constant. The cry-ion pump, as constructed and operated by us, did not work as anticipated. There are several reasons which may account for this failure.

A. The density of the solid was too low to retain any helium atoms which did impinge on the surface. One of the principal requirements for helium trapping is that the solid condensable pack densely enough to prevent the helium from diffusing back out. If the solid is porous, it will not make much difference in what form (ion or neutral) or velocity the helium atom arrives at the solid condensable surface.

* The terms positive and negative are relative.

B. It is possible that the electron current and path length were too small to cause significant ionization of the helium. This is particularly true when it is remembered that the helium was the minority component in the gas mixture. It is likely that significant helium ionization would only be accomplished by resorting to large electron currents and long electron path lengths. The path length could be increased by operating the device in a magnetic field, as is done with conventional getter-ion pumps.

APPENDIX 2 - SOME STUDIES OF HYDROGEN WALL ADSORPTION IN THE CRY-ION PUMP

Figure 29 shows the partial pressures of helium and hydrogen in the cry-ion pump when a mixture of pure helium and hydrogen was admitted (no condensables). Estimating the average gas temperature in the apparatus to be about 100°K, the leak rates were calculated to be 3.9×10^{11} H_2 molecules/sec. and 4.89×10^{10} He atoms/sec. It is readily seen that the behavior of the hydrogen and helium are markedly different. The helium pressure rose more or less linearly while the hydrogen pressure increased sharply at first, then leveled out for a period, followed by another abrupt rise which assumed a linear form. The hydrogen behavior was that expected for wall adsorption. Proof of the adsorption of hydrogen on the 20°K wall is shown in Figure 30. A warm metal rod was introduced into the liquid hydrogen container in the gas space above the liquid. This caused a momentary warming of the walls. Some of the adsorbed hydrogen was driven off the walls, but the helium pressure remained constant. There was no significant amount of helium adsorbed on the walls.

Although Figure 29 establishes hydrogen wall adsorption, the behavior is entirely different from that observed during cryotrapping with oxygen or nitrogen. If we assume that 30 min. (Figure 29) represents the time for complete wall coverage, then this coverage was 8.48×10^{11} molecules/cm^2 The total 20°K surface area was about 827 cm^2. In the cryotrapping pump 2.51×10^{11} molecules/cm^2 was obtained. Because the 20°K surfaces were different types of metals, better agreement cannot be expected.

•

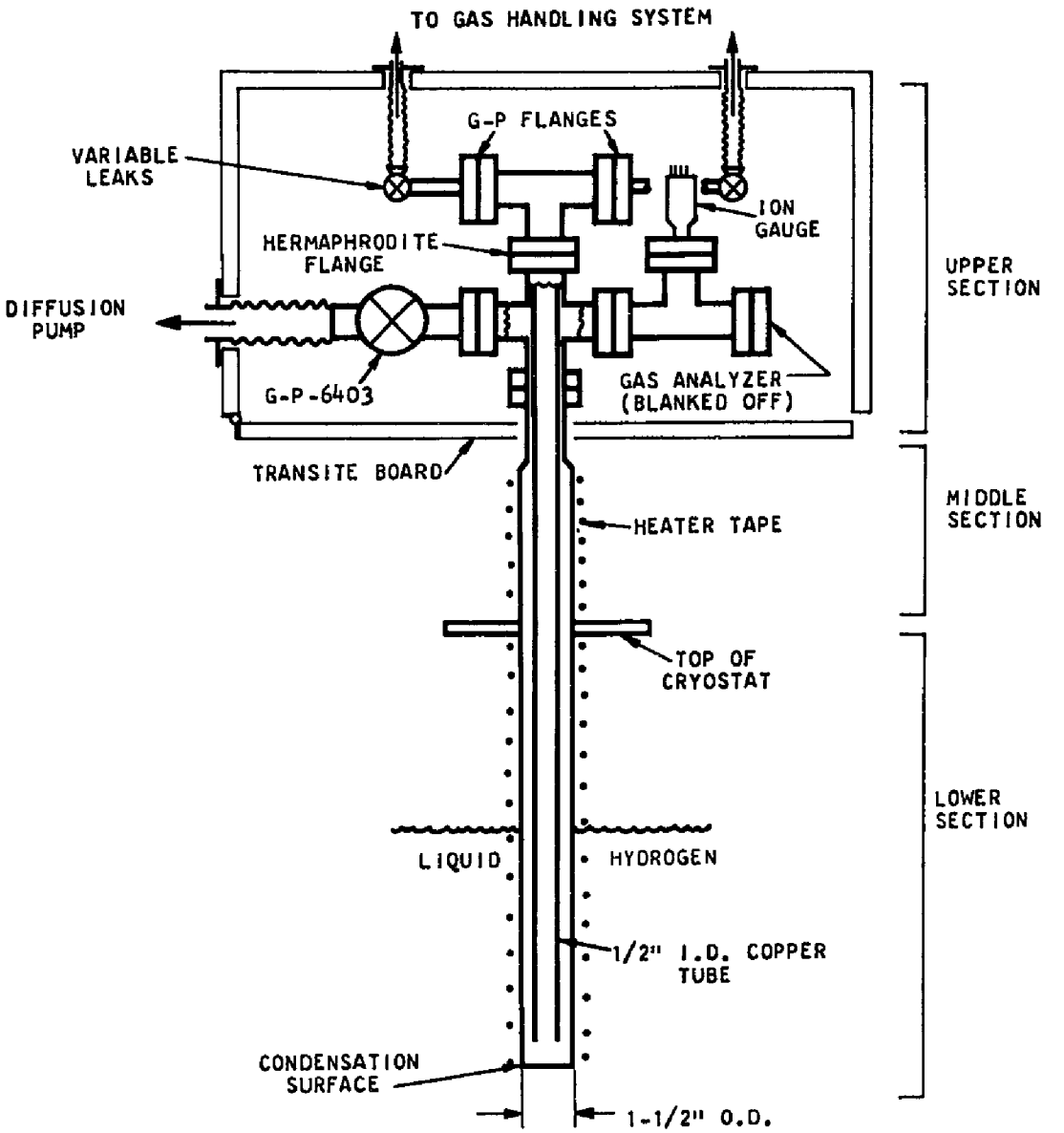

FIG. 1 CRYOPUMP DIAGRAM

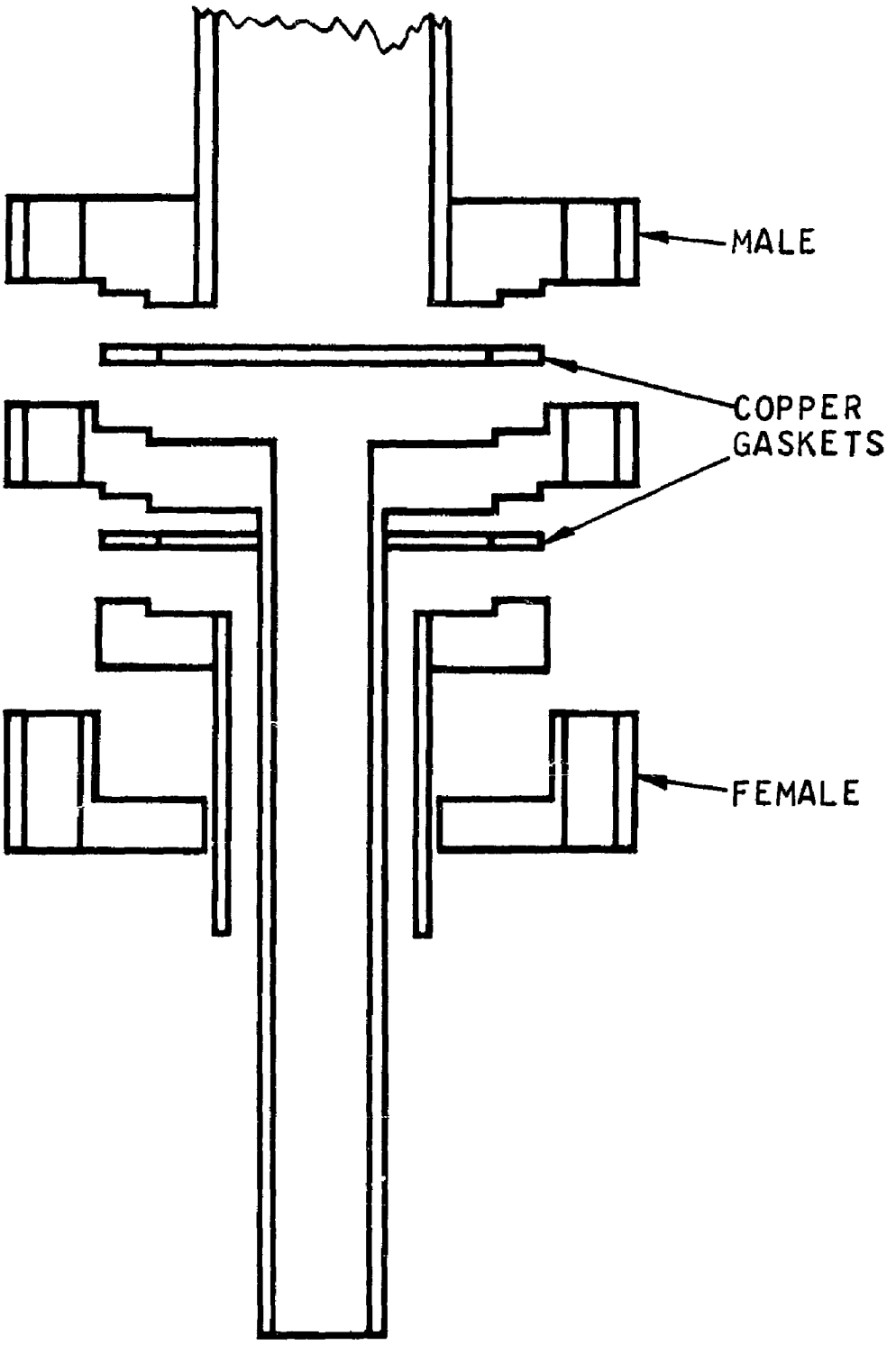

FIG. 2 HERMAPHRODITE FLANGE

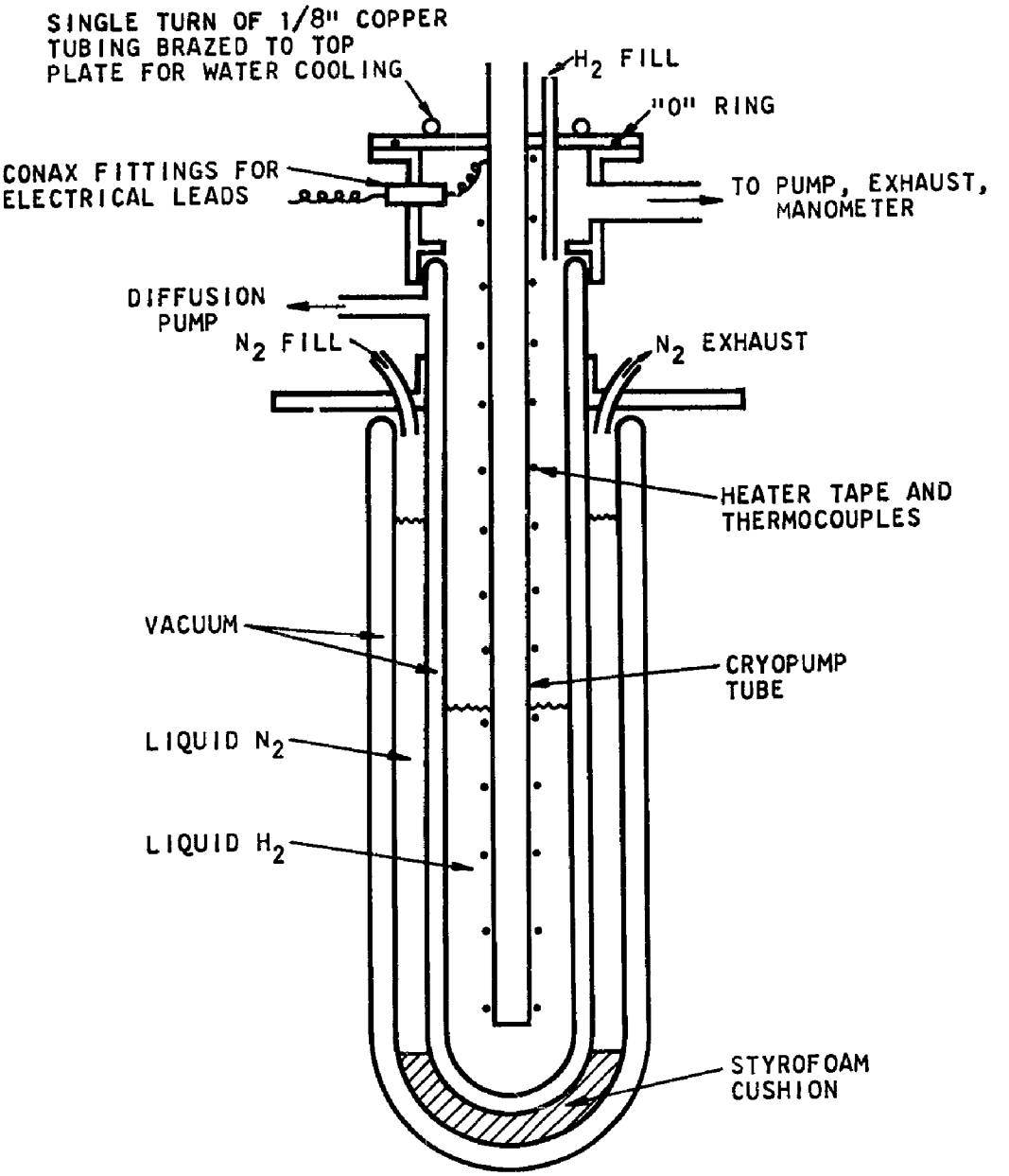

FIG. 3 CRYOSTAT SECTION

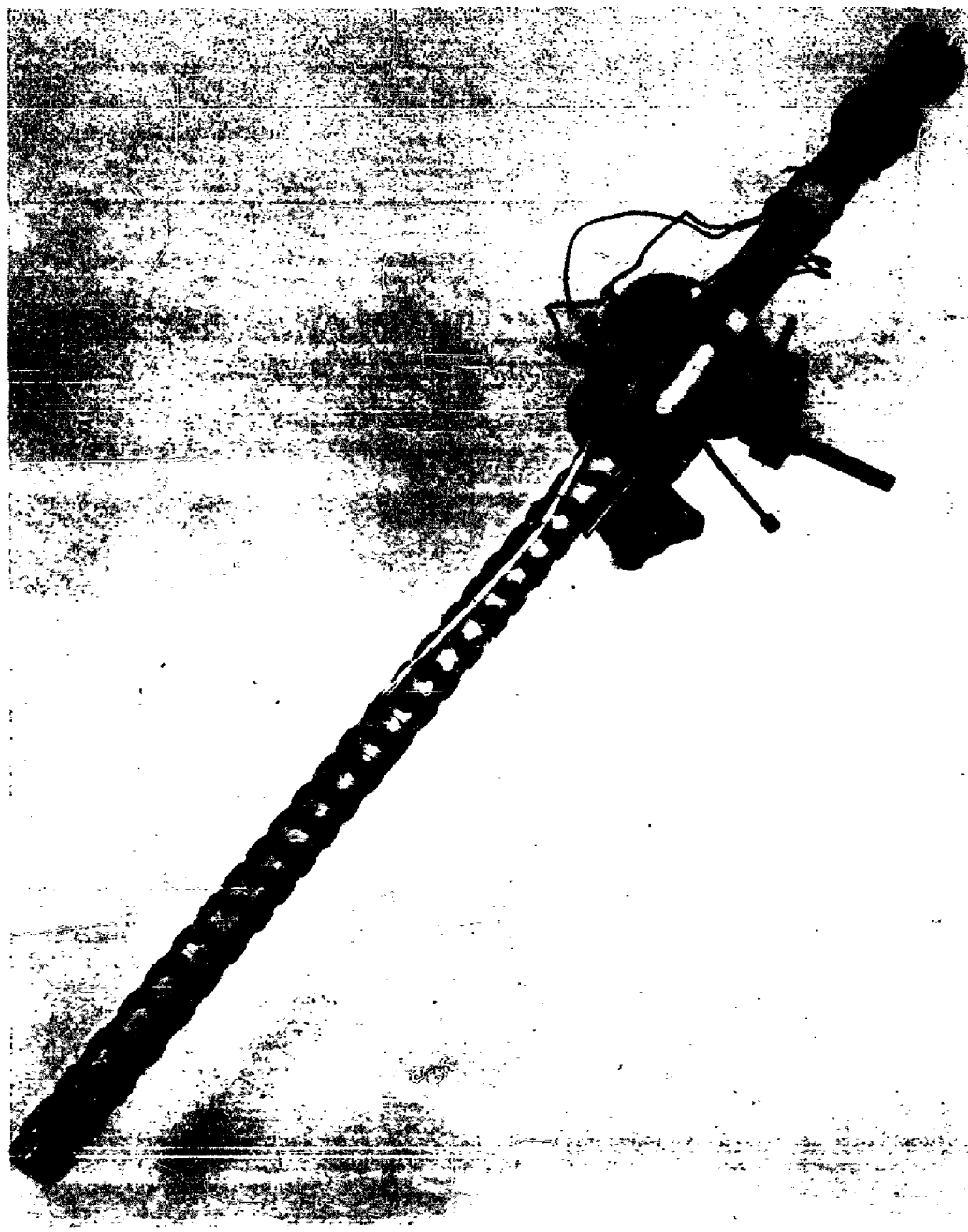

FIG. 4 LOW TEMPERATURE SECTION OF THE CRYOPUMP

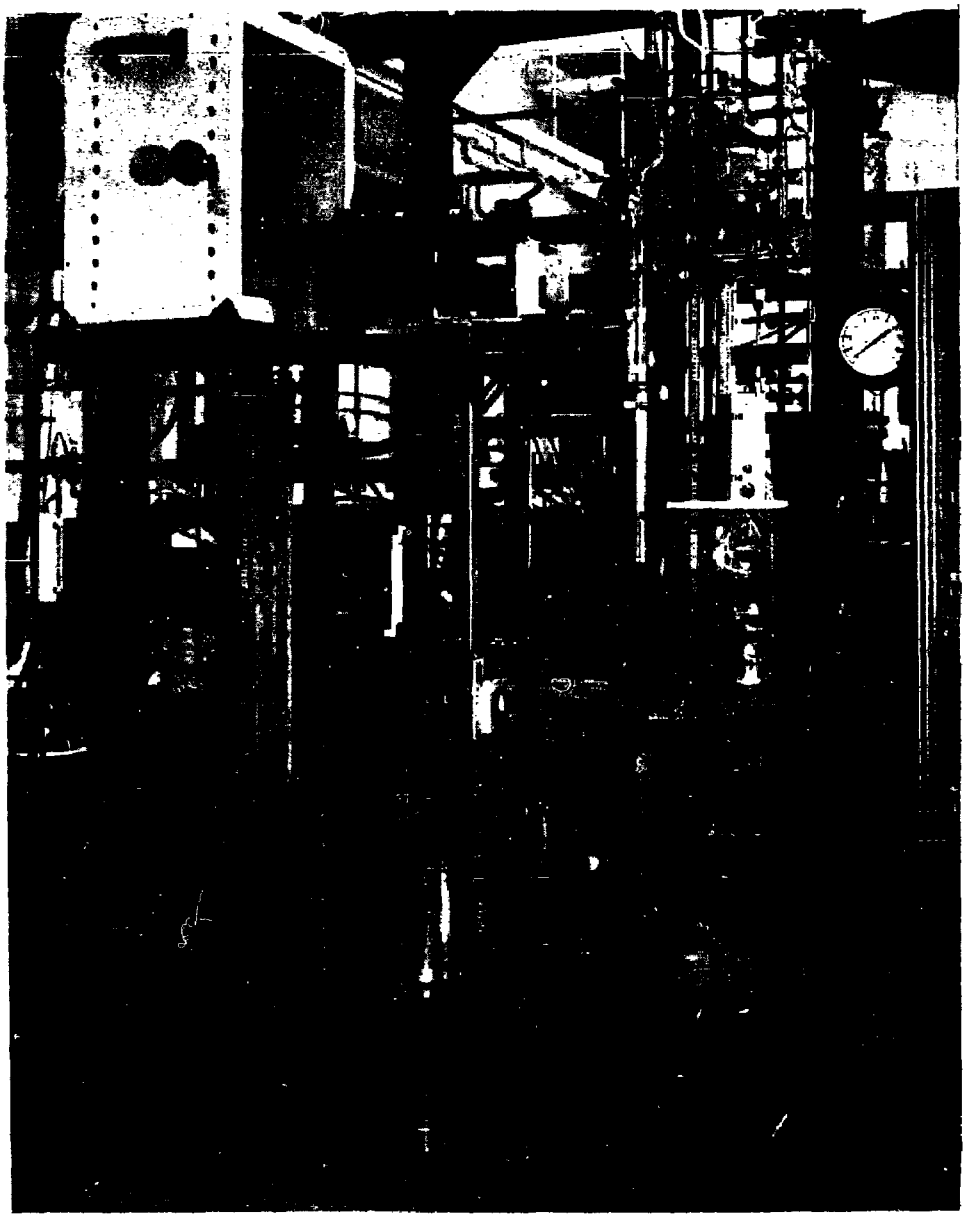

FIG. 5 EXPERIMENTAL EQUIPMENT

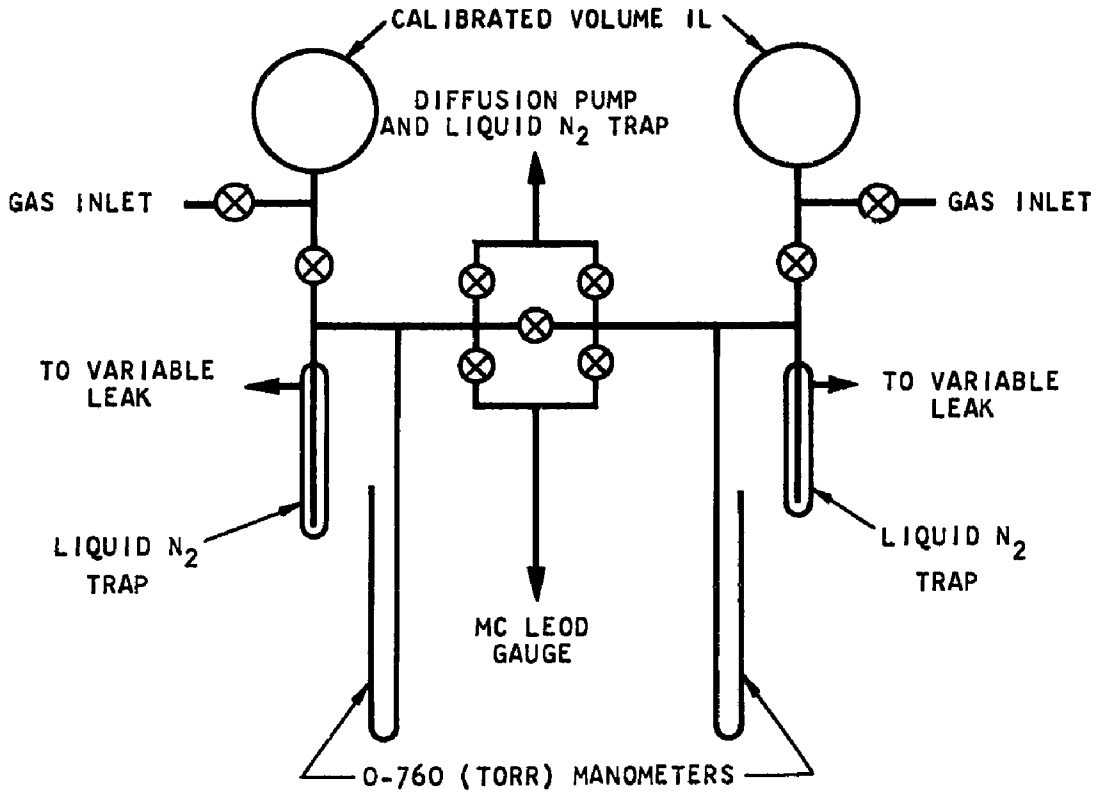

FIG. 6 GAS HANDLING SYSTEM

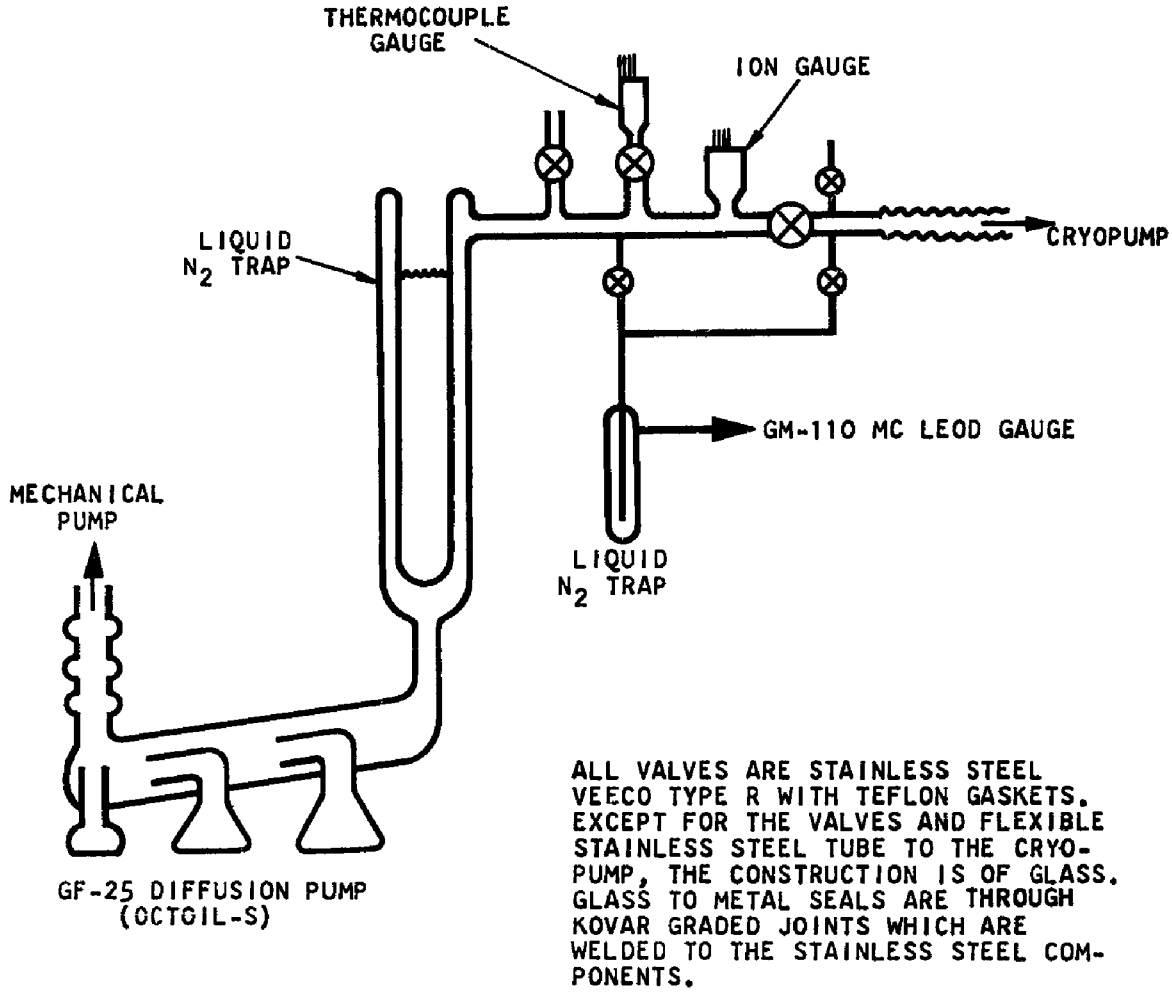

FIG. 7 DIFFUSION PUMP SYSTEM

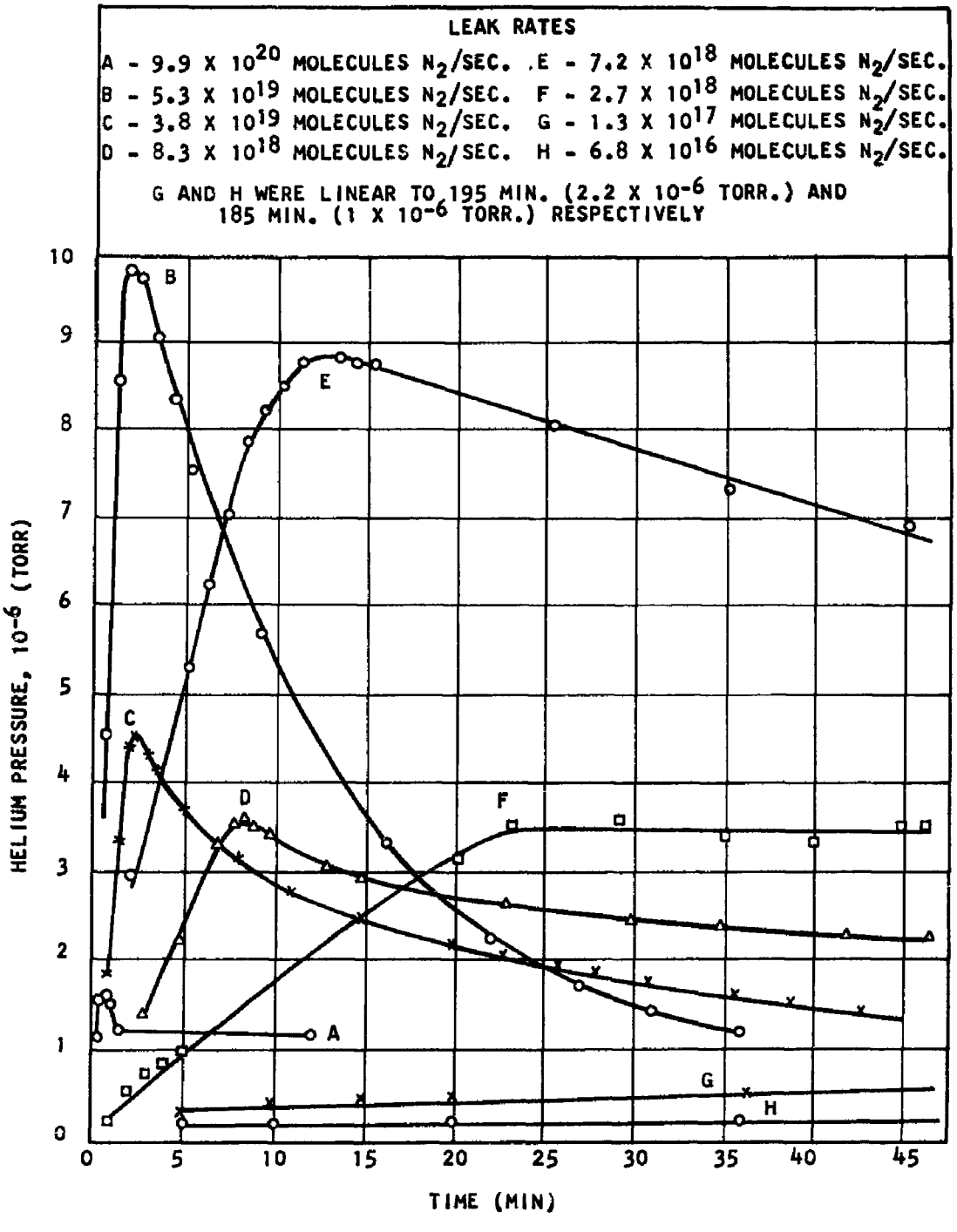

FIG. 8 HELIUM PRESSURE DURING CONDENSATION OF NITROGEN

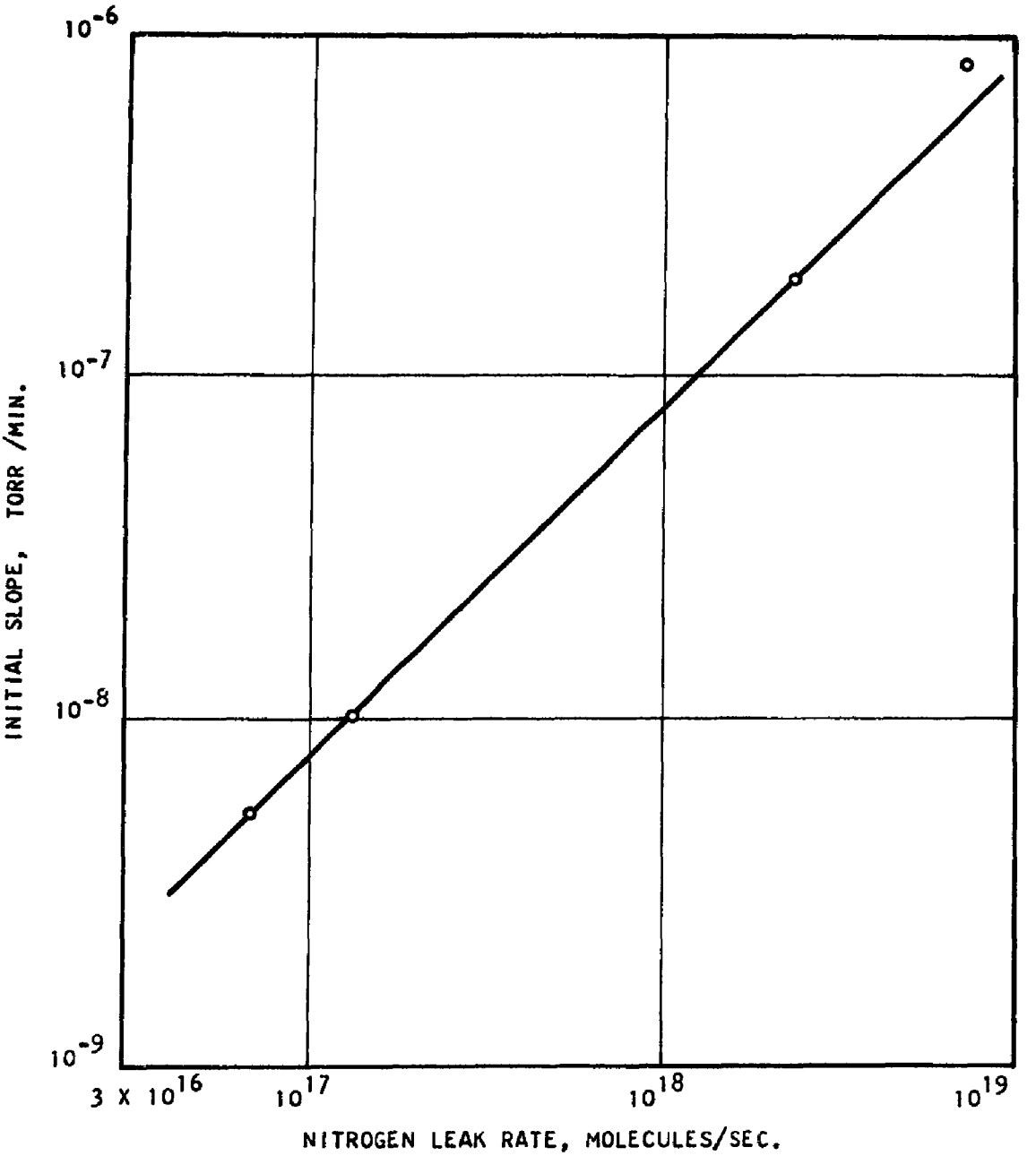

FIG. 9 INITIAL SLOPE OF HELIUM PRESSURE-TIME CURVE AS A FUNCTION OF NITROGEN LEAK RATE

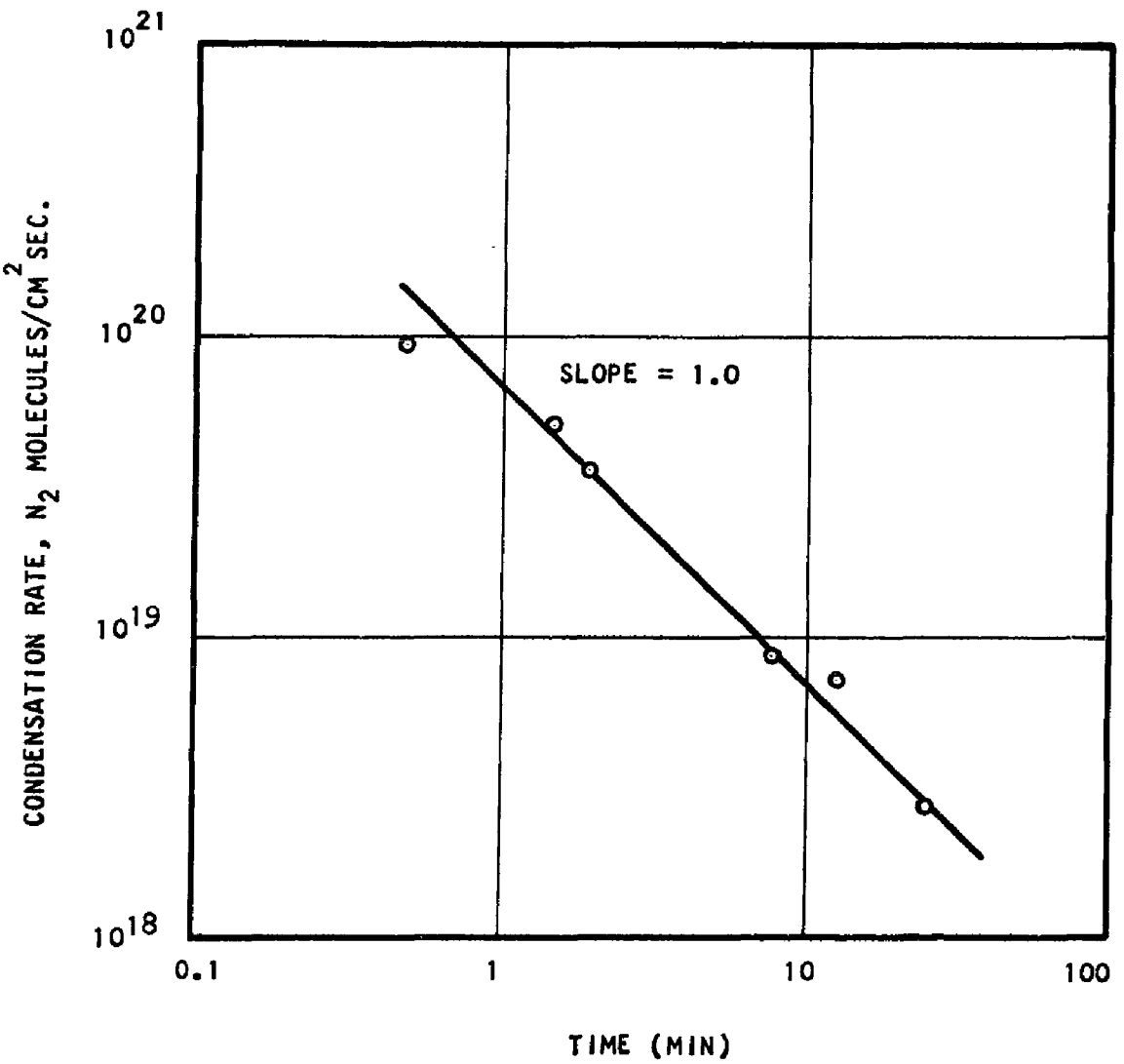

FIG. 10 TIME FOR MAXIMUM HELIUM PRESSURE AS A FUNCTION OF NITROGEN CONDENSATION RATE

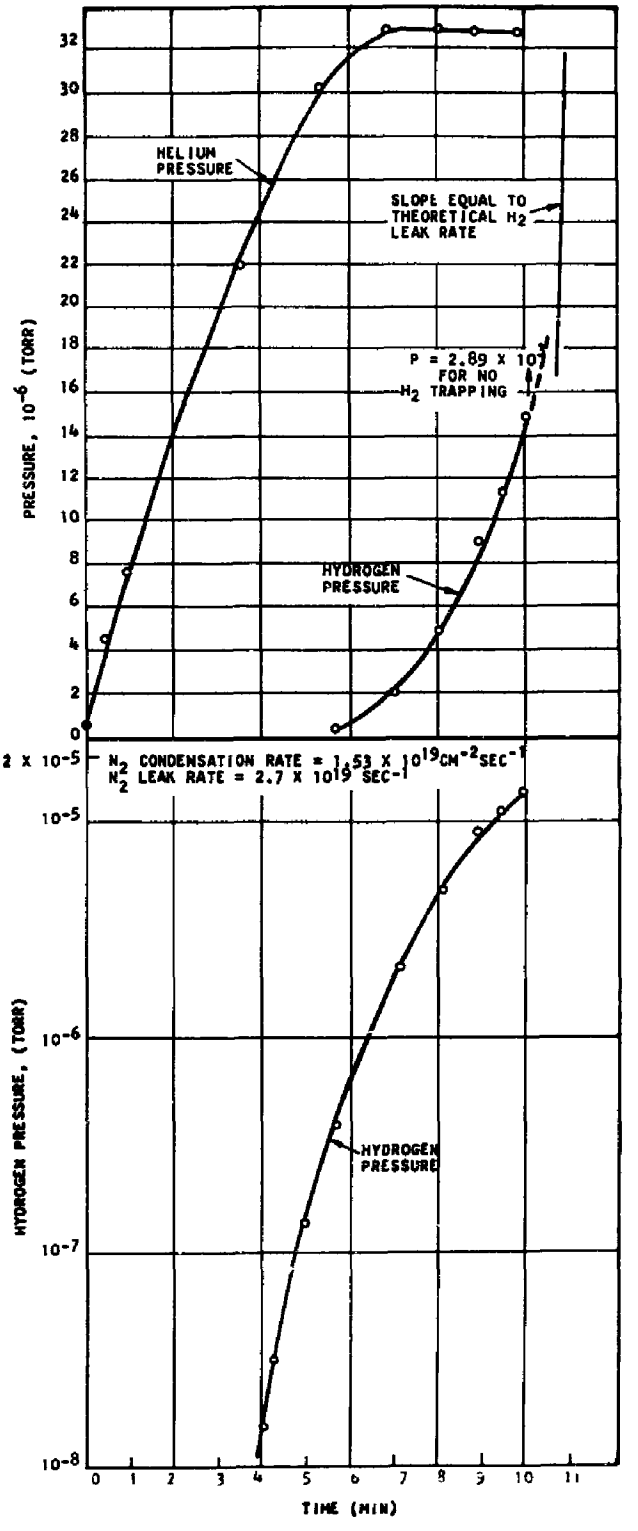

FIG. 11 HELIUM AND HYDROGEN PRESSURES DURING CONDENSATION OF NITROGEN CONTAINING 10 PPM H_2 AND 0.37 PPM He

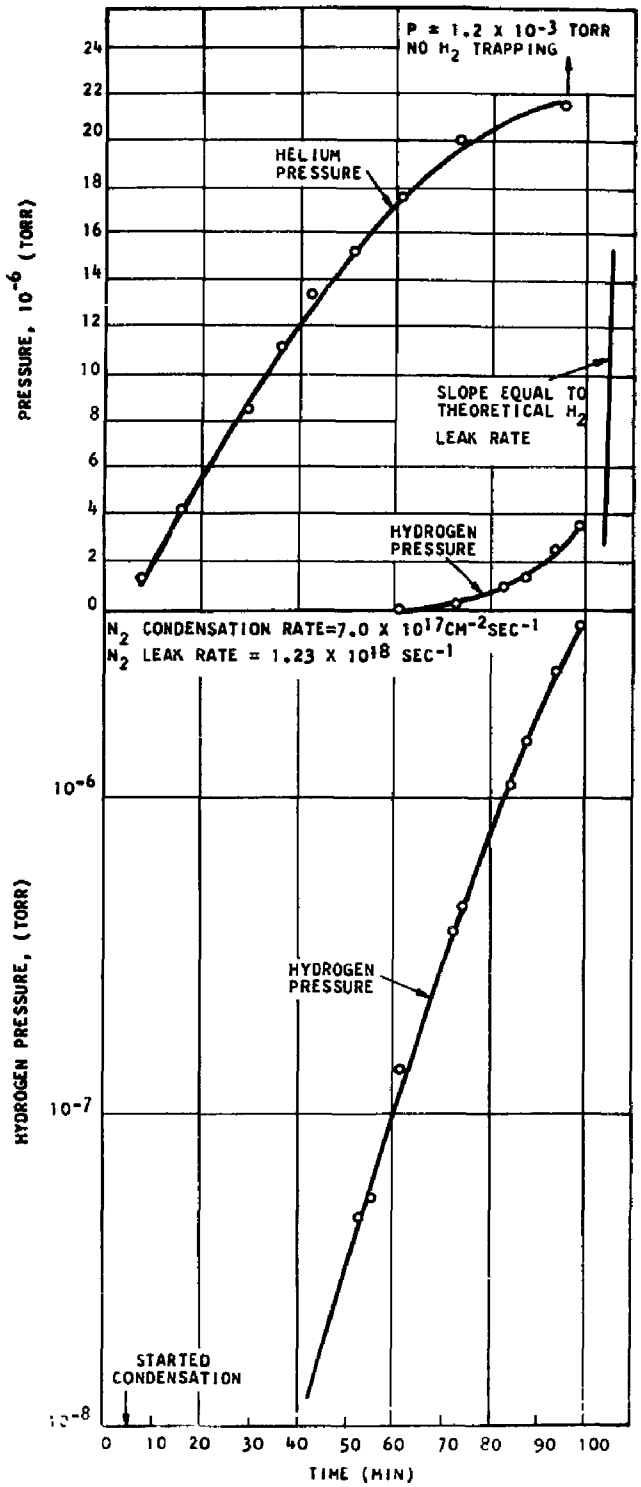

FIG. 12 HELIUM AND HYDROGEN PRESSURES DURING CONDENSATION OF NITROGEN CONTAINING 10 PPM H_2 AND 0.37 PPM He

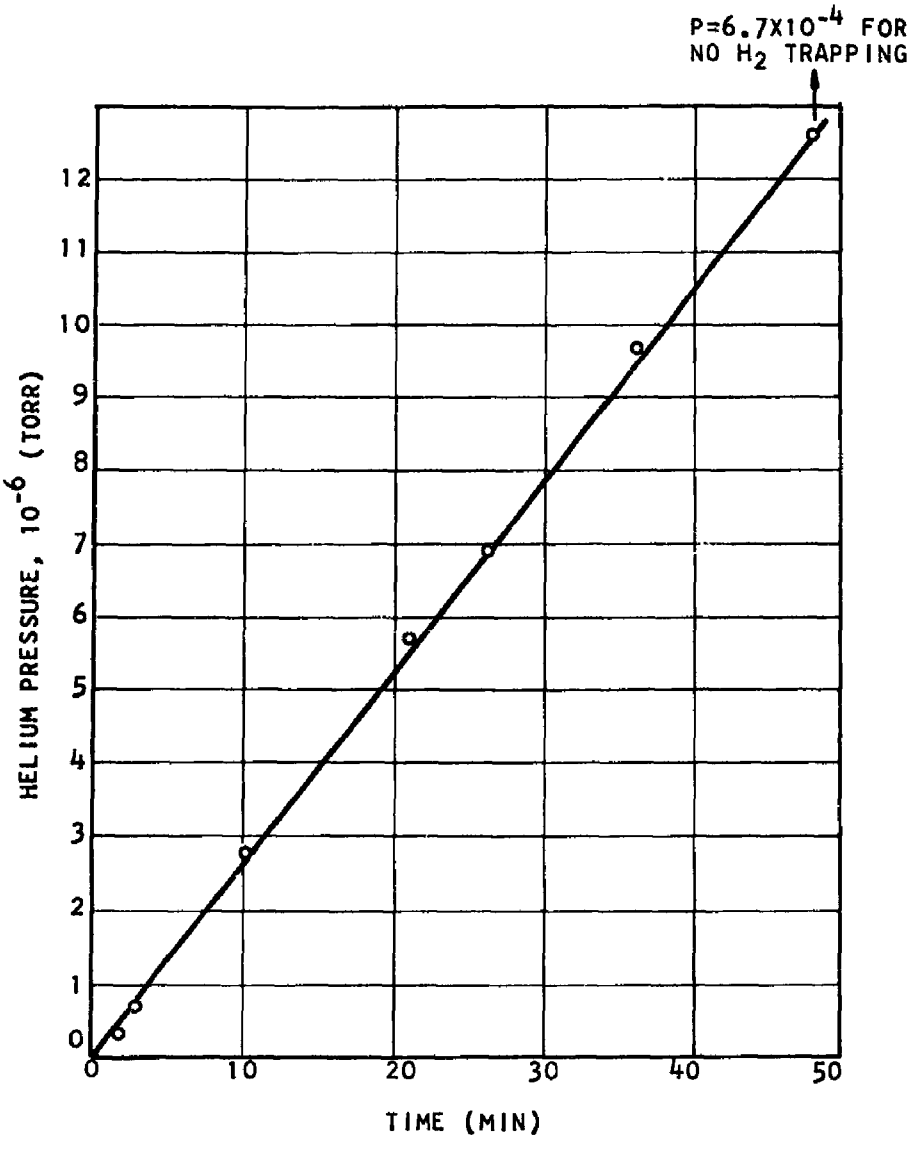

N_2 LEAK RATE = 6.74×10^{17} SEC.$^{-1}$
N_2 CONDENSATION RATE = 3.82×10^{17} CM^{-2} SEC.$^{-1}$
DURING THIS RUN THE HYDROGEN PRESSURE WAS 1-2 X 10^{-10} TORR

FIG. 13 HELIUM PRESSURE DURING CONDENSATION OF NITROGEN CONTAINING 10 PPM H_2 AND 0.37 PPM He

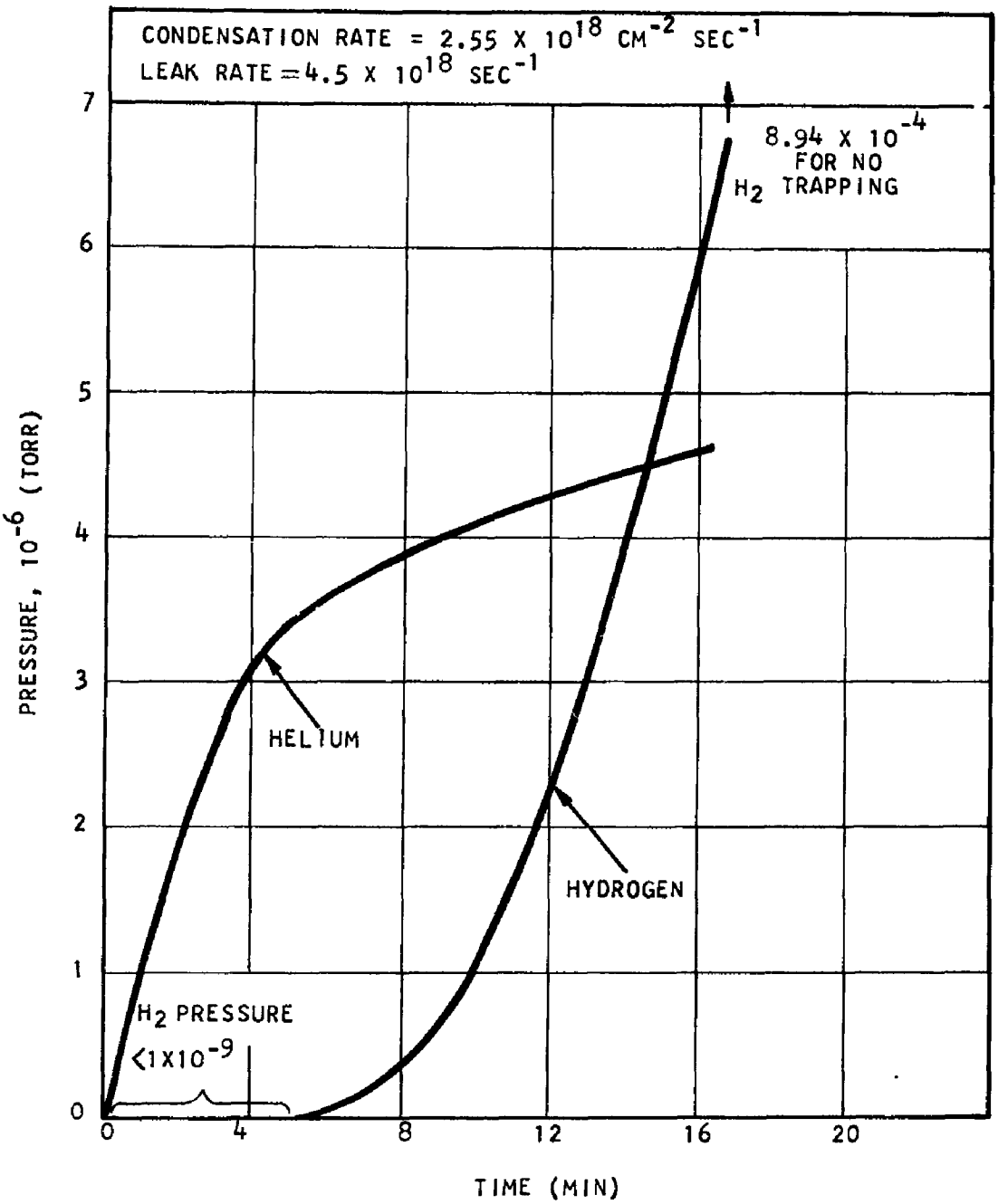

FIG. 14 HELIUM AND HYDROGEN PRESSURES DURING CONDENSATION OF OXYGEN CONTAINING 10.8 PPM H_2

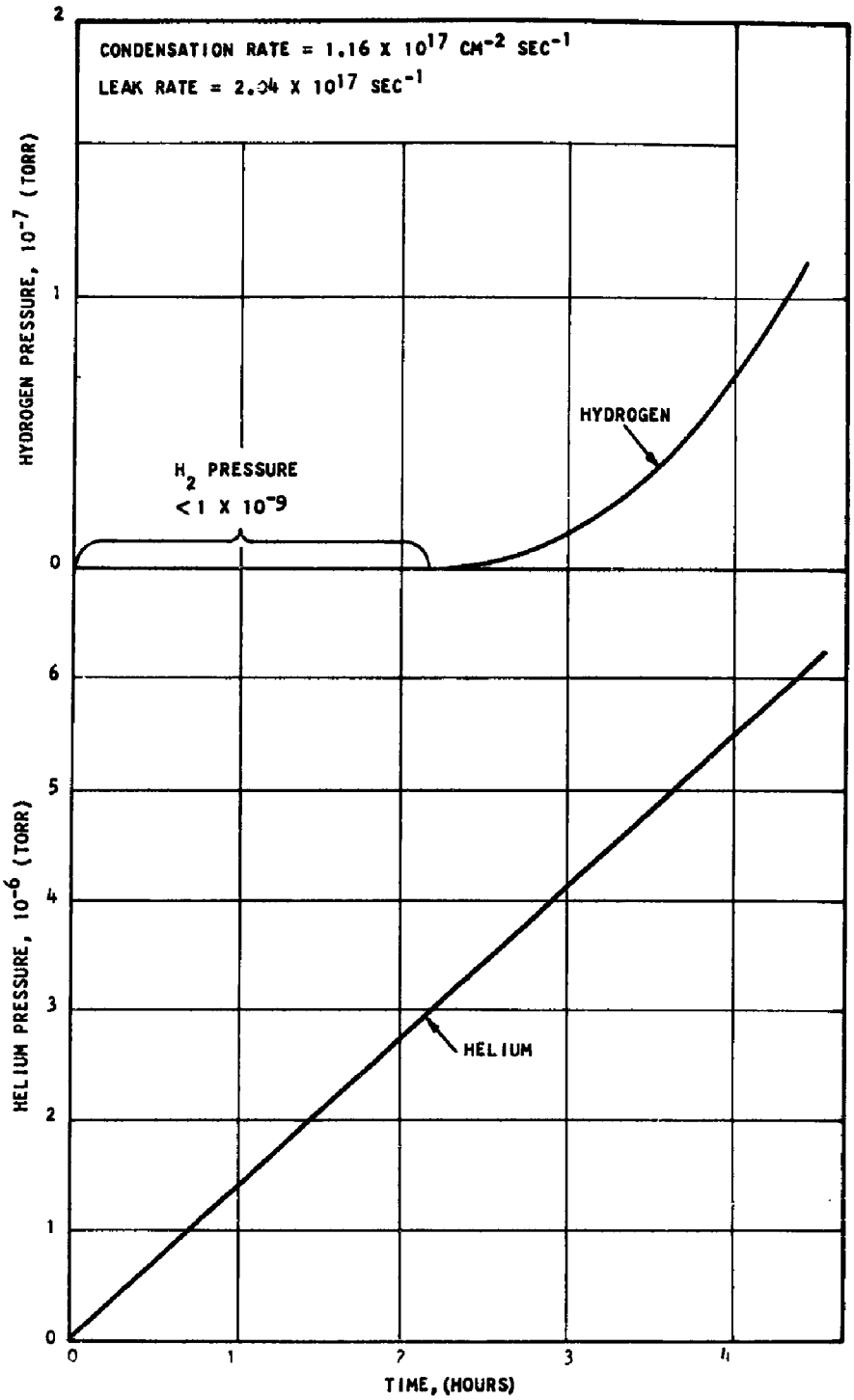

FIG. 15 HELIUM AND HYDROGEN PRESSURES DURING CONDENSATION OF OXYGEN CONTAINING 10.8 PPM H_2

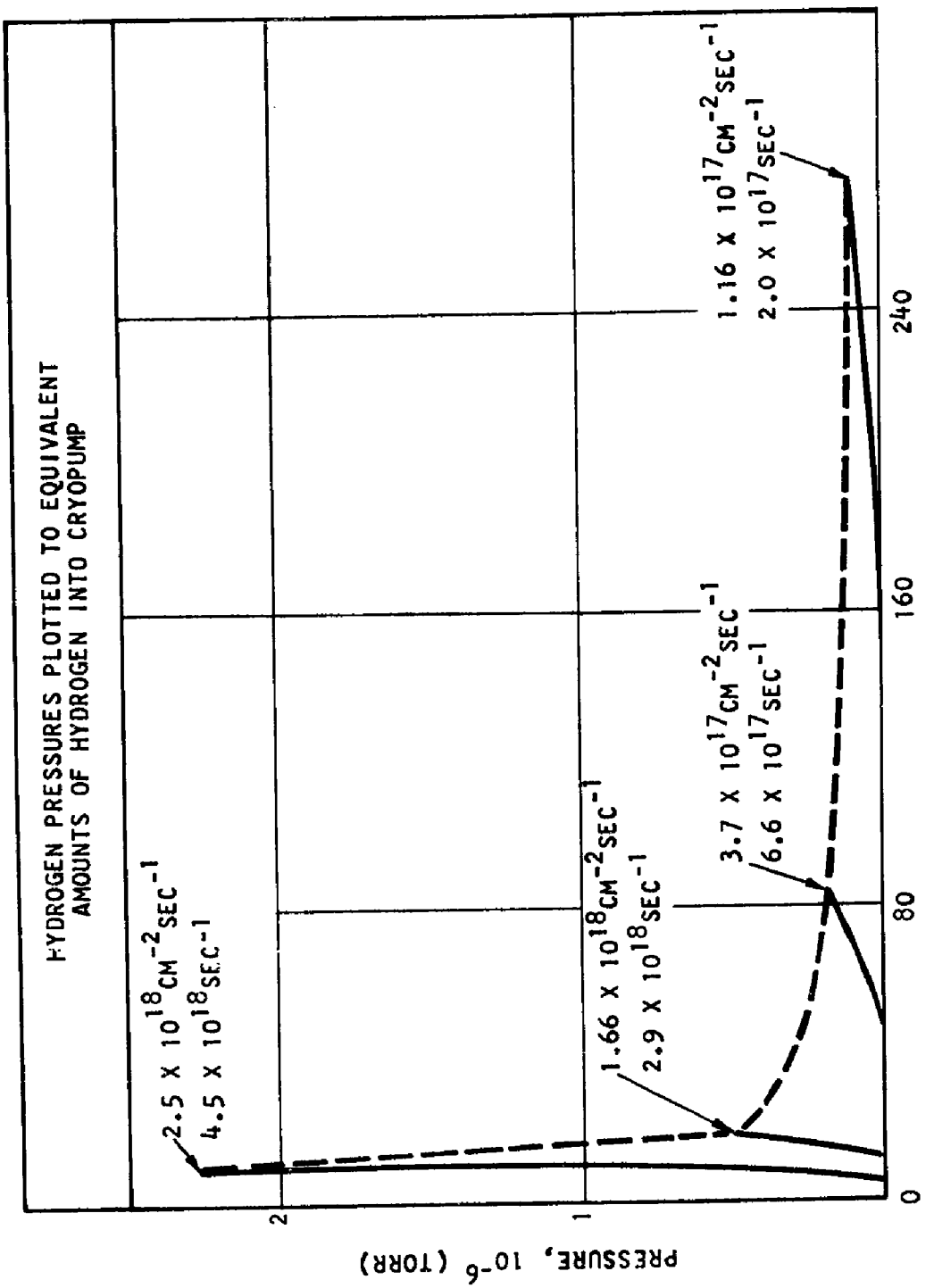

FIG. 16 HYDROGEN PRESSURES DURING CONDENSATION OF OXYGEN CONTAINING 10.8 PPM H_2

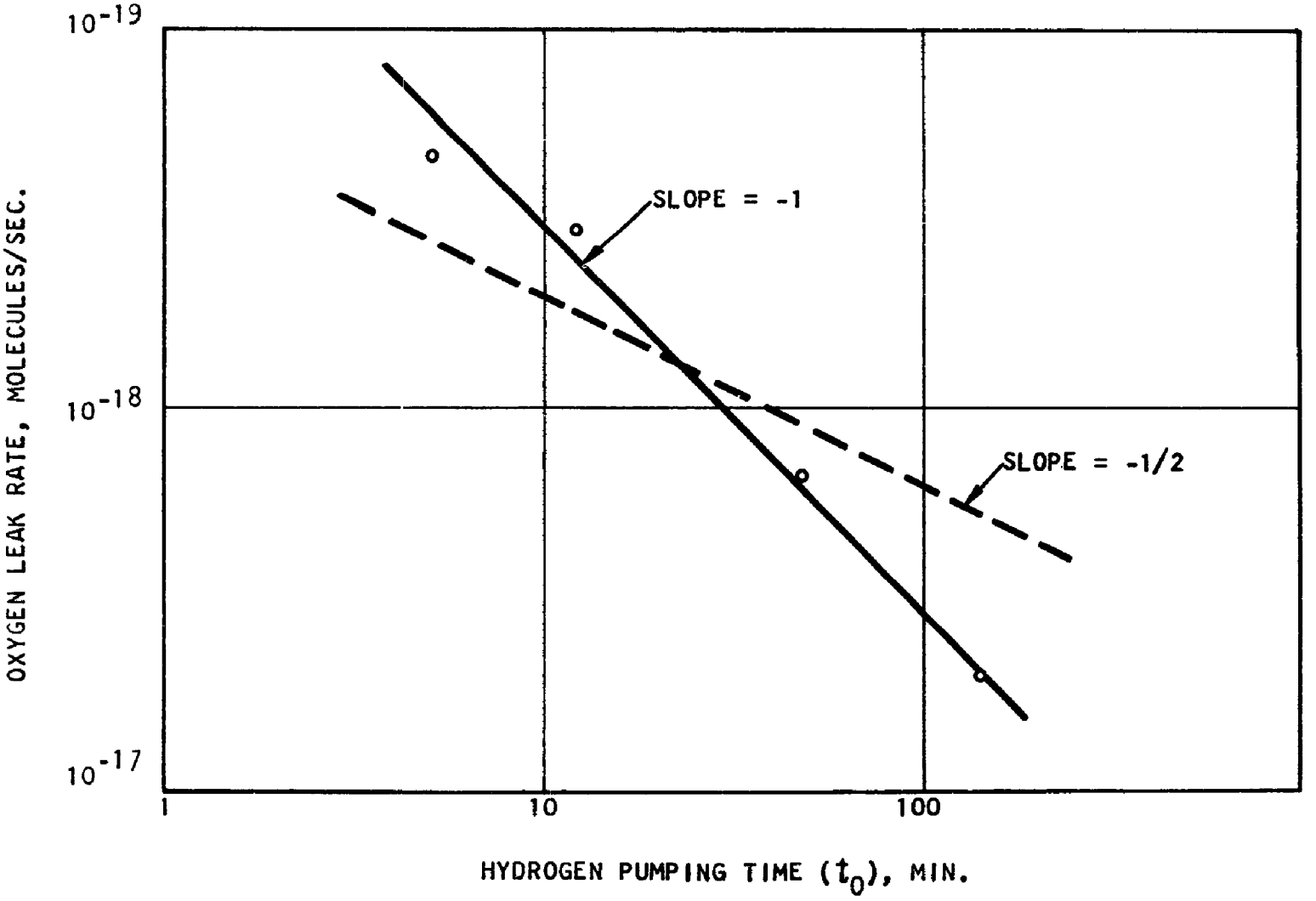

FIG. 17 HYDROGEN PUMPING TIME AS A FUNCTION OF OXYGEN LEAK RATE

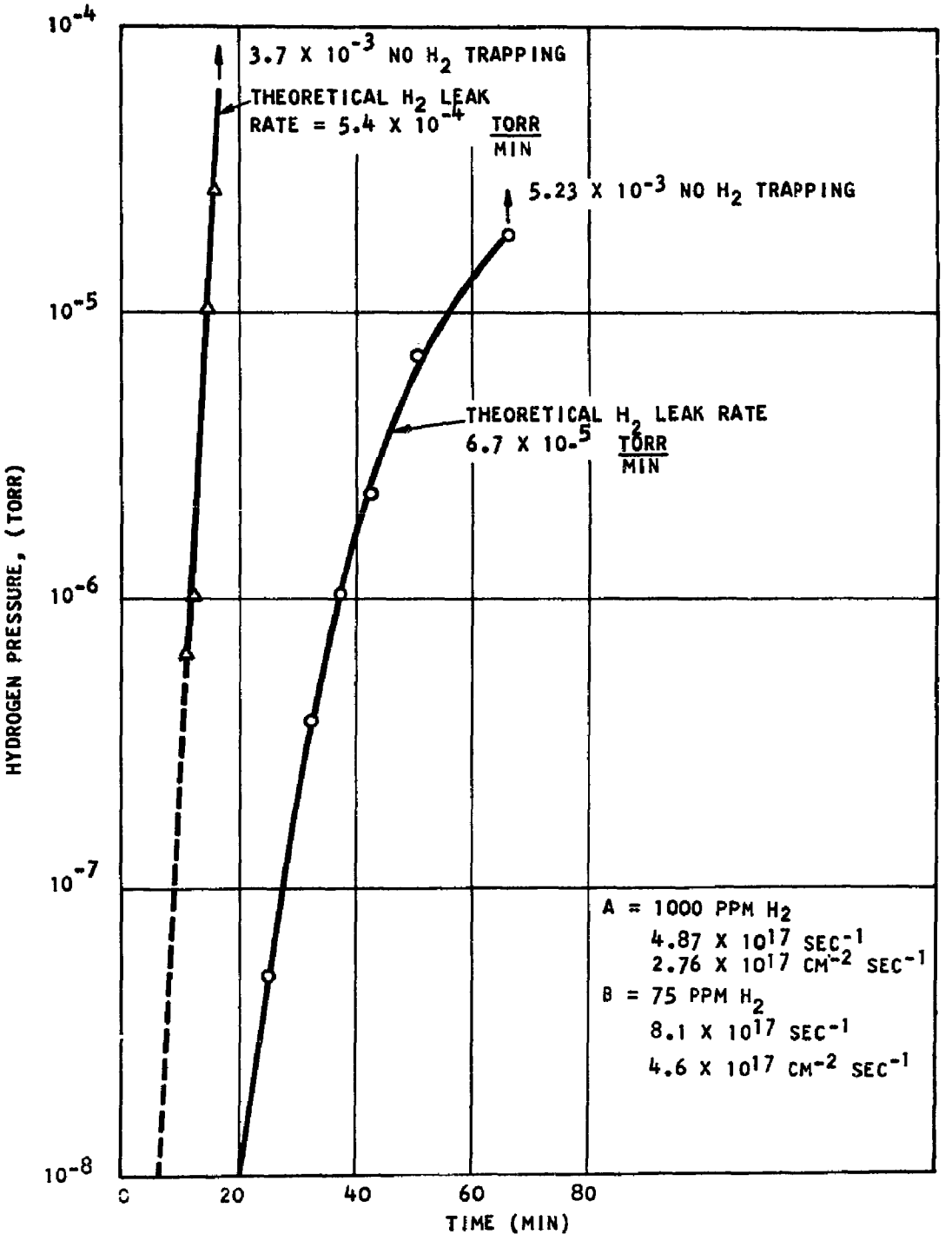

FIG. 18 HYDROGEN PRESSURE DURING CONDENSATION OF NITROGEN

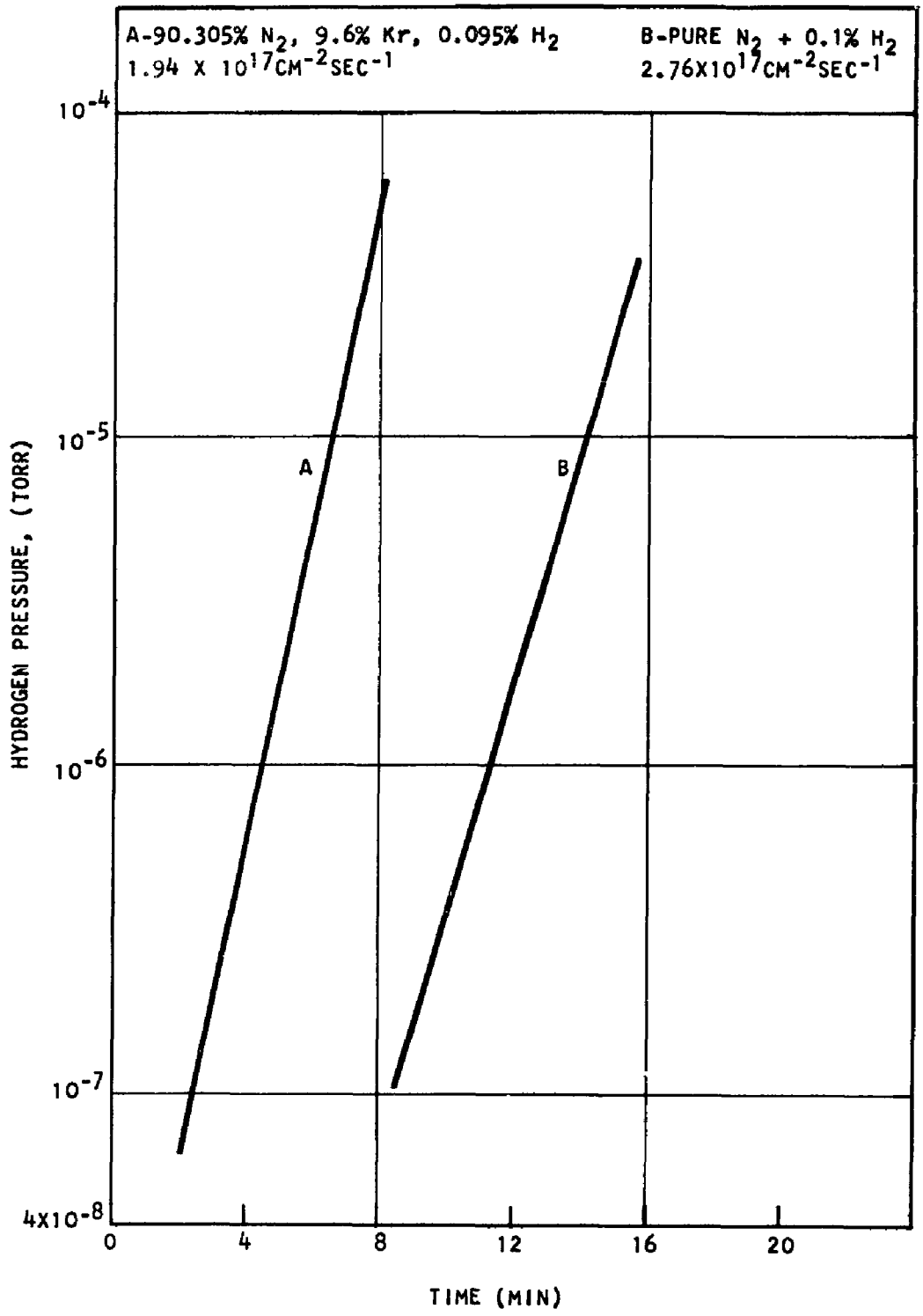

FIG. 19 HYDROGEN PRESSURE DURING CONDENSATION OF NITROGEN

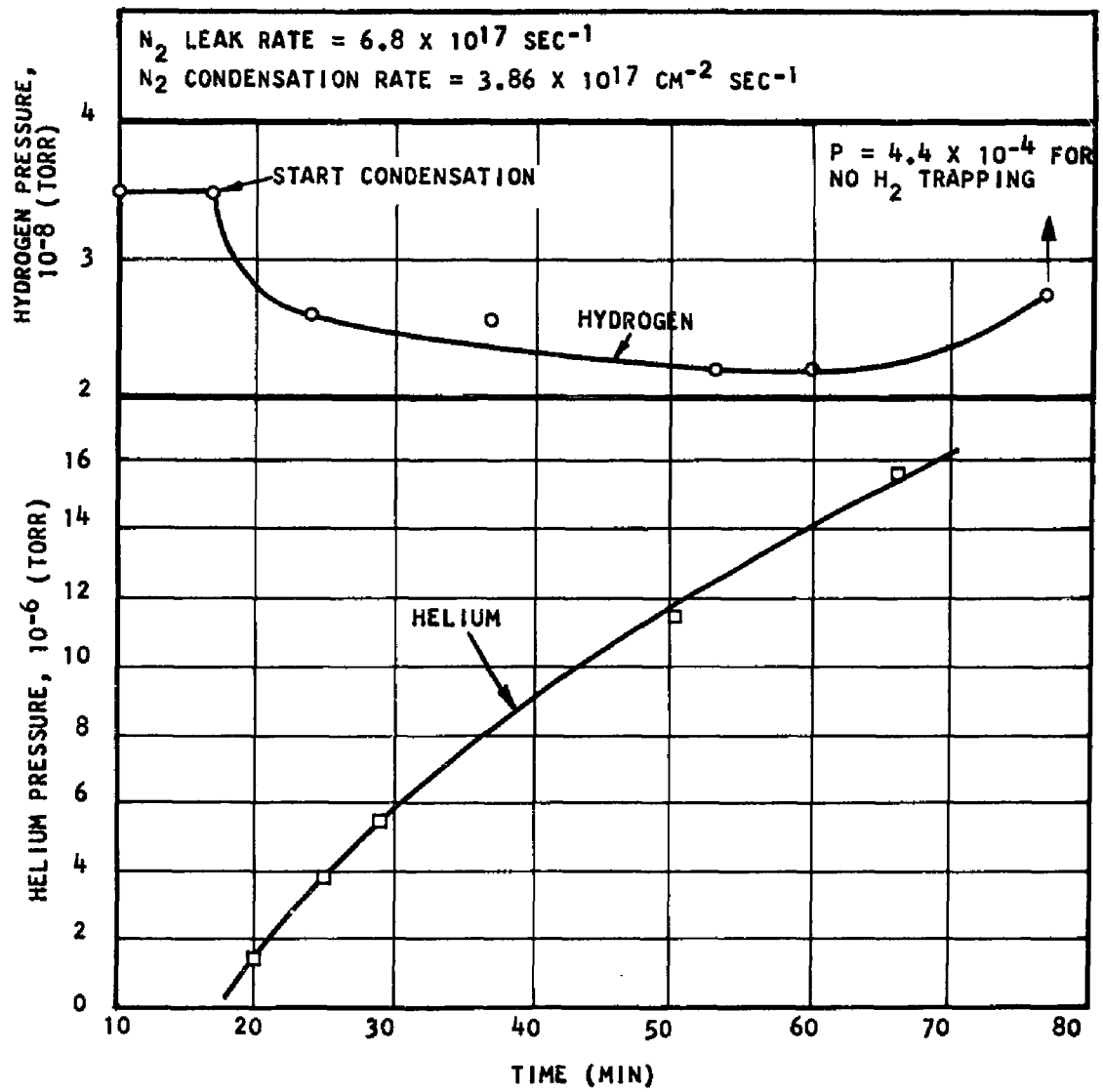

FIG. 20 HELIUM AND HYDROGEN PRESSURES DURING CONDENSATION OF NITROGEN CONTAINING 10 PPM H_2 AND 0.37 PPM He

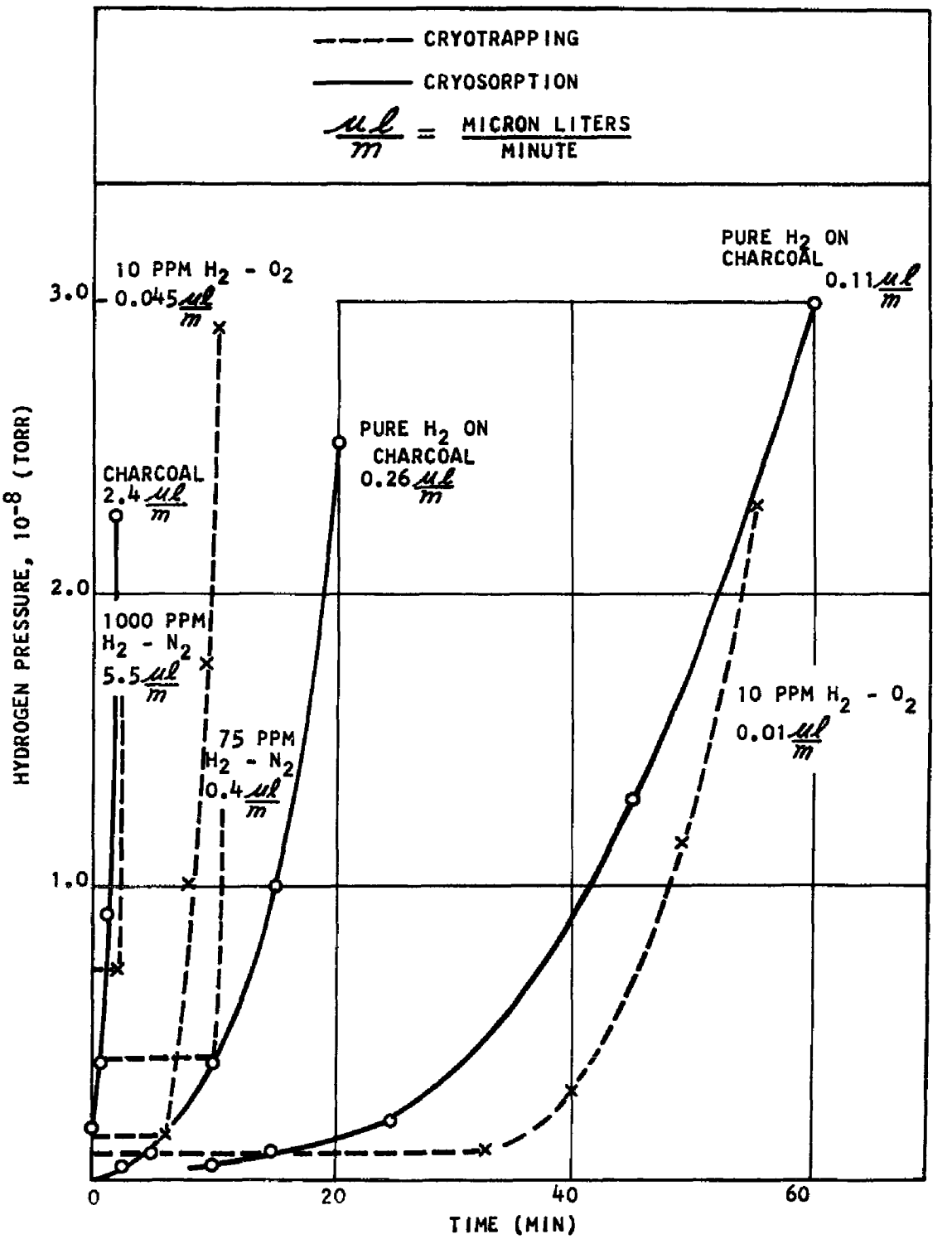

FIG. 21 COMPARISON OF HYDROGEN PRESSURE CURVES DURING CRYOTRAPPING AND CHARCOAL CRYOSORPTION

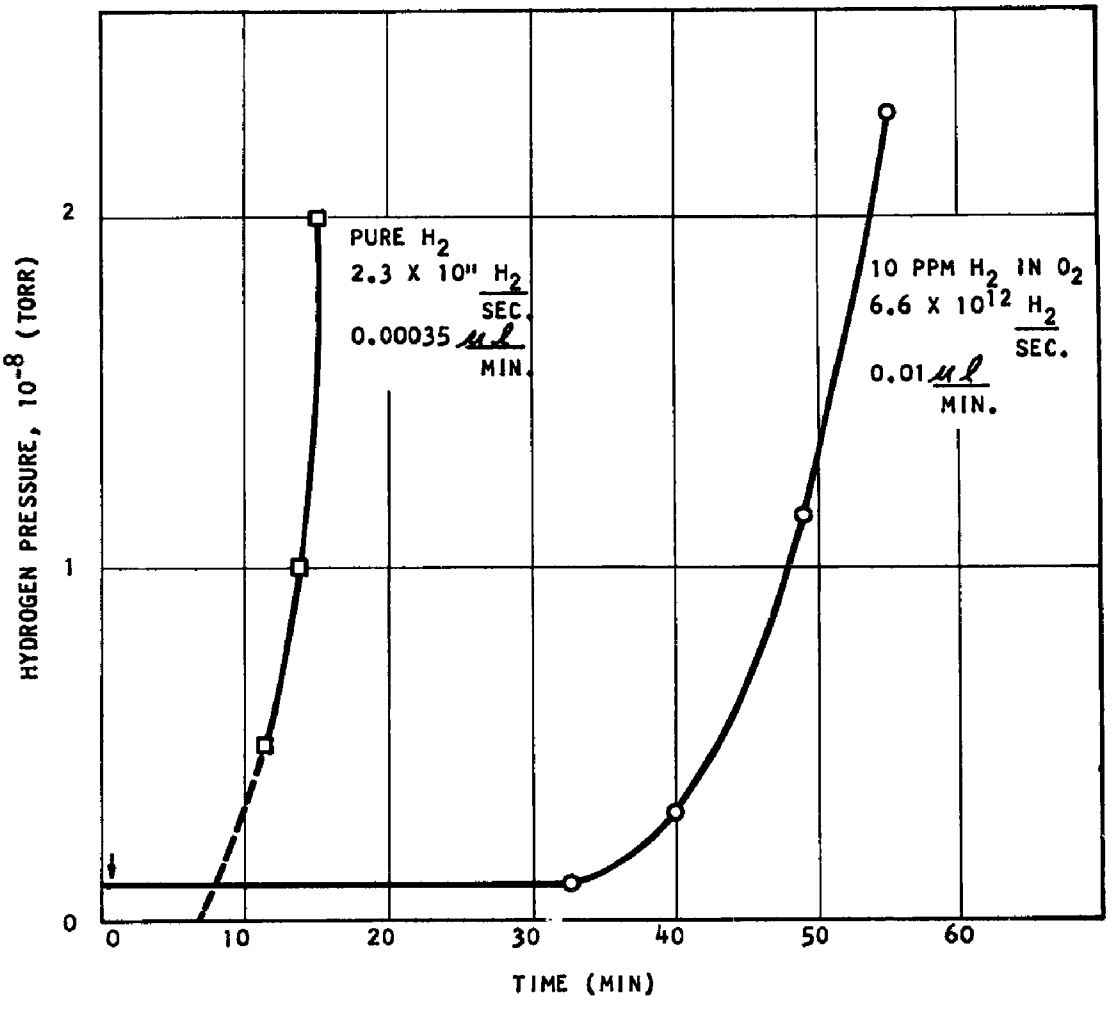

FIG. 22 COMPARISON OF HYDROGEN PUMPING BY WALL ADSORPTION AND CRYOTRAPPING

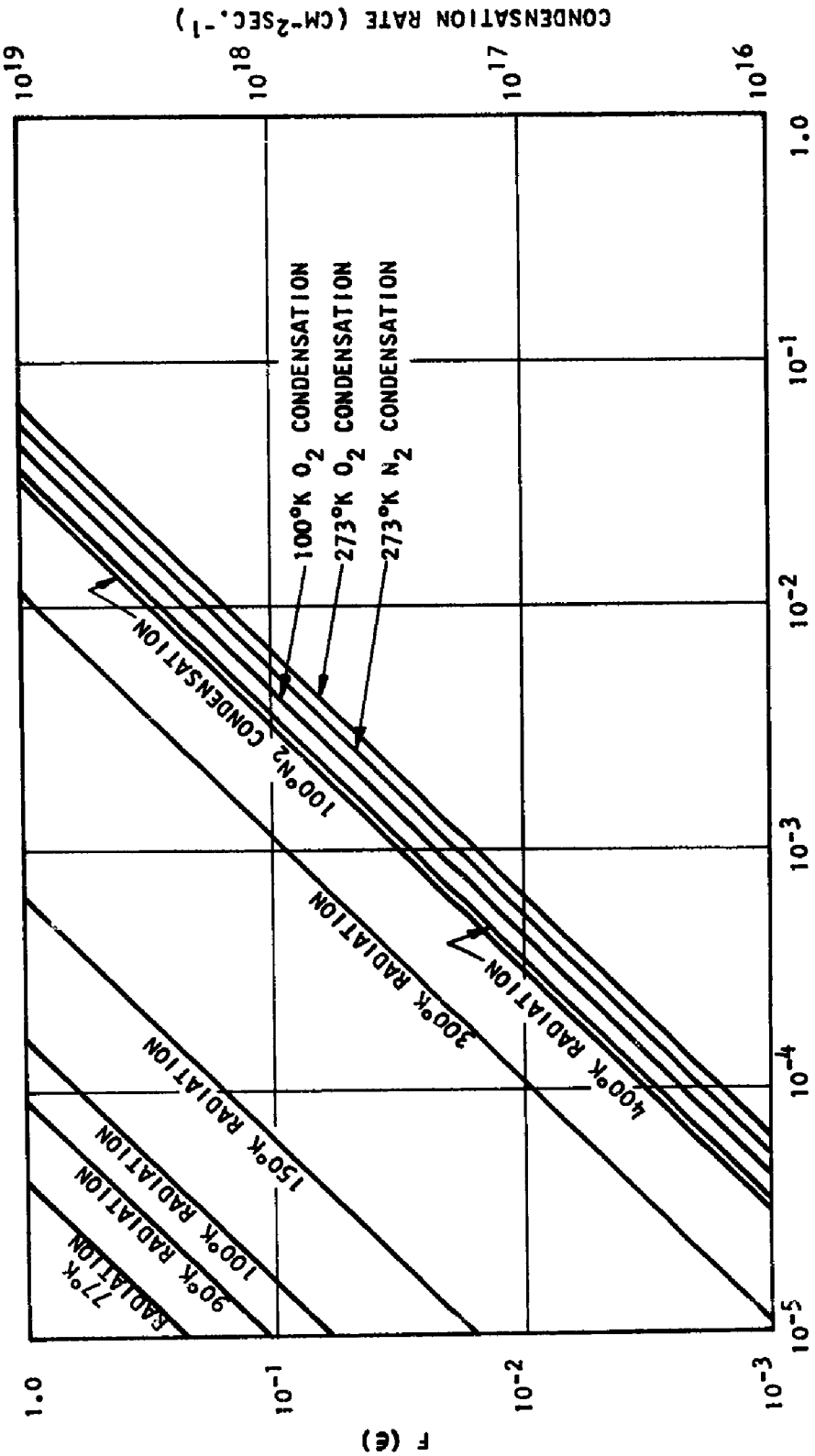

FIG. 23 COMPARISON OF RADIANT AND CONDENSATION HEAT FLUXES ON A 20°K SURFACE

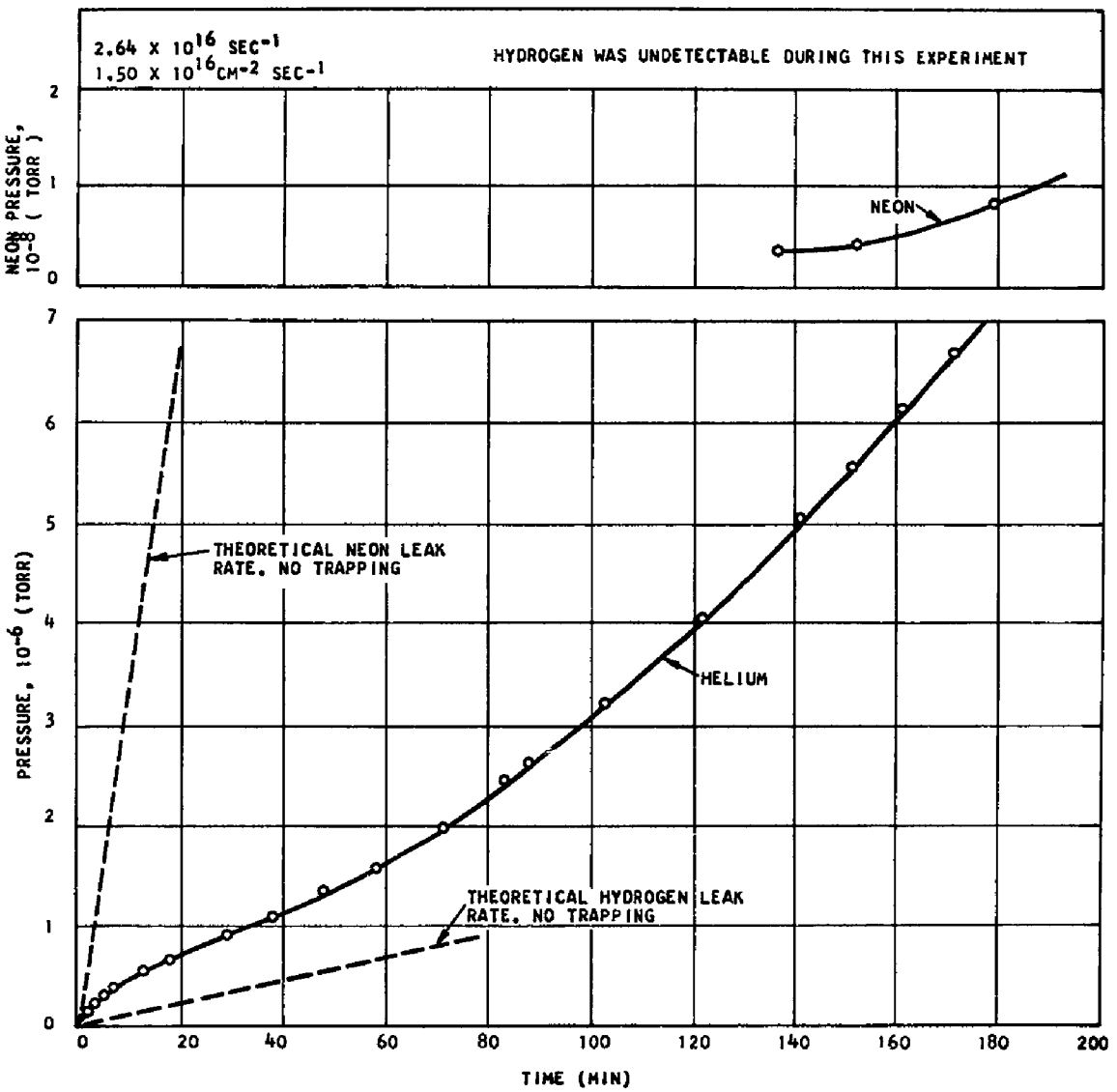

FIG. 24 NEON AND HELIUM PRESSURES DURING CRYOPUMPING OF AIR AT 20°K

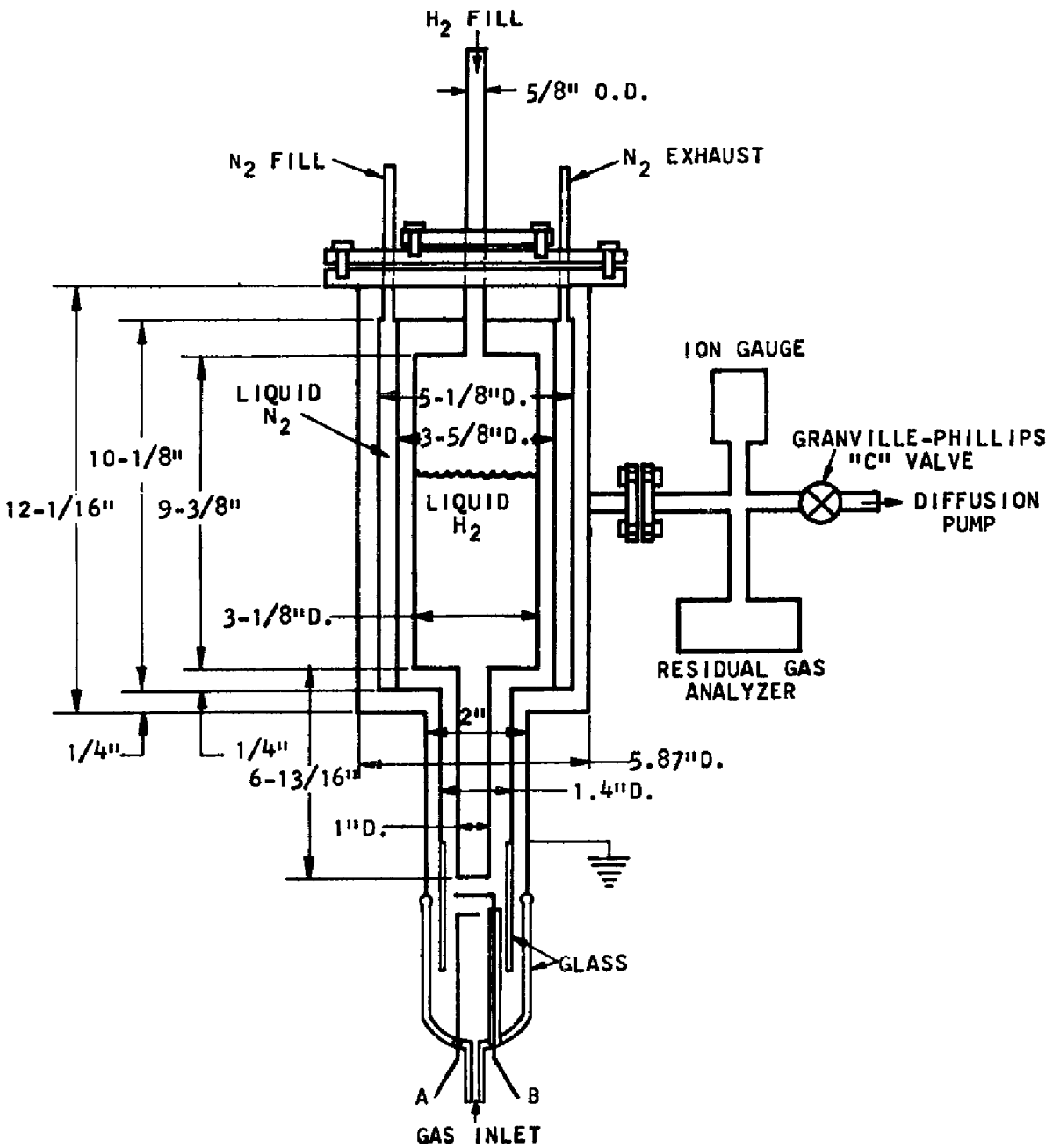

FIG. 25 CRY - ION PUMP

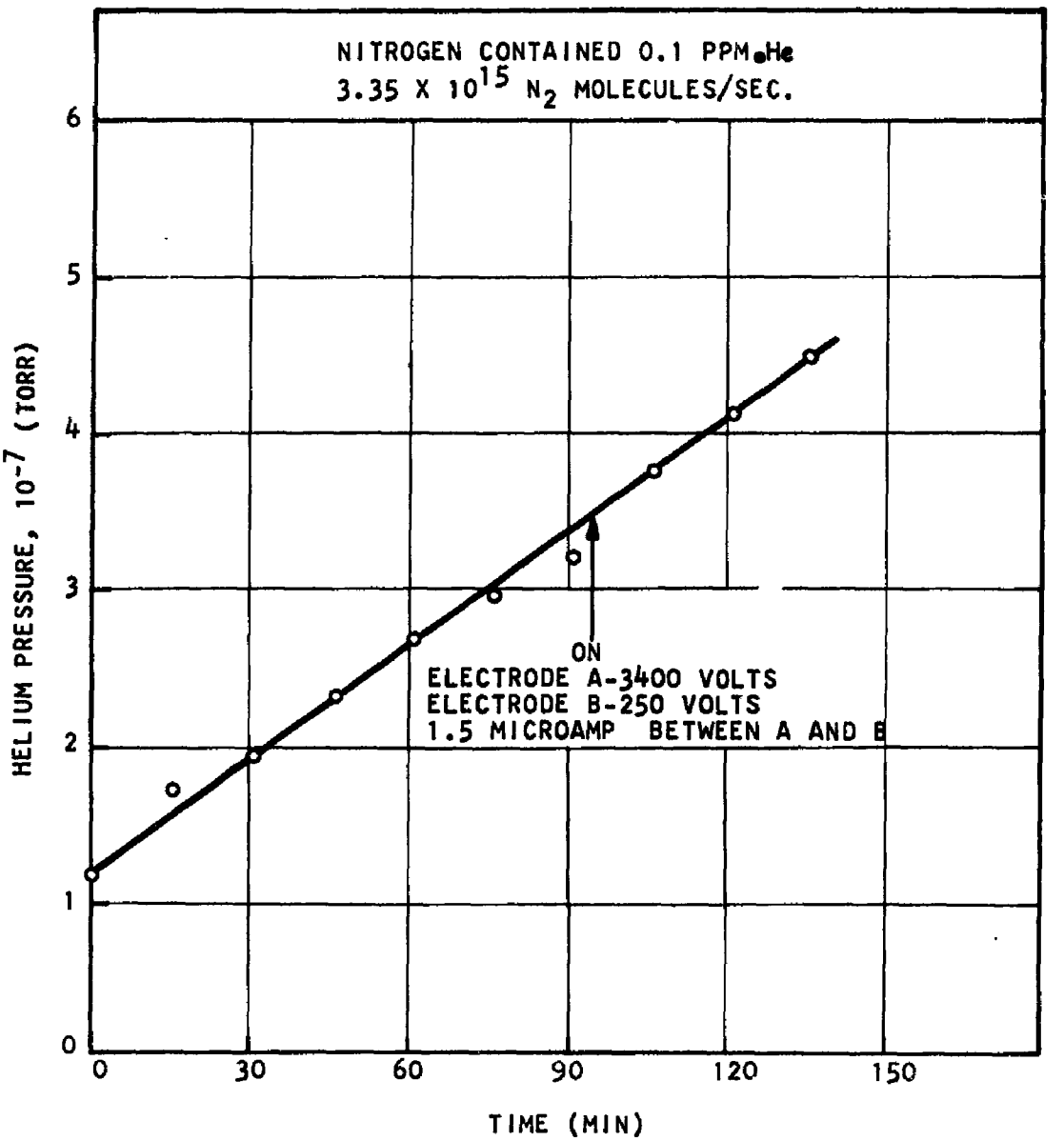

FIG. 26 HELIUM PRESSURE DURING CONDENSATION OF NITROGEN IN THE CRY-ION PUMP

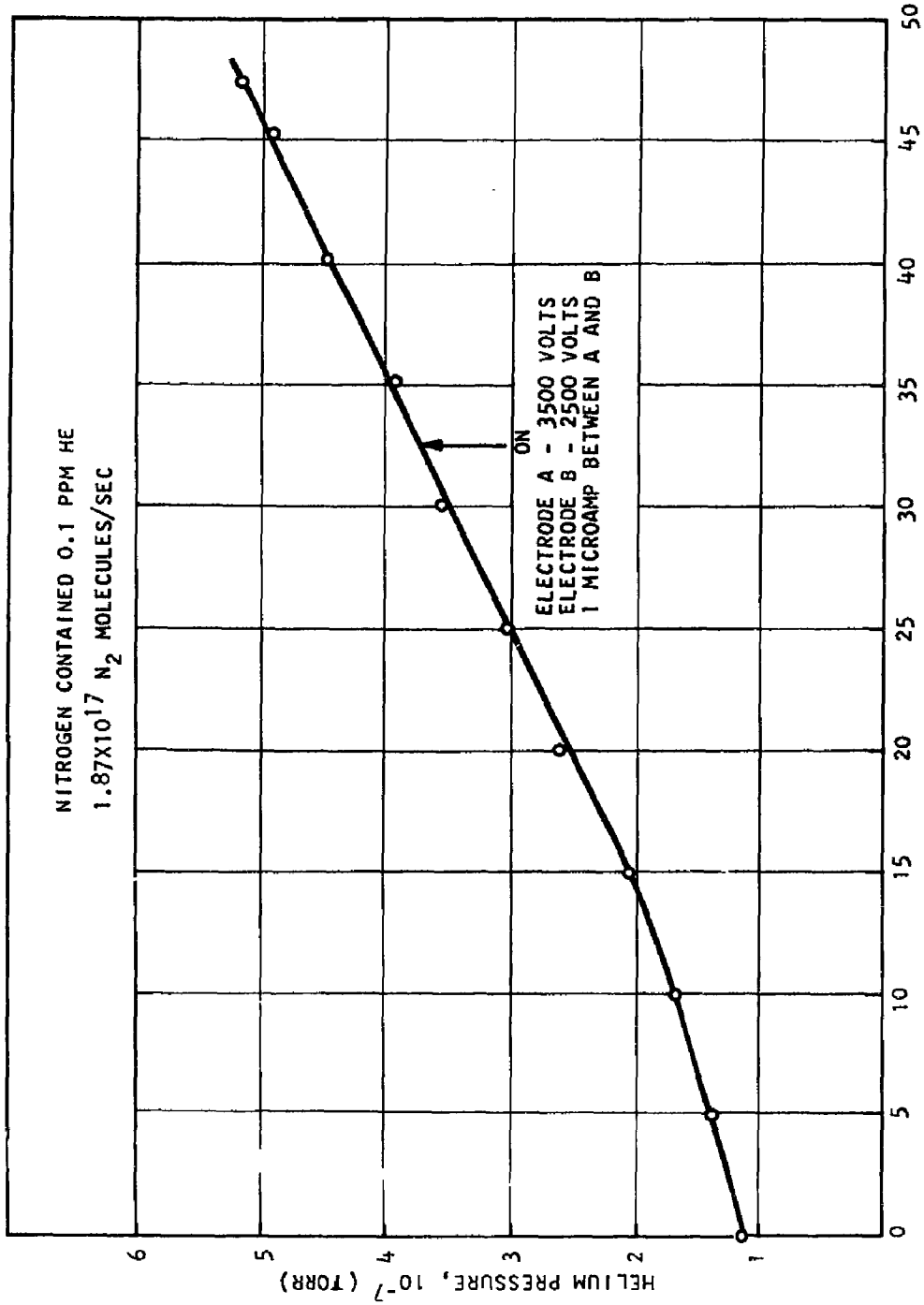

FIG. 27 HELIUM PRESSURE DURING CONDENSATION OF NITROGEN IN THE CRY-ION PUMP

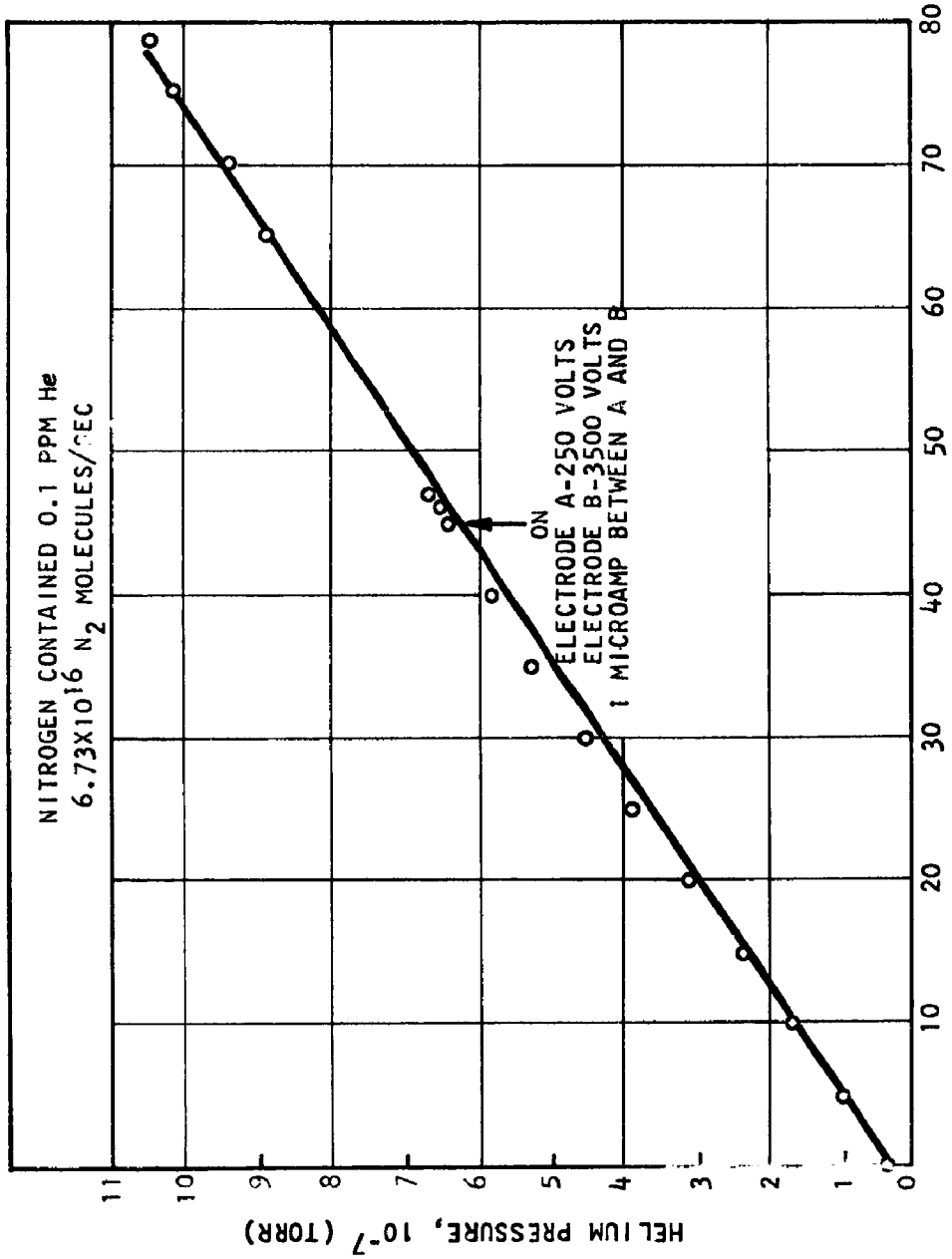

FIG. 28 HELIUM PRESSURE DURING CONDENSATION OF NITROGEN IN THE CRY-ION PUMP

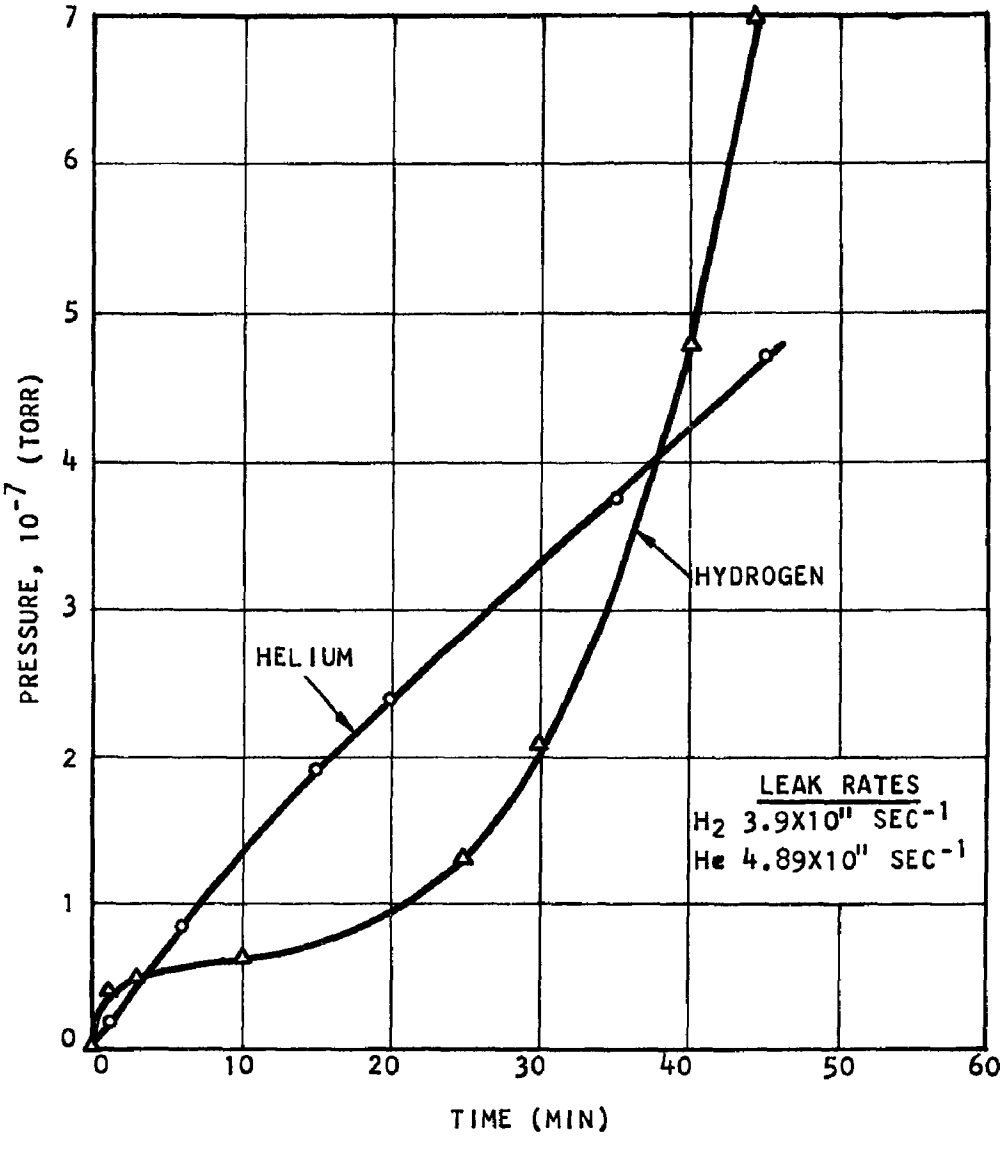

FIG. 29 PARTIAL PRESSURES DURING ADMISSION OF A HYDROGEN-HELIUM MIXTURE TO THE CRY-ION PUMP

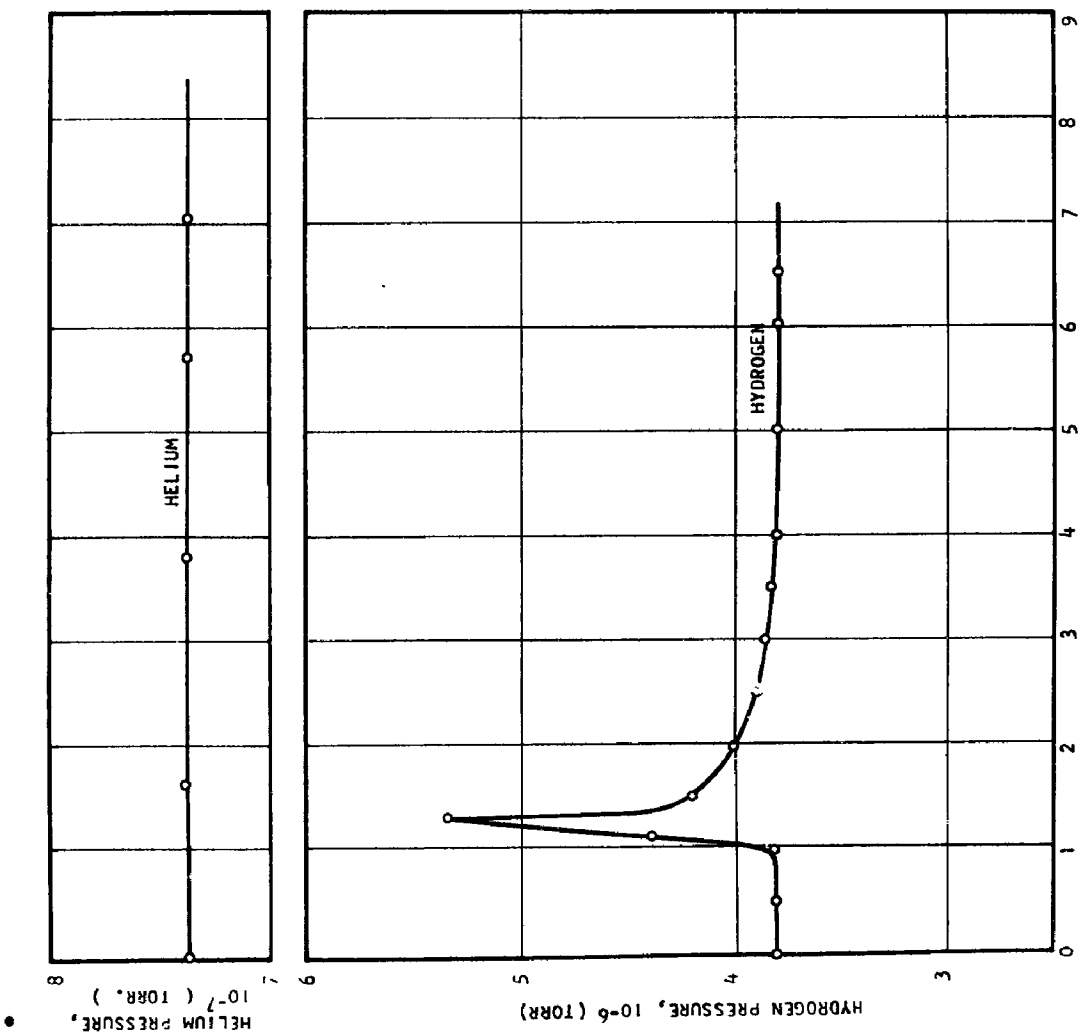

FIG. 30 DESORPTION OF HYDROGEN FROM 20°K WALL OF THE CRY-ION PUMP

AEDC-TDR-63-127

CRYOTRAPPING OF HELIUM AND HYDROGEN BY CONDENSED GASES AT 20°K (PHASE II)

by

R.A. Hemstreet, D.M. Ruttenbur
W.J. Wirth, and J.R. Hamilton

Research Laboratories, Linde Company

a division of Union Carbide Corporation

ABSTRACT

The trapping of hydrogen by nitrogen condensed on a 20°K surface has been studied under conditions where the surface was shielded from ambient temperature radiation. The process is shown to be an inefficient means for hydrogen pumping and is likely to have value only as a bonus in the operation of a large space chamber.

Hydrogen trapping by methane, some simple fluorocarbons, and carbon dioxide condensed on a 20°K surface not shielded from ambient temperature radiation has been studied. CCl_2F_2 and carbon dioxide show rather large capacities for hydrogen and may be useful for the pumping of hydrogen in a space chamber and in special applications.

1.0 INTRODUCTION

Cryotrapping is the phenomenon whereby non-condensable gases are removed from a volume during the normal cryopumping of condensable gases. The process has been used extensively for the stabilization of unstable chemical species in solids at low temperatures (Ref. 1), but Chuan (Ref. 2) first observed the phenomenon in conjunction with the operation of a cryopumping installation and recognized its potential value as a pumping technique. Fite (Ref. 3), using water frozen at 77°K, employed the trapping phenomena to pump oxygen and nitrogen. This work was an outgrowth of studies of the trapping of atomic hydrogen in solid, molecular hydrogen in the neighborhood of 4°K. Wang and co-workers (Ref. 4) have investigated the trapping of oxygen and nitrogen with water and carbon dioxide at 77°K and have determined that the dominant physical process governing the trapping of oxygen and nitrogen is physical adsorption. Nichols (Ref. 5) used the trapping of nitrogen by water, carbon tetrachloride, methanol, ethanol, and acetone at 77°K in the operation of a "cold diffusion pump".

With the exception of Chuan who observed some pumping of non-condensables during the operation of a 20°K cryopump, previous studies have been concerned with the trapping of oxygen and nitrogen in condensed gases at temperatures in the neighborhood of the normal boiling point of liquid oxygen and nitrogen (90-77°K). Nichols (Ref. 5) did not observe any hydrogen or helium trapping at 77°K, but this is not surprising because, if trapping is an adsorption process, it would not be expected to be of much significance at temperatures above the critical temperatures of the trapped (or adsorbed) gases.

Because many large space chambers will use 20°K cryopumping as the principal means of evacuation and maintenance of the necessary high vacuum, there exists the problem of the removal of hydrogen, helium, and to a lesser extent, neon. At 20°K, these gases will not condense to form solids with very low vapor pressures. Thus, in addition to the use of 20°K cryopumping for the removal of oxygen, nitrogen, etc., the cryopumping installation must be backed up with another pumping system for the removal of hydrogen, helium, and neon. The use of diffusion pumps is obvious, but it would be very desirable to use a system which could be integrated with, or be a part of, the cryopumping installation. This report gives the results of a study of the cryotrapping of non-condensables at 20°K. Another project (Ref. 6) is considering the use of conventional adsorption at 20°K for the pumping of non-condensables.

2.0 SUMMARY OF PREVIOUS HELIUM AND HYDROGEN CRYOTRAPPING STUDIES

In the Phase I report the experimental and theoretical studies of helium and hydrogen trapping by solid nitrogen and oxygen at 20°K were given. The experimental results were obtained in an apparatus

where the condensing surface was exposed to thermal radiation from a surface near ambient temperatures. It was assumed in the interpretation of helium and hydrogen trapping that, at the beginning of the formation of solid nitrogen or oxygen on a 20°K surface, the solid forms in a disordered, non-crystalline state. This is due to the low surface mobility of nitrogen and oxygen molecules, which inhibits their migration from their random impact points to the minimum energy lattice sites in the crystalline solid. It was further assumed that, as the solid became thicker with time during continuous condensation, the surface temperature of the solid steadily increased due to the constant heat flux to its surface. This heat flux was due to the thermal radiation on the surface and the heat liberated by gas condensation on the surface, and it was determined that thermal radiation probably was the most important factor in the total heat flux. The final assumption concerning the nature of solid nitrogen and oxygen condensates was that, as the surface temperature increased, the surface mobility of molecules increased, thus making it progressively easier for the surface molecules to migrate to lattice positions in the well ordered crystalline state. There was a continuous transition from a disordered to an ordered form in each succeeding layer of solid nitrogen or oxygen. Coinciding with the transition from a disordered to an ordered state was a decrease in the effective surface area of the condensate.

With these concepts of the structure of nitrogen and oxygen condensates, the general principles of helium and hydrogen trapping as given in the Phase I Report may be summarized.

2.1 HELIUM TRAPPING

Helium trapping is a physical burying process. During the condensation of nitrogen or oxygen, helium atoms impact on the solid surface. When the surface temperature is much higher than the critical temperature of helium, very few helium atoms are adsorbed on the surface. However, the collision time of each atom is not zero but some small but finite value. Trapping was postulated to occur if a helium atom could be buried by condensing nitrogen or oxygen molecules during the collision time of the helium atom with the surface. However, burying is not sufficient to insure the removal of a helium atom from the gas phase. The atom may diffuse through the solid back to the surface. The most effective helium trapping occurs after the solid has started packing in a dense form, some time after the beginning of the condensation when the surface temperature becomes large enough to permit significant surface migration of nitrogen or oxygen molecules.

In addition to the requirement of dense packing to minimize the diffusion of buried helium atoms out of a condensate, there was the requirement that the condensation rate must be large enough to give a reasonable probability that a helium atom will be buried during its collision time with the surface. Both of these requirements led to the conclusion that the helium trapping efficiency (or probability) increased with the nitrogen or oxygen condensation rate.

The experimental results substantiated the theoretical model of helium trapping, but the dependence on the condensation rate of the condensable gases was just the opposite to that desired in the operation of a space chamber. Furthermore, even at very high condensation rates, the helium trapping probability is very low and the process is regarded as being uninteresting for the attainment and maintenance of high vacua.

2.2 HYDROGEN TRAPPING

It was postulated that at 20°K the dominant pumping mechanism is the adsorption of the hydrogen gas by the solid condensate of nitrogen and oxygen. This agrees with the mechanism of nitrogen and oxygen trapping at 77°K given by Wang (Ref. 4). However, the structural properties and changes in nitrogen and oxygen condensates introduce complexities not found in a trapping medium such as water at 77°K. Hydrogen adsorption is dependent on the heat of adsorption and the surface area of the adsorbent (solid nitrogen or oxygen in the present case). During the initial formation of a solid nitrogen or oxygen condensate, the solid is a highly porous or disordered material. Because of this, there is available a large surface area for hydrogen adsorption and almost complete hydrogen trapping occurs. However, the condensate surface temperature increases with its thickness, and a point is reached where the condensate starts forming in a well ordered, crystalline state. This densely packed solid has a much lower surface area than the disordered solid formed initially, so that a decrease in the hydrogen adsorptive capacity occurs rather abruptly. Theoretical calculations indicate that the breakdown in hydrogen pumping occurred at a surface temperature near 23°K, when the principal heat flux to the surface was due to thermal radiation from surfaces at ambient temperatures.

At 20°K, helium and hydrogen trapping take place under opposite conditions. Because hydrogen trapping appears to be most efficient under conditions of low condensate surface temperatures and low condensation rates, it is most likely to find application in high vacuum technology. This report presents the results of hydrogen trapping studies in an apparatus where the condensate was shielded from thermal radiation. In addition, a survey of hydrogen trapping media other than solid oxygen and nitrogen is given.

3.0 APPARATUS

3.1 SHIELDED CRYOPUMP

A diagram of the apparatus is shown in Figure 1. Basically, the cryopump consisted of three concentric sections. The inner part was a copper can for holding liquid hydrogen. A fill tube of stainless steel passed out through the upper flange. The bottom surface of the liquid hydrogen container was flat and highly polished. Gases were condensed on this surface.

Surrounding the liquid hydrogen container was a 77°K radiation shield constructed of copper. The shield was cooled by circulating liquid nitrogen through a copper coil soldered to the outside of this shield. There was a well in the bottom of the 77°K shield where gases were admitted to the apparatus. Gases were admitted through a copper tube which entered the apparatus through the top flange and then passed through the wall of the 77°K shield. The open end of the gas inlet tube was directed towards the bottom of the well in the 77°K shield. Because of the construction of the gas inlet system, gases reaching the 20°K surface were at a temperature very near 77°K and the gas flow was diffuse. This was in contrast to the apparatus described in the Phase I Report where the gas flow was highly directed at the condensing surface and was at a temperature near 273°K or higher. The 20°K condensing surface area of the shielded cryopump was estimated to be 11.1 cm^2.

The low temperature portions of the apparatus were located inside of a stainless steel vacuum jacket. The 20°K and the 77°K sections were suspended from separate flanges which were sealed with indium gaskets.

The pressure measuring instruments used were the Consolidated Electrodynamics Corporation Bakeable Residual Gas Analyzer (Mass Spectrometer), the Consolidated Vacuum Corporation GIC-011 Bayard-Alpert Gauge, and the Consolidated Vacuum Corporation GM-110 McLeod Gauge. The Residual Gas Analyzer was used for all partial pressure measurements and was calibrated against the ion gauge and McLeod gauge as described in the Phase I Report. A schematic diagram of the placement of gauges, valves, diffusion pump, and traps is shown in Figure 2.

Prior to each experiment the apparatus was prepared for use as follows: The Residual Gas Analyzer and ion gauge were baked overnight at 400°C and 300°C, respectively. The valves and connecting lines were not baked. The jacket of the cryopump was heated to 100°C and inner portions of the apparatus were heated to 140°C by forcing hot air through the coils of the 77°K shield. During the mild bake-out period the entire apparatus was pumped with a diffusion pump to 10^{-7} torr. After the bake-out period liquid nitrogen was circulated through the 77°K shield for several hours and then liquid hydrogen was transferred to the central copper can. Following the liquid hydrogen transfer, the valves were closed and the ion gauge indicated pressures of 1-3 x 10^{-9} torr. This pressure could be maintained for periods up to 12 hours without addition of more liquid hydrogen.

After cool-down of the apparatus, experiments were performed by admitting gas mixtures at known rates through a variable leak. The leak rates were determined by the pressure drop in a calibrated gas reservoir.

3.2 UNSHIELDED CRYOPUMP

This was the same apparatus described in the Phase I Report. No modifications or changes were made and its operation was exactly as described previously. This apparatus was used in a survey of hydrogen trapping media which could be more useful than either solid nitrogen or oxygen. Although the apparatus had some deficiencies (a directed gas flow, warm gas impinging on the condensation surface, and the condensation surface exposed to 300°K thermal radiation), it was used in the survey because the results could be directly compared with the nitrogen and oxygen results obtained previously.

4.0 EXPERIMENTAL RESULTS AND INTERPRETATION

4.1 CRYOTRAPPING OF HYDROGEN BY SOLID NITROGEN

The theory of hydrogen trapping by solid oxygen and nitrogen developed in the Phase I Report suggested that hydrogen trapping could be improved if the condensing surfaces were shielded from thermal radiation from surfaces at ambient temperatures. It was the purpose of this work to test this prediction in an apparatus where the 20°K condensing surface was completely shielded by a 77°K shield. The apparatus is described in section 3.0. Nitrogen-hydrogen mixtures were condensed on the 20°K surface and the residual hydrogen pressure was monitored during the condensation. The pressures quoted in this section were the pressures measured at ambient temperatures. No corrections for the thermonuclear effect were made.

The residual hydrogen pressure during the condensation of a nitrogen-hydrogen mixture containing 0.1% hydrogen is shown in Figure 3. The experiment consisted of two parts. In the first part, the condensation was started on the bare 20°K copper surface. With the possible exception of a short period at the beginning of the condensation the pressure rose continuously. The dotted lines on Figure 3 are hydrogen pressures calculated assuming that none of the hydrogen admitted to the apparatus was trapped by the solid nitrogen. These pressures were calculated for assumed apparatus temperatures of 300°K and 20°K. The effective gas temperature was unknown, but the pressures expected in the absence of any trapping should have been between the value calculated using temperatures of 300°K and 20°K. The fact that the measured pressure lay below the calculated values indicated that a small amount of trapping did occur.

Following the first part of the experiment shown on Figure 3, the residual hydrogen was pumped out with the diffusion pump and the condensation of the nitrogen-hydrogen mixture restarted. The results are shown in Part II of Figure 3. In Part II, the pressure rise was slower than in Part I, but the difference was no greater than would be expected on the basis of the difference in condensation rates. Figure 4 is basically a repeat of Part II of Figure 3, but shows that there was no initial period where the hydrogen was strongly pumped, as was observed in the experiments where the condensing surface was unshielded from thermal radiation (Phase I). This directly contradicts the prediction made in Phase I.

Because the pressure curves of Parts I and II of Figure 3 differed only by the condensation rate (and the hydrogen leak rate), it is concluded that the solid nitrogen present before the condensation of a nitrogen-hydrogen mixture had little or no ability to trap hydrogen. The curves of Parts I and II appear to be the results of two independent experiments, each starting with a bare metal condensing surface. Apparently, the hydrogen molecules were unable to penetrate very deeply into the solid nitrogen, and adsorption took place only on or near the surface. Figure 5 gives the results of a series of experiments in which the number of hydrogen molecules trapped in the solid is plotted as a function of the pressure over the solid as the condensation of the nitrogen-hydrogen mixture proceeds. The number of molecules trapped in the solid was obtained by the difference between those admitted to the apparatus and those in the gas phase calculated from the pressure. The results were insensitive to the assumed gas temperature. Because the experiments were performed over a range of condensation rates and ratios of hydrogen-to-nitrogen in the mixture admitted to the apparatus, the fact that the curves of Figure 5 lie so close together can only be explained by assuming that hydrogen adsorption takes place on the surface of the solid nitrogen, and hydrogen does not penetrate into the material below the surface. The only parameter which was constant in the experiments of Figure 5 was the gross surface area of the solid.

Since surface adsorption of hydrogen is the dominant process in hydrogen trapping, the question arises as to whether hydrogen adsorbed on the surface of solid nitrogen is displaced by subsequently condensing nitrogen molecules. This is answered by the experiment shown in Figure 6. This experiment consisted of two parts. In the first, a nitrogen-hydrogen mixture was condensed for a short period of time. The condensation was stopped and the residual pressure allowed to drop near an equilibrium value. The condensation was then continued as shown in Part II, and again the pressure was allowed to drop to an approximately constant value. The pressure drops are shown in Figure 7 and it is apparent that the final equilibrium pressure does not depend on the condensation rate or the amount of nitrogen condensed, but only on the hydrogen-nitrogen ratio in the gas mixture. Since the equilibrium pressures at the ends of Parts I and II of Figures 6 or 7 were the same, it follows that no hydrogen molecules were displaced from the solid nitrogen surface by the second condensation because such a displacement would have been equivalent to increasing the hydrogen-nitrogen ratio in the original gas mixture which would have caused a higher equilibrium pressure at the end of the second condensation.

The theory of hydrogen trapping developed in Phase I viewed a nitrogen condensate forming at 20°K in the absence of strong thermal fluxes to its surface as being an irregular, porous material having very little crystalline structure. This picture is substantiated by Roder (Ref. 7) who concluded that solid nitrogen, formed by condensation of the gas on a very cold surface, may contain from 10 to 30 per cent voids. There are two surfaces that should be considered; the exterior, gross surface of a solid mass of nitrogen which may have a large area if the solid is not highly crystalline, and the interior surface formed by defects or vacancies in the solid. When the surface of such a nitrogen solid is shielded from strong

thermal radiation, so that the solid remains in a disordered condition, and when the hydrogen molecules impinging on this surface have relatively low thermal energies, hydrogen molecules are adsorbed only on the exterior surface of the solid mass. The adsorbed hydrogen molecules are buried by subsequent layers of solid nitrogen and become incorporated into the solid, but a hydrogen molecule impinging on the exterior surface of the mass cannot penetrate into the defects or vacancies within the solid. It was found to be impossible to operate at condensation rates or hydrogen-to-nitrogen ratios low enough such that the rate of surface adsorption equaled the rate of hydrogen admission to the apparatus, i.e. conditions could not be achieved where constant pressure hydrogen pumping resulted. It is estimated that condensation rates much less than 10^{15} $cm^{-2}sec^{-1}$ and/or hydrogen-to-nitrogen ratios much less than 10^{-4} would be required.

To explain the basic differences between shielded and unshielded hydrogen trapping experiments, it is postulated that, when the hydrogen molecules impinging on the solid nitrogen surface have relatively high thermal energies, they may penetrate into the solid. Thus they may be adsorbed on the exterior surface and within the solid mass. This could cause the initial period of complete hydrogen pumping observed when the condensing surface was unshielded (Phase I) and the absence of this period in the shielded experiments. Ordering of the solid nitrogen, caused by an increase in the surface temperature due to thermal radiation, causes an almost complete breakdown of hydrogen pumping because this ordering reduces the exterior surface area available for adsorption and also increases the solid density, making it even more difficult for hydrogen molecules to penetrate the surface.

No matter what conditions are used for hydrogen trapping with solid nitrogen (and oxygen), the phenomenon does not appear to have much practical value for pumping hydrogen in a space chamber, although it may serve as a bonus in normal cryopump operation. Whether the condensing surface is shielded or not, the amount of hydrogen which can be trapped by solid nitrogen or oxygen is small and the trapping rate is low. Furthermore, the process is very sensitive to structural changes in the solid nitrogen or oxygen and it would be difficult to control these effects during the long term operation of a large installation.

4.2 SURVEY OF NEW HYDROGEN TRAPPING MEDIA

The results of section 4.1 show that solid nitrogen is a poor material for trapping hydrogen at 20°K; therefore a survey was made of new substances which might be more efficient than nitrogen for hydrogen trapping. The survey was restricted to materials which are gaseous at ambient temperatures and pressures, and which have freezing points near to or higher than that of nitrogen. The compounds studied were CH_4 (methane), some simple fluorocarbons, and carbon dioxide. The studies were carried out in the unshielded cryopump in order to prevent the gases from freezing in the gas inlet system and to permit a direct comparison with the results obtained in the Phase I Report. In all cases, a mixture of condensable gases and hydrogen was frozen on a 20°K surface and the residual hydrogen pressure monitored during the freezing process.

The experimental results for each trapping medium are discussed separately.

4.2.1 CF_4, Carbon Tetrafluoride (Boiling Point = 145°K, Freezing Point = 89°K)

A carbon tetrafluoride-hydrogen mixture containing 0.17% hydrogen was condensed at two different rates. The residual hydrogen pressures during these condensations are shown in Figures 8 and 9. In each case, the hydrogen pressure rose continuously during the course of the experiment. As in section 4.1, two hydrogen pressures are quoted on Figures 1 and 2, which were calculated assuming that none of the hydrogen admitted to the apparatus was trapped by the solid carbon tetrafluoride. The pressures were calculated for assumed apparatus temperatures of 300°K and 20°K. From Figures 8 and 9, it is seen that, although the hydrogen pressure rose steadily during condensation, a large fraction of the hydrogen admitted to the apparatus was trapped in the solid carbon tetrafluoride. In each experiment, there was an initial period where the hydrogen pressure rose very slowly indicating almost complete trapping. This behavior was similar to that observed with oxygen and nitrogen (Phase I), but, in the case of carbon tetrafluoride, the initial "pumping" period was very short and not as well defined as with oxygen or nitrogen.

The performance of carbon tetrafluoride as a hydrogen trapping medium was not sufficiently different from that of oxygen or nitrogen to be of practical value.

4.2.2 CH_4, Methane (Boiling Point = 111°K, Freezing Point = 89°K)

Figure 10 shows the residual hydrogen pressure during the condensation of a mixture of methane and hydrogen containing 0.15% hydrogen. The hydrogen pressure rose linearly with time and there was no evidence of a delay in the appearance of the hydrogen after condensation was started. The dotted lines show the hydrogen pressures expected in the absence of trapping for apparatus temperatures of 300°K and 20°K., and, because the experimental curve lies between the calculated curves, it was concluded that there was no evidence of hydrogen trapping. As a hydrogen trapping medium, methane is much inferior to oxygen or nitrogen.

4.2.3 $CClF_3$, Ucon 13 or Freon 13 (Boiling Point = 192°K, Freezing Point = 92°K)

A mixture of Ucon 13 and hydrogen containing 0.97% hydrogen was used. The residual hydrogen pressures during the condensation of this mixture are shown on Figures 11 and 12. There is clear evidence of hydrogen trapping, and Ucon 13 appears to be superior to nitrogen, oxygen, carbon tetrafluoride, or methane as a hydrogen trapping medium.

4.2.4 $CHClF_2$, Ucon 22 or Freon 22 (Boiling Point = 233°K, Freezing Point = 113°K)

Mixtures containing 0.1, 1.1, and 1.4% hydrogen were used. The results are shown in Figures 13 and 14 for the 1.4 and 1.1% hydrogen mixtures. Using the 0.1% hydrogen mixture and a condensation rate of 2.44×10^{17} cm^{-2} sec^{-1}, no hydrogen (less than 1×10^{-8} torr) was found at the end of an experiment lasting one hour. The hydrogen pressure curves in Figures 13 and 14 are entirely different from those obtained with oxygen, nitrogen, carbon tetrafluoride, methane, or Ucon 13. There was an initial period where the hydrogen pressure rose rather rapidly (but no faster than with the other trapping media) followed by a reduction in the rate of pressure increase. It appears that the situation was being approached where the hydrogen trapping rate equaled the influx rate, i.e. constant pressure pumping. This was the first evidence of hydrogen trapping which could have practical significance.

4.2.5 CCl_2F_2, Ucon 12 or Freon 12 (Boiling Point = 244°K, Freezing Point = 115°K)

A mixture containing 1.01% hydrogen was used. Figure 15 shows the residual hydrogen pressure during the condensation of this mixture. The experiment was carried out using three different condensation rates. The first part of the experiment was conducted at a very low condensation rate and hydrogen trapping is evident in view of the approach to constant pressure pumping. However, accumulated evidence indicated that at very low leak rates there was an enrichment of hydrogen on passing the gas mixture through the variable leak controlling the gas flow into the apparatus. This caused the actual hydrogen - Ucon 12 ratio introduced into the apparatus to be higher than expected. Therefore, the condensation rate (and leak rate) was increased. A pressure drop occurred and a period of constant pressure pumping resulted.

In the third part of the experiment shown in Figure 15, the condensation rate was increased again and the hydrogen pressure rose sharply, probably due to strong heating of the condensate surface. At the end of the experiment, based on the total amount of gas admitted, the hydrogen pressure calculated assuming no trapping was between 0.13 and 2 torr. The measured pressure was 2 to 5×10^{-4} torr.

During the course of the experiment shown in Figure 15 occassional pressure pulses were observed. They were of short duration and are indicated by numbered arrows on Figure 15, Figures 16 and 17 show these pulses in detail.

4.2.6 Carbon Dioxide (Melting Point 216°K at 5.2 atm)

Figure 18 shows the hydrogen pressure during the condensation of a mixture of carbon dioxide and 1.04% hydrogen. It is seen that pressures less than 10^{-6} torr were maintained during the course of the experiment. The condensation rate decreased during the experiment due to a reduction in the pressure in the reservoir holding the gas mixture. As the

condensation rate decreased, the residual hydrogen pressure diminished. A further decrease in the hydrogen pressure after termination of the condensation rate is shown in Figure 19. At equilibrium, there were 0.123 cm^3 (STP) of hydrogen trapped per gram of carbon dioxide. During the condensation of the carbon dioxide-hydrogen mixture, the hydrogen pumping speed was 499 micron liters in^{-2} min^* at a carbon dioxide condensation rate of 4.40×10^{18} cm^{-2} sec^{-1}.

Figure 20 shows that the hydrogen pressure during a continuous condensation was a linear function of the condensation rate and suggests that even lower pressures could be maintained at lower condensation rates. Figure 21 demonstrates that this was the case. The hydrogen pressure was reduced about one order of magnitude with a corresponding reduction in the carbon dioxide condensation rate. Figure 22 shows the pressure drop following termination of the condensation of Figure 21.

Figure 23 shows the hydrogen pressure during the condensation of a mixture of carbon dioxide and 5.39% hydrogen. An attempt was made to hold the condensation rate constant by manual adjustment of the variable leak controlling the gas flow. The pressure remained constant at about 2.3×10^{-5} torr at a condensation rate of about 7×10^{16} cm^{-2} sec^{-1}.

4.2.7 Summary

Carbon dioxide must be regarded as the best hydrogen trapping medium studied in this program. None of the substances trapped helium at condensation rates less than 10^{18} cm^{-2} sec^{-1}. Table 1 lists the hydrogen trapping media studied and orders the materials qualitatively according to their usefulness for hydrogen trapping at 20°K when the condensing surface is not shielded from ambient temperature radiation.

With the single exception of methane, the ability of these gases to trap hydrogen was directly related to their melting point (or triple points). However, methane has a specific heat anomaly near 20°K which may be due to the onset of free rotation of the molecules in the solid. This could cause the solid to show very little adsorptive capacity for hydrogen.

There are two possible explanations for the dependence shown in Table I. The trapping theory developed in Phase I stated that it is important that the condensable gas form a highly porous solid, with a large surface area, so that significant amounts of hydrogen can be adsorbed. As the solid thickness increases, the surface temperature rises and ordering occurs causing a reduction in the surface area for adsorption and a consequent reduction in the hydrogen trapping rates. It would be expected that this type of process would be most important for solids of low melting points. However,

---

* The condensation rates are given in units of cm^{-2} sec^{-1} because this corresponds with the data. The pumping rates are given in units of in^{-2} min^{-1} to facilitate use in possible engineering applications.

in the case of solids having high melting points, it would be quite difficult for the solid surface temperature to rise high enough for the molecules to have sufficient surface mobility to form a densely packed solid. These materials would be expected to continuously form a porous or high surface area condensate and to be relatively insensitive to changes in the surface temperature. The occurrence of constant pressure hydrogen pumping indicates the continuous formation of disordered solid and, as one moves up the melting point scale of Table 1, the first trace of this phenomenon is encountered with Ucon 22. True constant pressure hydrogen pumping is found with Ucon 12 and is well established with carbon dioxide. Using the relative ordering of the melting point scale, it is interesting to note that Ucon 12, being the first to exhibit true constant pressure pumping, also demonstrated hydrogen pressure pulses during its condensation with hydrogen. The structure of the solid Ucon 12 surface is believed to be unstable and frequent ordering of the solid near the surface occurs during the condensation. The surface temperature builds up to the point where ordering can occur and a highly crystalline or densely packed state results and some adsorbed hydrogen is ejected. Because the dense state has a higher thermal conductivity than the porous state, the surface temperature drops and the process repeats itself. This phenomenon was observed by Hemstreet and Hamilton (Ref. 8) in the case of nitrogen condensing on a 4°K surface and Brackmann and Fite (Ref. 9) with hydrogen at 4°K.

In the case of carbon dioxide, ordering probably had no influence because the surface temperature never became high enough for the molecules to have sufficient mobility to migrate to the lattice positions of the well ordered solid. In this case, the differential equation governing the hydrogen pressure P over the condensate is:

$$\frac{dP}{dt} = aR - bP \qquad (1)$$

where a and b are constants and R is the hydrogen influx rate. bP is the trapping or surface adsorption rate which is of the same form as Henry's Law. A constant pressure is obtained when aR = bP; the influx rate equals the adsorption rate. In the case of Ucon 22, a truly constant hydrogen pressure was not obtained. This may be because this substance was subject to a slow but progressive surface ordering which caused the term b in equation 1 to have a time dependence, i.e. decrease with time.

Table 2 compares the hydrogen adsorptive capacities of some conventional adsorbents with solid carbon dioxide. Solid carbon dioxide has a much lower capacity for hydrogen than charcoal or Molecular Sieve 5A, but it does have a fairly high pumping rate on a unit area basis. Since solid carbon dioxide pumps hydrogen as a true adsorbent, it may be of value because it is one adsorbent which does not have to be activated before use. It could be sprayed onto a 20°K surface as needed. Probably it could be applied to the same panels used for cryopumping oxygen and nitrogen.

There is one problem which could arise in the use of a substance like carbon dioxide for hydrogen pumping. Most likely, the 20°K condensing surface will be surrounded by 77°K - 100°K radiation shields or

baffles. The carbon dioxide would have to be passed through these shields at a rate such that its pressure is less than the vapor pressure of the solid at the shield temperature. Otherwise the carbon dioxide would condense on the shield. The evaporation rate of a solid in equilibrium with its vapor is:

$$f = 3.513 \times 10^{22} \frac{P}{(MT)^{1/2}} \text{ cm}^{-2} \text{ sec}^{-1} \qquad (2)$$

where P is the pressure in torr, M the molecular weight, and T the absolute temperature. If carbon dioxide is to be passed through a 77°K shield, the collision frequency of the molecules with this shield would have to be less than 1.2×10^{13} cm^{-2} sec^{-1} from equation 2. If the shield temperature is 100°K, the rate is of the order of 10^{17} cm^{-2} sec^{-1}. It would be possible to inject carbon dioxide warm onto a 20°K surface and this might not greatly increase the 20°K refrigeration requirement if the amount of hydrogen to be pumped is small.

5.0 CONCLUSIONS

The results of this study indicate that hydrogen trapping by solid oxygen or nitrogen is not likely to be of value for pumping hydrogen in a large space chamber.

Solidified gases with relatively high melting points such as Ucon 12 and carbon dioxide have rather large capacities for hydrogen and may find applications for pumping hydrogen in a space chamber or in special applications. One such application could be the pumping of gases from propulsion devices operated in a vacuum chamber.

REFERENCES

1. Bass, A. M. and Broida, H. P., Formation and Trapping of Free Radicals, Academic Press, New Yor, 1960.

2. Chuan, R. L., Research on Rarefied Gas Dynamics, University of Southern California Engineering Center, Report No. 56-101, November 1960.

3. Brackmann, R. T. and Fite, W. L., J. Chem. Phys. 34, 1572 (1961).

4. Wang, E. S. J. and Collins, J. A., General Cryopumping Study, AEDC-TN-61-114, October 1961. Haygood, J. D. and Wang, E. S. J., The Trapping Effect in Cryopumping, AEDC-TDR-62-133, August 1962.

5. Nichols, J. E., Trapping and Sorption of Noncondensable Gases in the Cold Diffusion Pump, AEDC-TDR-62-124, August 1962.

6. Stern, S. A., Mullhaupt, J. T., DiPaolo, F.S. and Marasco, L., The Cryosorption Pumping of Hydrogen and Helium at 20°K, AEDC-TDR-62-200, October 1962.

7. Roder, H. M., Cryogenics 2, 302 (1962).

8. Hemstreet, R. A. and Hamilton, J. R., J. Chem. Phys. 34, 948 (1961).

9. Brackmann, R. T. and Fite, W. L., Atomic Beam Studies on the Formation of Free Radical Solids, Fourth International Symposium on Free Radical Stabilization, Washington, D.C., August 31 - September 2, 1959.

TABLE 1

Relative Hydrogen Trapping Efficiencies
of Various Solidified Gases at 20°K

	Substance	Melting Point, °K
1.[a]	Carbon Dioxide	216 at 5.2 atm
2.	Ucon 12	115
3.	Ucon 22	113
4.	Ucon 13	92
5.	Carbon Tetrafluoride	89
6.	Nitrogen	63
7.	Oxygen	54
8.[b]	Methane	89

---

a. Best trapping medium

b. Least effective trapping medium

TABLE 2

Hydrogen Adsorptive Capacities of Charcoal, Molecular Sieve 5A, and Solid Carbon Dioxide at 20°K

Adsorbent	Pressure, Torr.	Equilibrium Capacity for Hydrogen
Coconut Charcoal[a]	7×10^{-7}	160 cm^3(STP)/gm
Molecular Sieve 5A[a]	7×10^{-7}	70 cm^3(STP)/gm
Solid Carbon Dioxide	7×10^{-7}	0.123 cm^3(STP)/gm[b]

a. Data taken from Reference 6.

b. Based on data of Figure 19 assuming uniform distribution of the hydrogen throughout the solid.

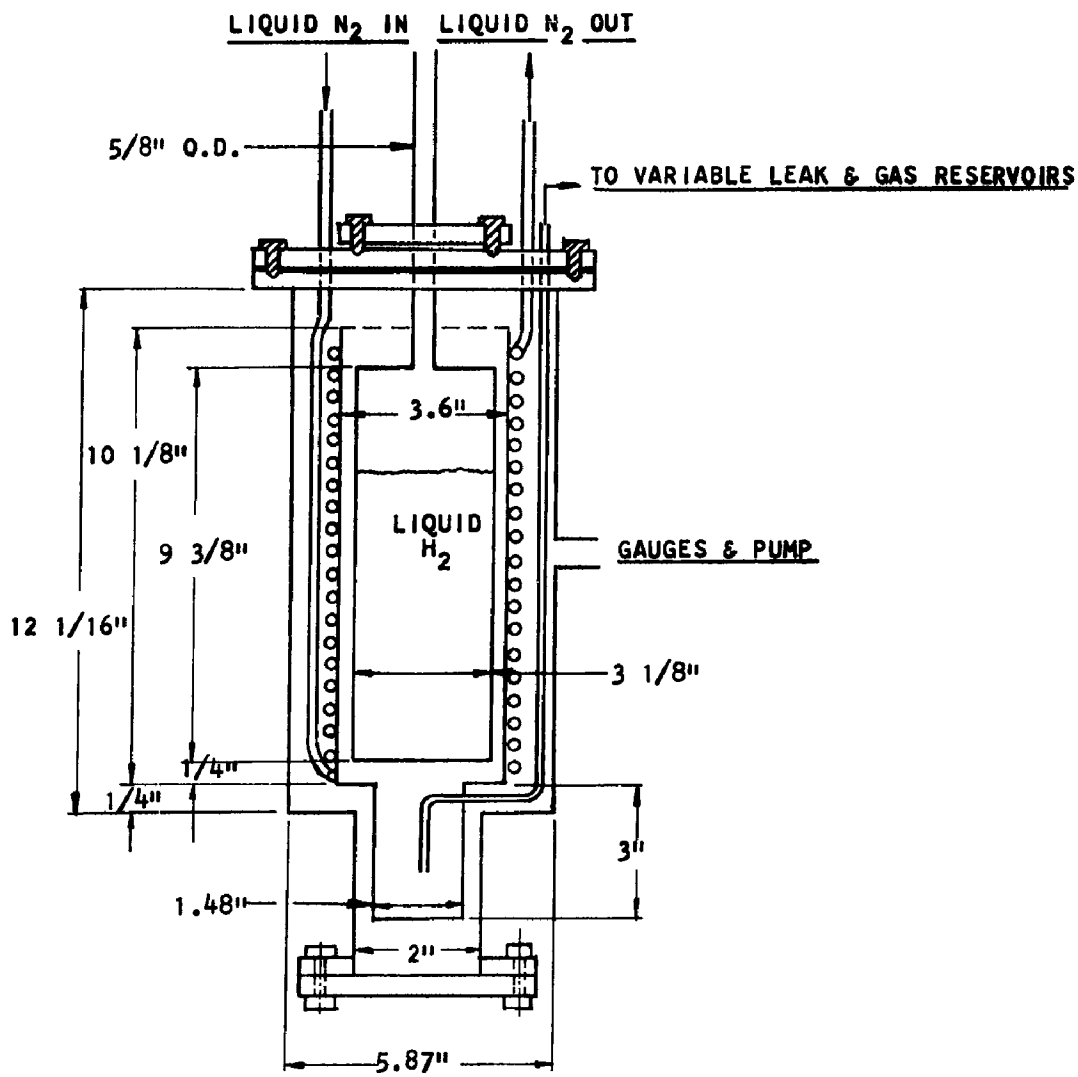

Figure 1 - Cryopump Diagram

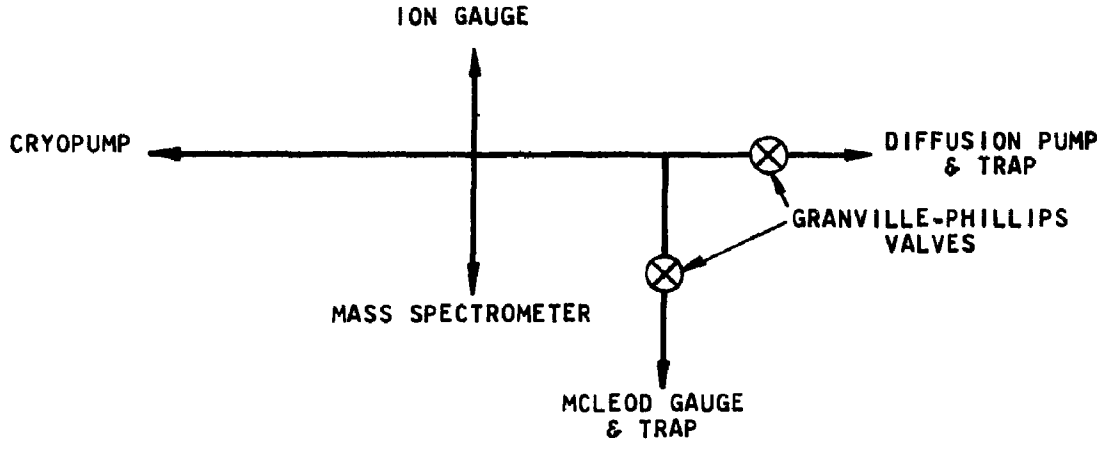

Figure 2 - Layout of Pressure Gauges, Valves, and Diffusion Pump

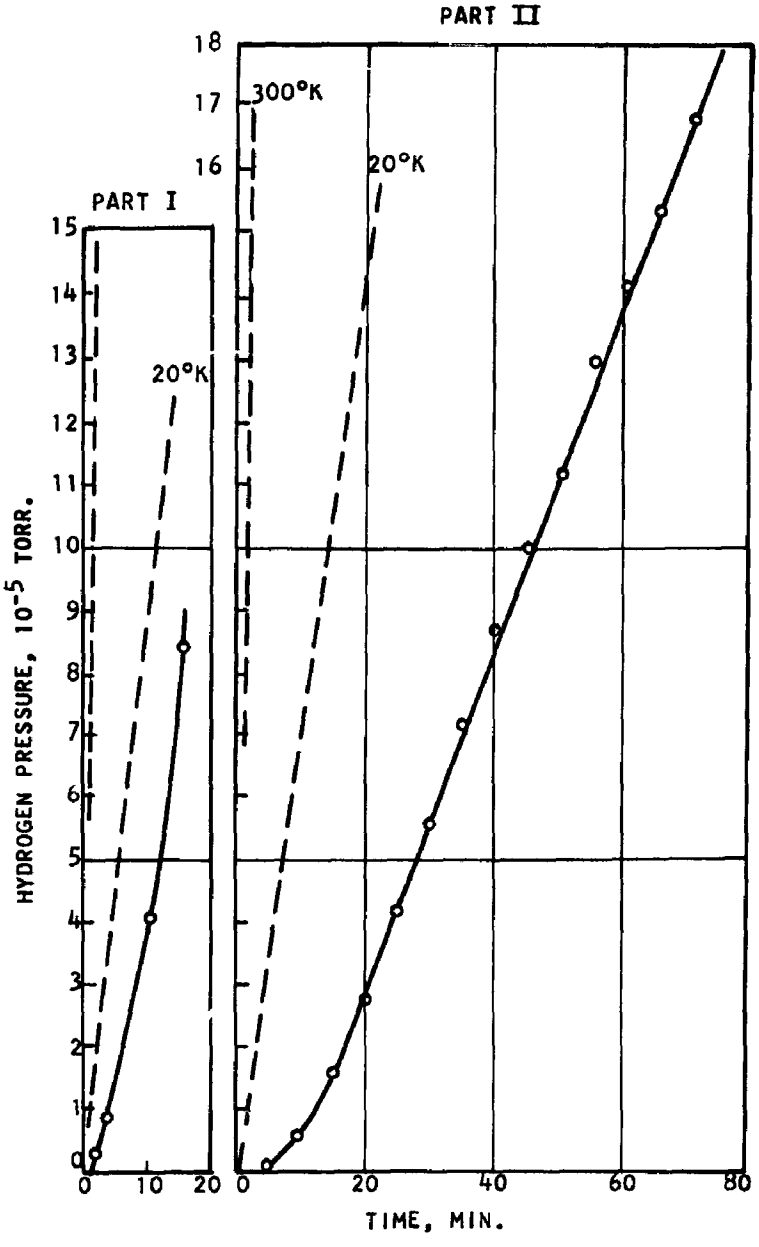

Figure 3 - Hydrogen Pressure During Condensation of Nitrogen Containing 0.1% Hydrogen. The Dotted Lines are Calculated Pressures Assuming No Trapping. Condensation Rates: Part I - $3.02 \times 10^{15} cm^{-2} sec^{-1}$, Part II - $2.56 \times 10^{15} cm^{-2} sec^{-1}$.

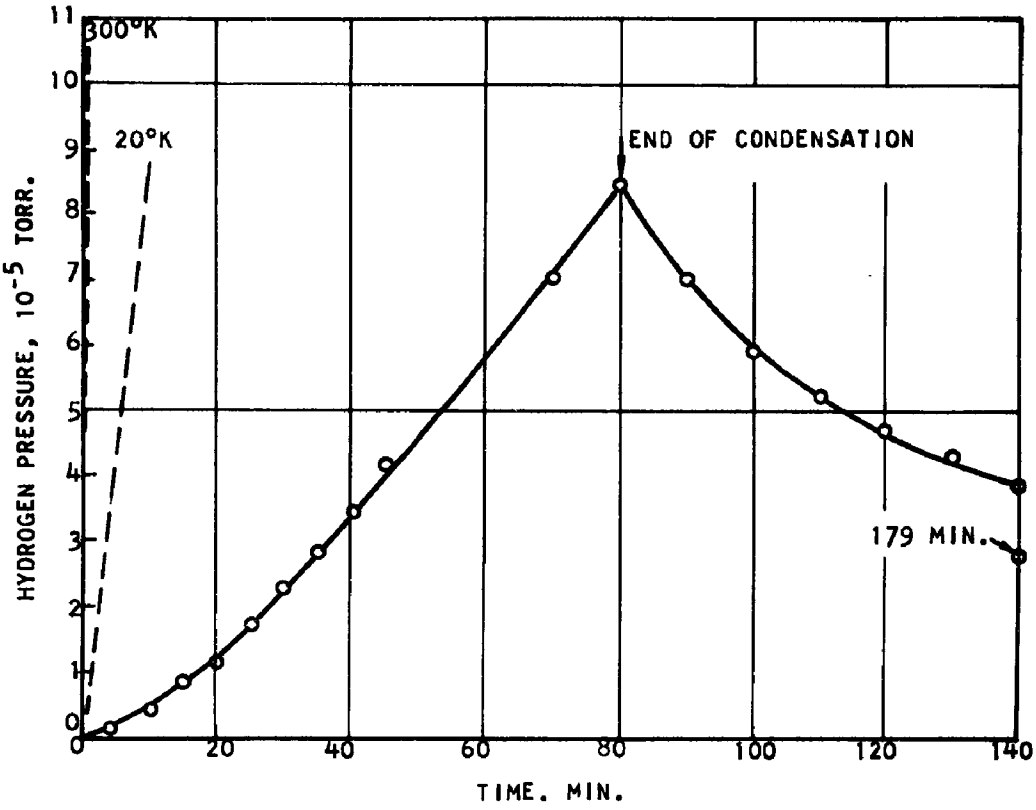

Figure 4 - Hydrogen Pressure During Condensation of Nitrogen Containing 0.103% Hydrogen. 1.67×10^{21} Molecules of Pure Nitrogen Condensed Before Admission of N_2-H_2 Mixture. Condensation Rate of the N_2-H_2 Mixture = $2.55 \times 10^{15} cm^{-2} sec^{-1}$. The Dotted Lines are Calculated Pressures Assuming No Trapping.

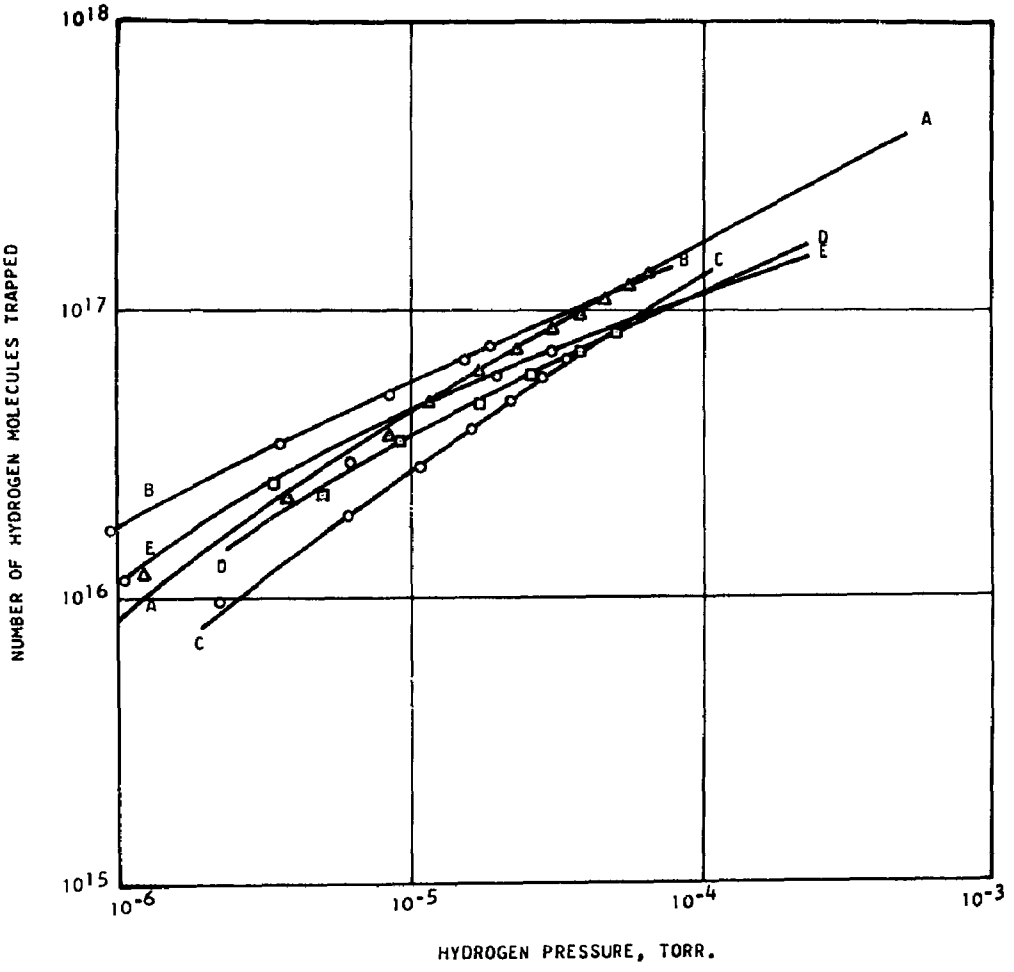

Fig. 5 Residual Hydrogen Pressure as a Function of the Number of Trapped Hydrogen Molecules.

	Percent Hydrogen in H_2-N_2 Mixtures	Condensation Rate
A.	0.103	$1.96 \times 10^{16} cm^{-2} sec^{-1}$
B.	0.019	$1.48 \times 10^{17} cm^{-2} sec^{-1}$
C.	0.019	$8.44 \times 10^{16} cm^{-2} sec^{-1}$
D.	0.103	$1.93 \times 10^{16} cm^{-2} sec^{-1}$
E.	0.019	$2.57 \times 10^{17} cm^{-2} sec^{-1}$

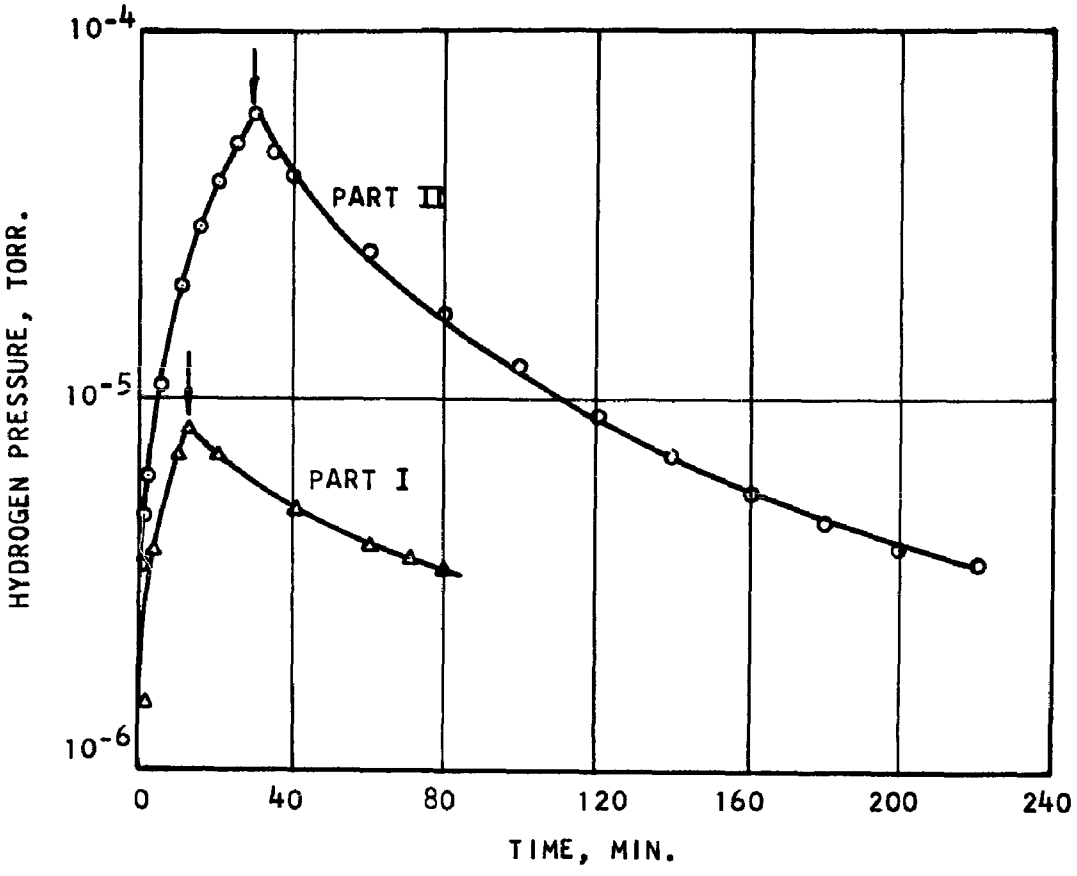

Figure 6 - Hydrogen Pressure During Condensation of Nitrogen Containing 0.001% Hydrogen. The Arrows Indicate Termination of the Condensation. Condensation Rates: Part I - $5.03 \times 10^{16} cm^{-2} sec^{-1}$, Part II - $1.13 \times 10^{18} cm^{-2} sec^{-1}$.

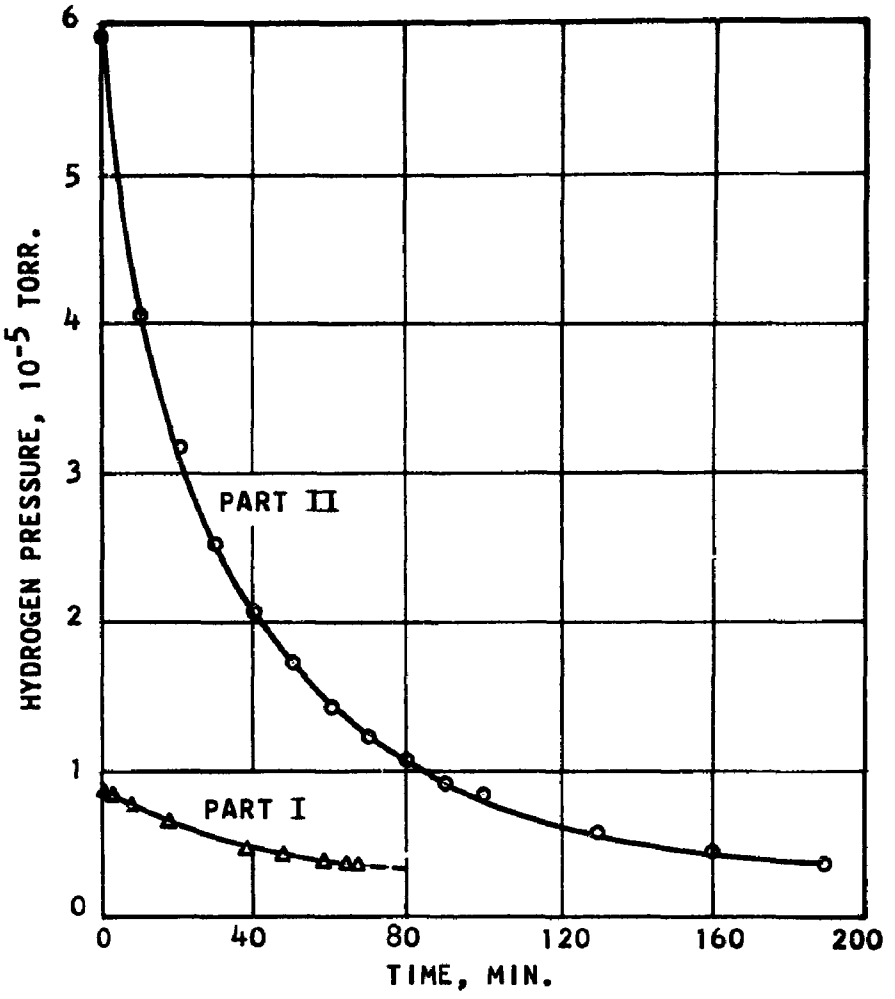

Figure 7 - Hydrogen Pressure After Termination of Nitrogen Condensations. See Figure 6.

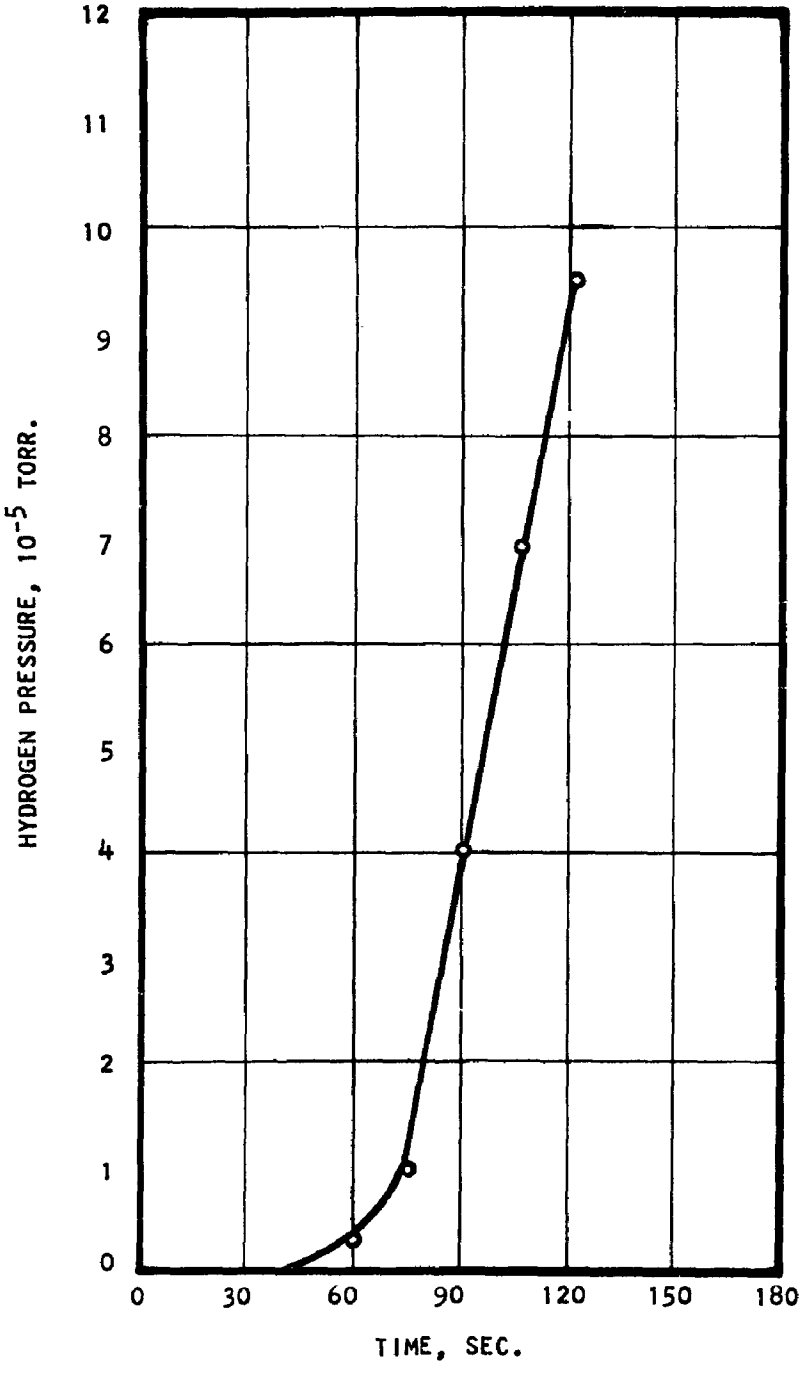

Figure 8 - Hydrogen Pressure During Condensation of CF_4 Containing 0.17% Hydrogen. Condensation Rate = $9.26 \times 10^{17} cm^{-2} sec^{-1}$. Assuming No Trapping, Pressures at the End of the Experiment were Calculated to be 1.01×10^{-2} Torr. (300°K) or 6.71×10^{-4} Torr. (20°K).

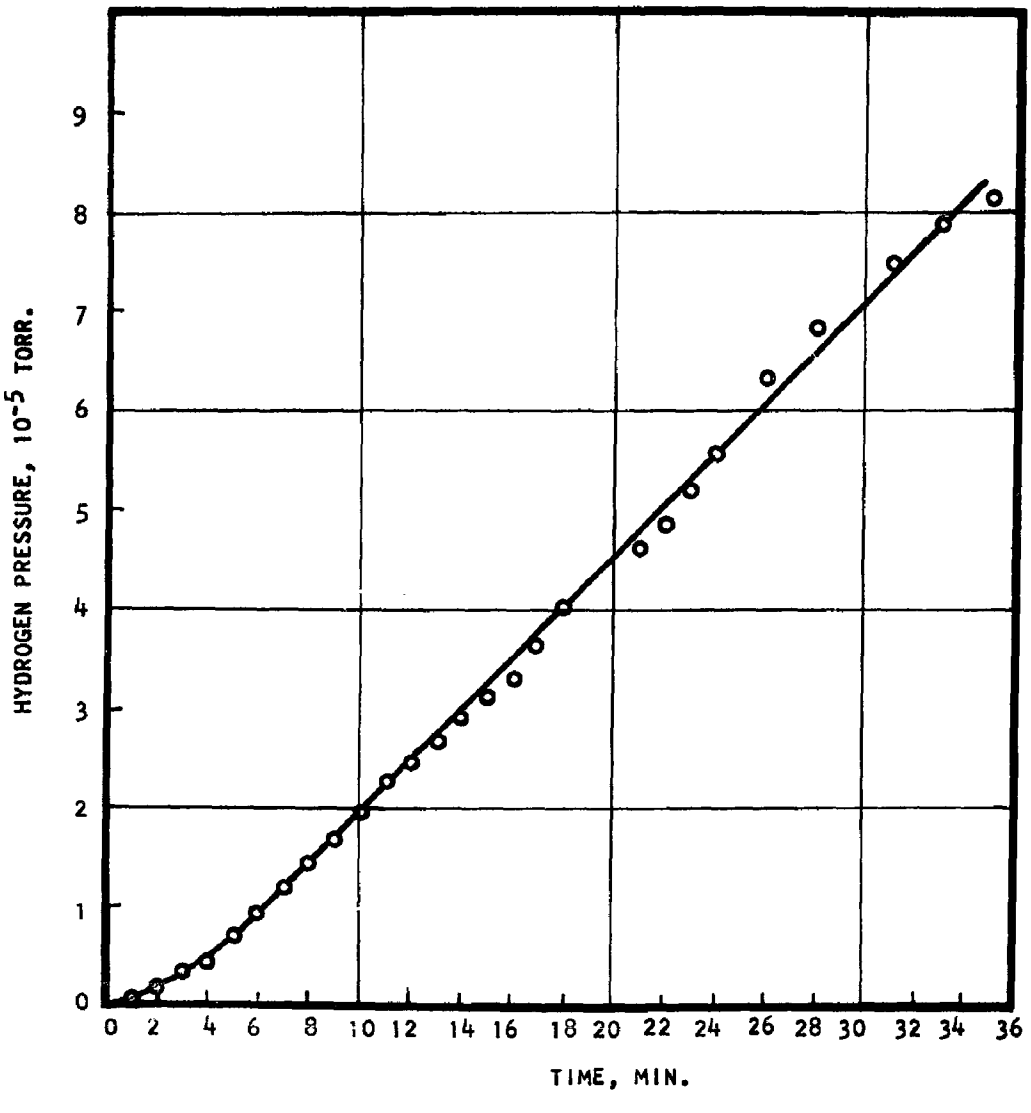

Figure 9 - Hydrogen Pressure During Condensation of CF_4 Containing 0.17% Hydrogen. Condensation Rate = $6.5 \times 10^{16} cm^{-2} sec^{-1}$. Assuming No Trapping, Pressures at the End of the Experiment were Calculated to be 7.5×10^{-3} Torr. (300°K) or 5.03×10^{-4} Torr. (20°K).

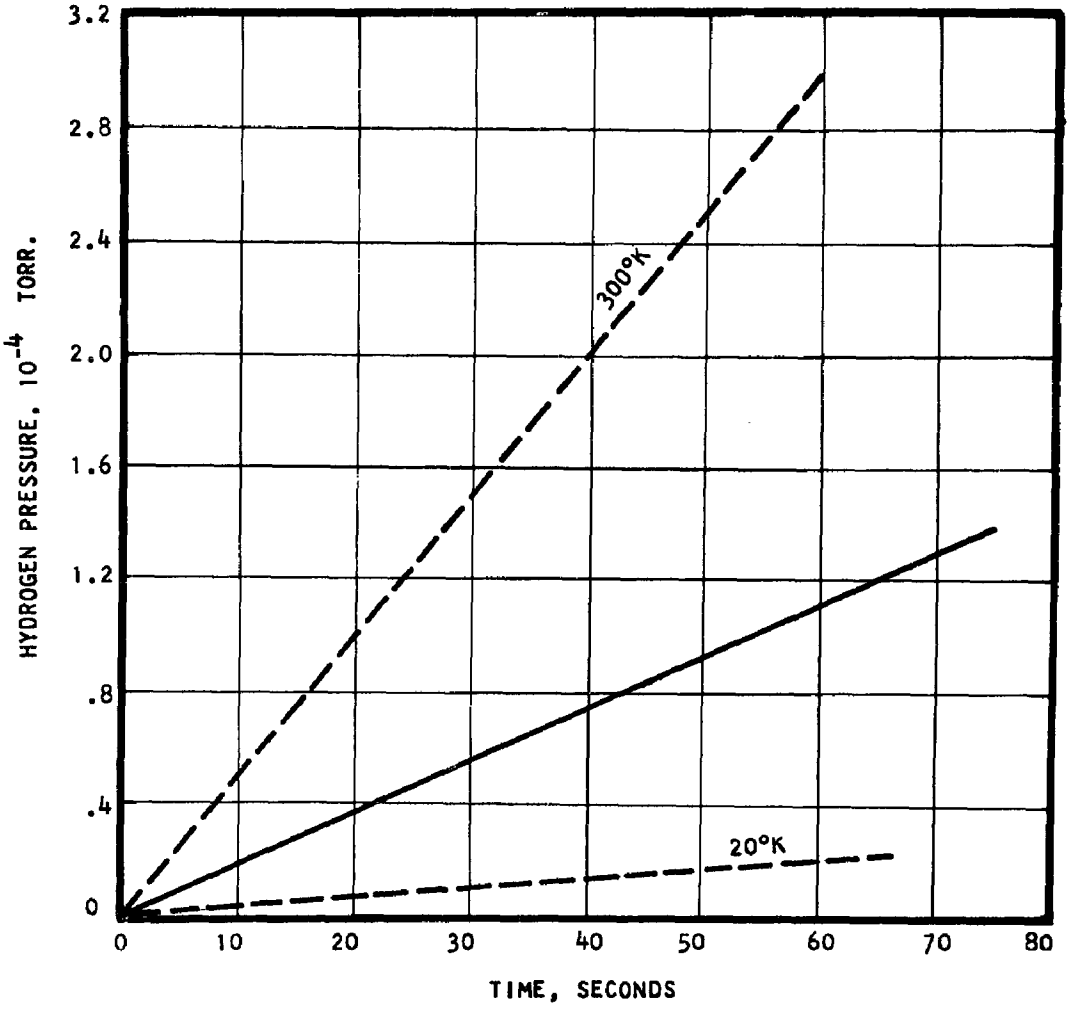

Figure 10 - Hydrogen Pressure During Condensation of CH_4 Containing 0.15% Hydrogen. Condensation Rate = $1.11 \times 10^{17} cm^{-2} sec^{-1}$. The Dotted Lines are Calculated Pressures Assuming No Trapping.

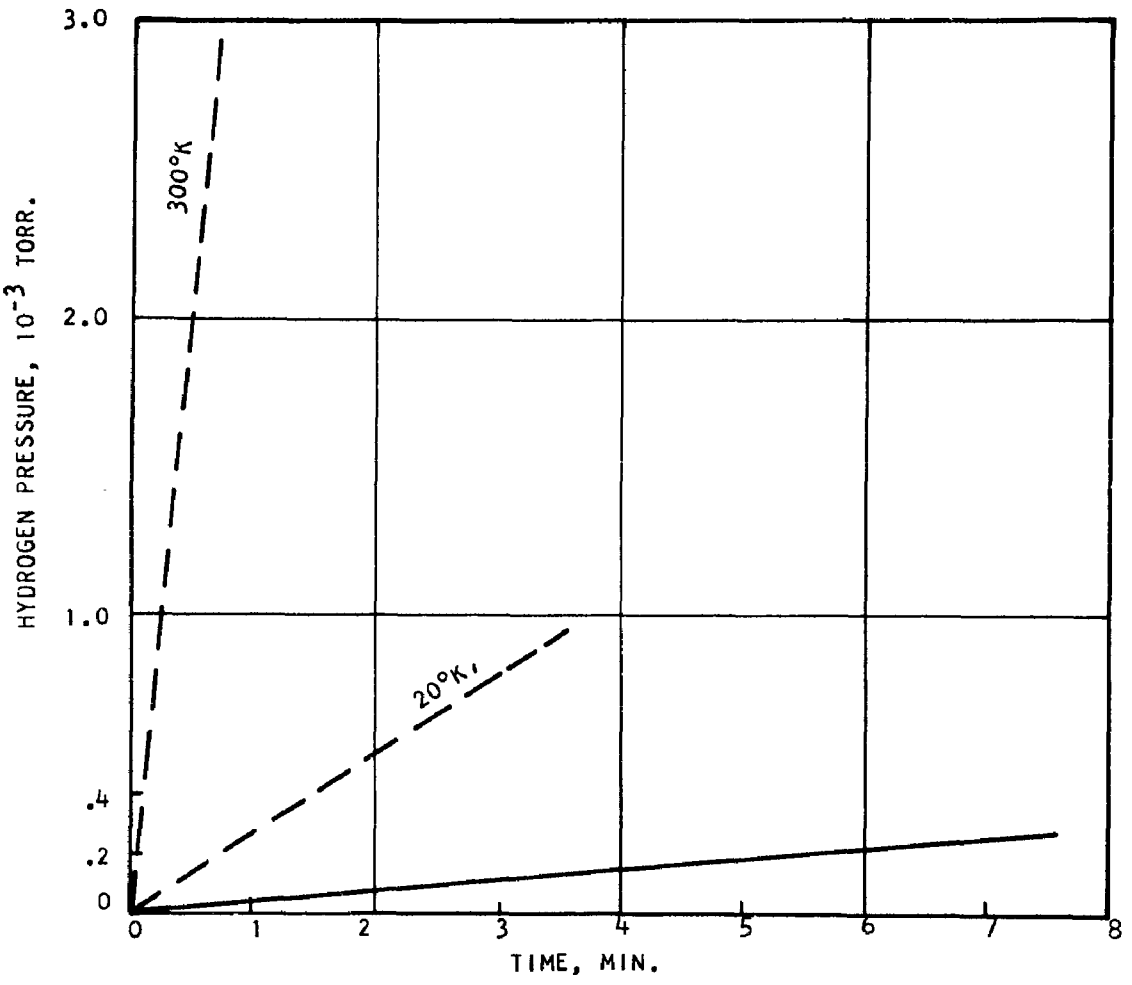

Fig. 11 Hydrogen Pressure During Condensation of C ClF_3 Containing 0.97% Hydrogen. Condensation Rate = 2.29×10^{17} $cm^{-2}sec^{-1}$. The Dotted Lines are Calculated Pressures Assuming No Trapping.

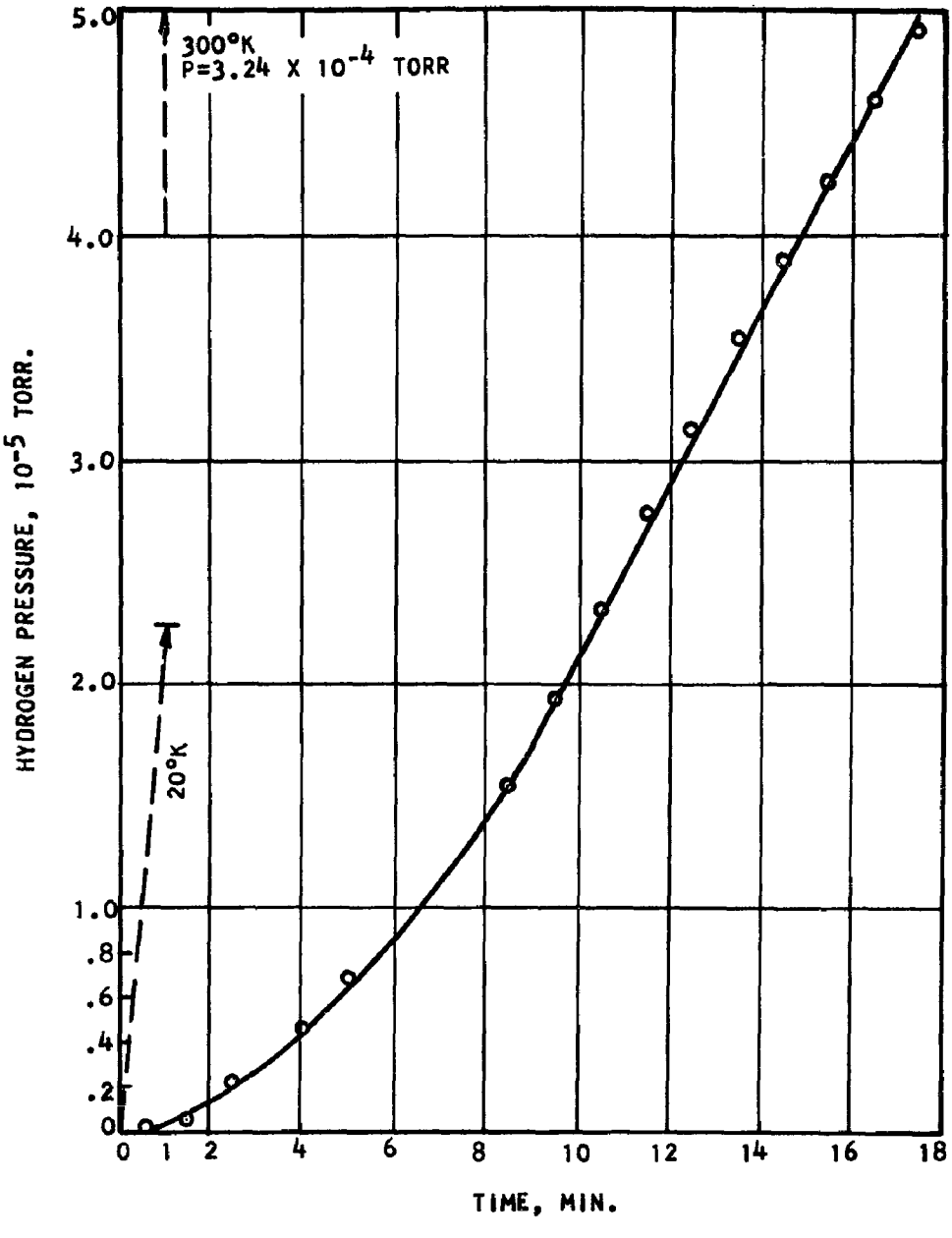

Fig. 12 Hydrogen Pressure During Condensation of $CClF_3$ Containing 0.97% Hydrogen. Condensation Rate = 1.99×10^{16} $cm^{-2}sec^{-1}$. The Dotted Lines Indicate the Hydrogen Pressures After One Minute Calculated Assuming No Trapping.

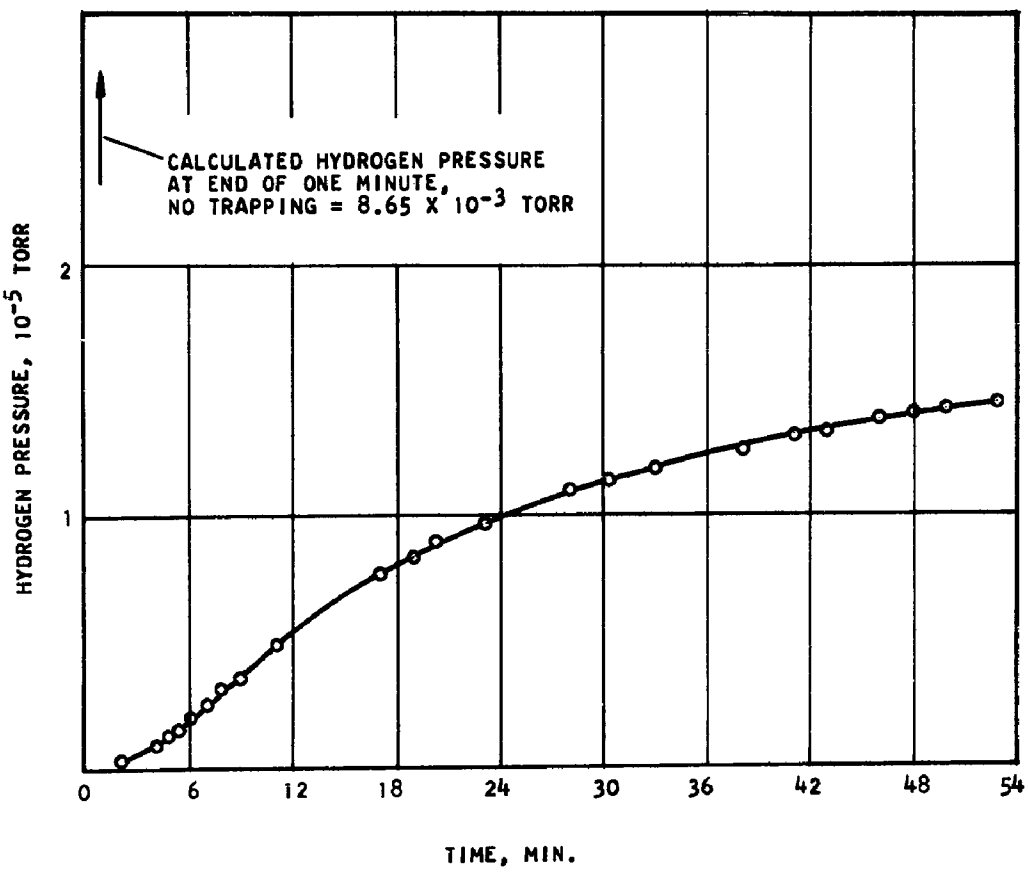

Figure 13 - Hydrogen Pressure During Condensation of $CHClF_2$ Containing 1.4% Hydrogen. Condensation Rate = $3.3 \times 10^{16} cm^{-2} sec^{-1}$.

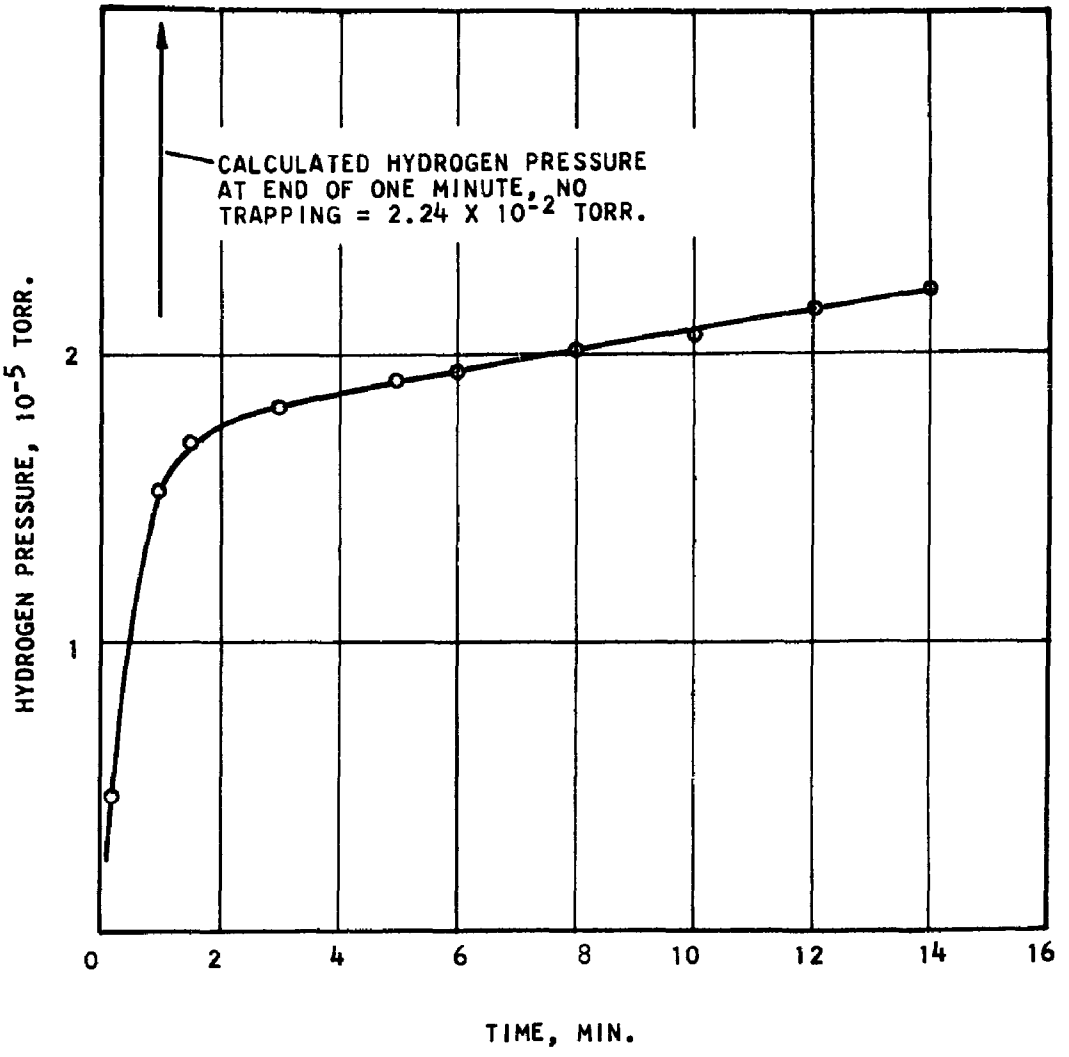

Figure 14 - Hydrogen Pressure During Condensation of $CHClF_2$ Containing 1.1% Hydrogen. Condensation Rate = $1.23 \times 10^{18} cm^{-2} sec^{-1}$.

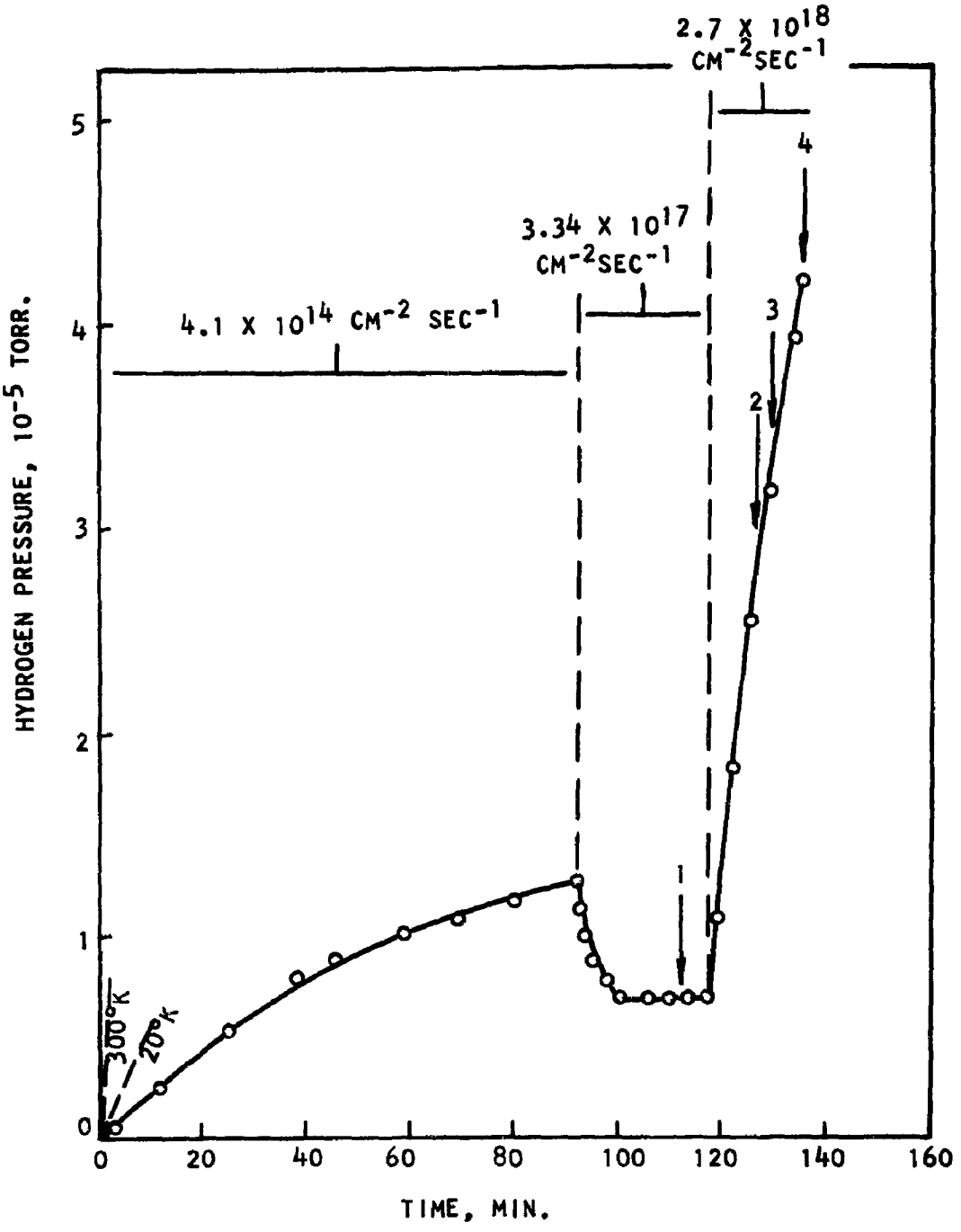

Figure 15 - Hydrogen Pressure During Condensation of CCl_2F_2 containing 1.01% Hydrogen. The Dotted Lines are Calculated Pressures Assuming No Trapping. The Numbered Arrows Indicate the Occurrence of Pressure Pulses.

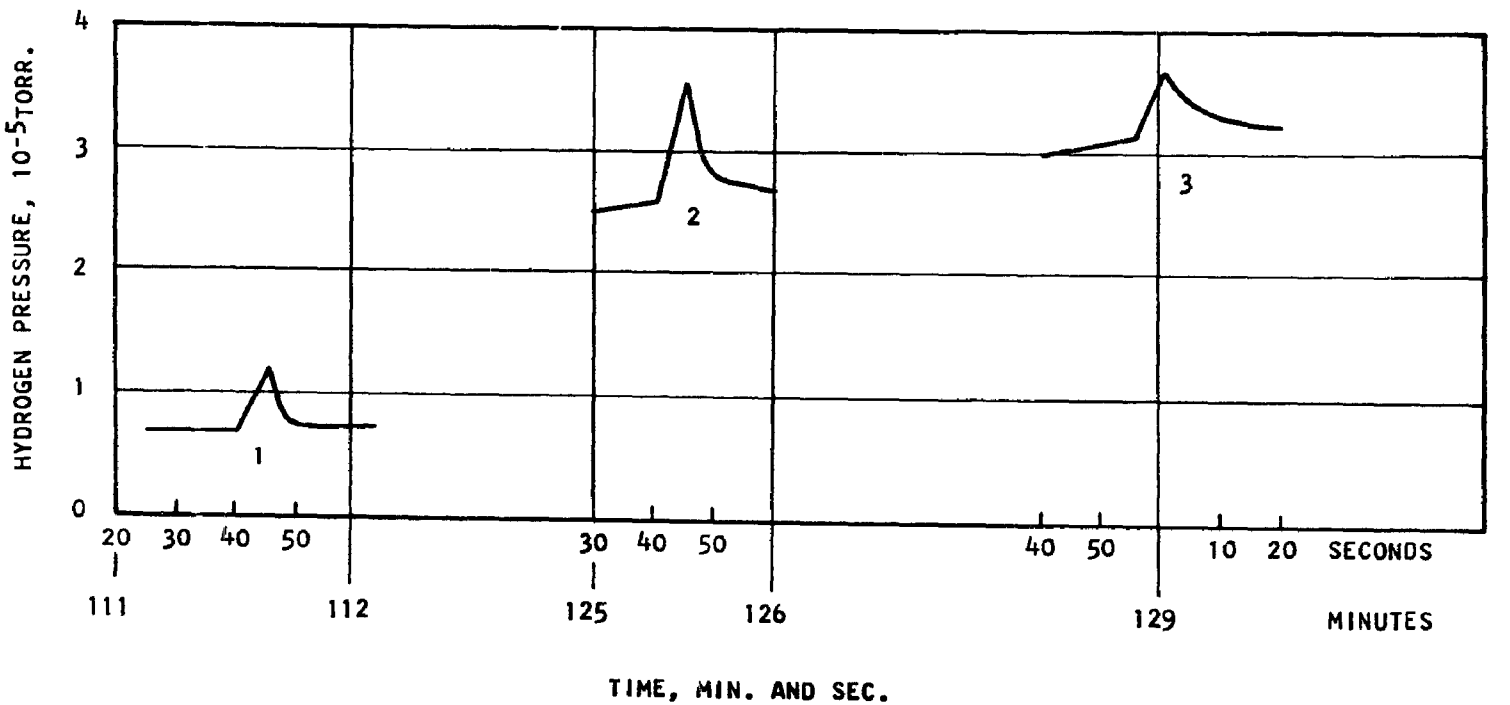

Figure 16 - Pressure Pulses During Condensation of CCl_2F_2 Containing 1.01% Hydrogen. (See Figure 15)

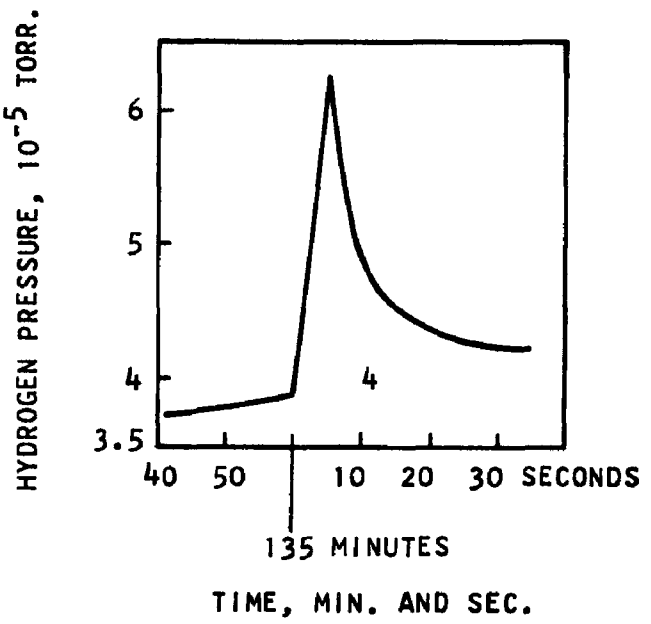

Fig. 17 Pressure Pulse During Condensation of C Cl_2F_2 Containing 1.01% Hydrogen. (See Fig. 15)

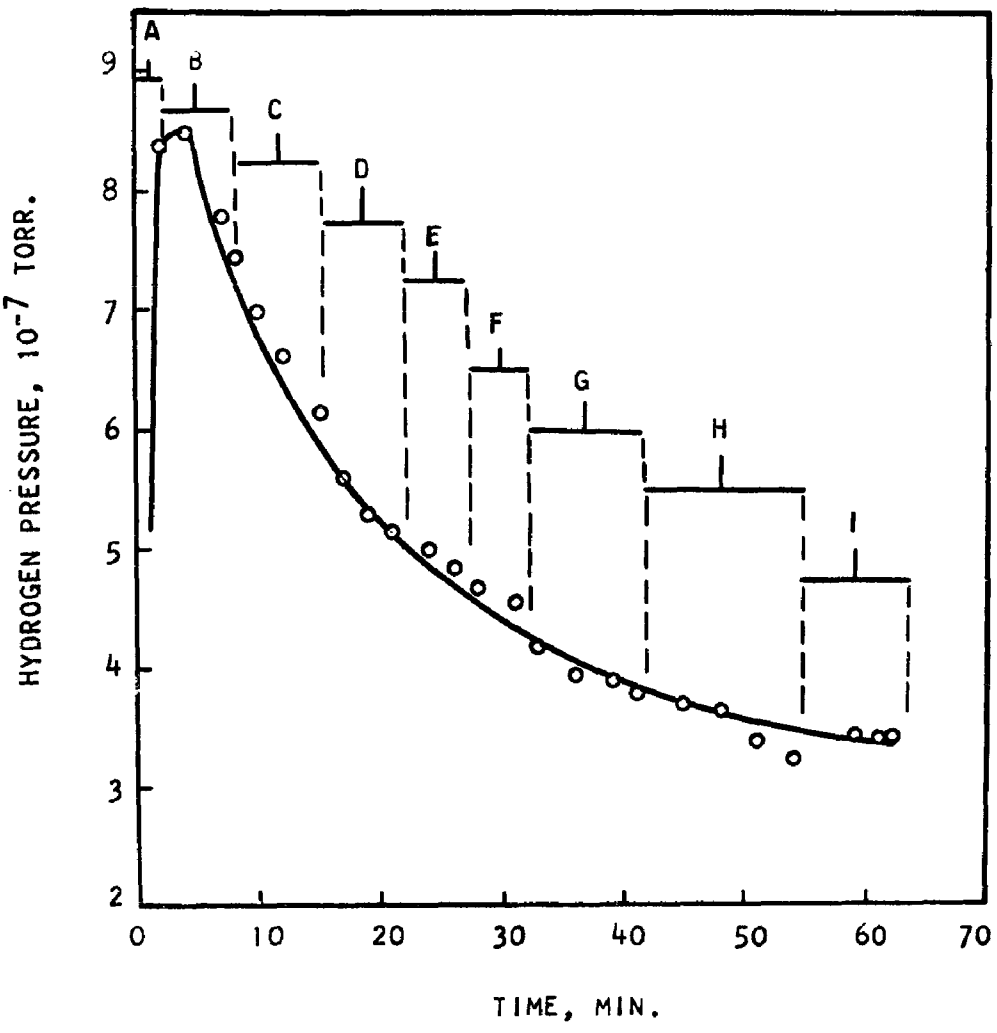

Fig. 18 Hydrogen Pressure During Condensation of Carbon Dioxide Containing 1.04% Hydrogen. Condensation Rates: A-8.65 x 10^{18} $cm^{-2}sec^{-1}$, B-4.40 x 10^{18} $cm^{-2}sec^{-1}$, C-3.47 x 10^{18} $cm^{-2}sec^{-1}$, D-2.78 x 10^{18} $cm^{-2}sec^{-1}$, E-2.36 x 10^{18} $cm^{-2}sec^{-1}$, F-1.96 x 10^{18} $cm^{-2}sec^{-1}$, G-1.69 x 10^{18} $cm^{-2}sec^{-1}$, H-1.37 x 10^{18} $cm^{-2}sec^{-1}$, I-1.14 x 10^{18} $cm^{-2}sec^{-1}$. The Condensation Rates are Averages over the Indicated Time Periods.

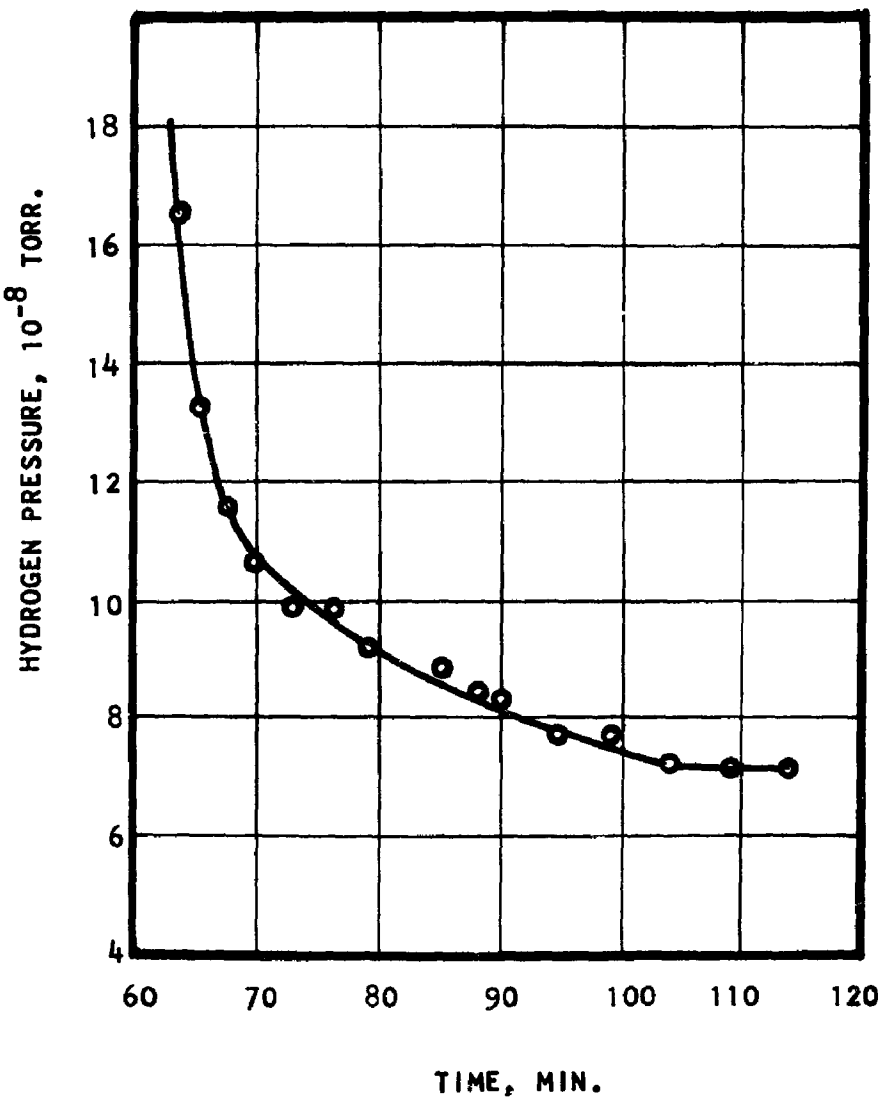

Fig. 19 Hydrogen Pressure After Termination of Carbon Dioxide Condensation. (See Fig. 18)

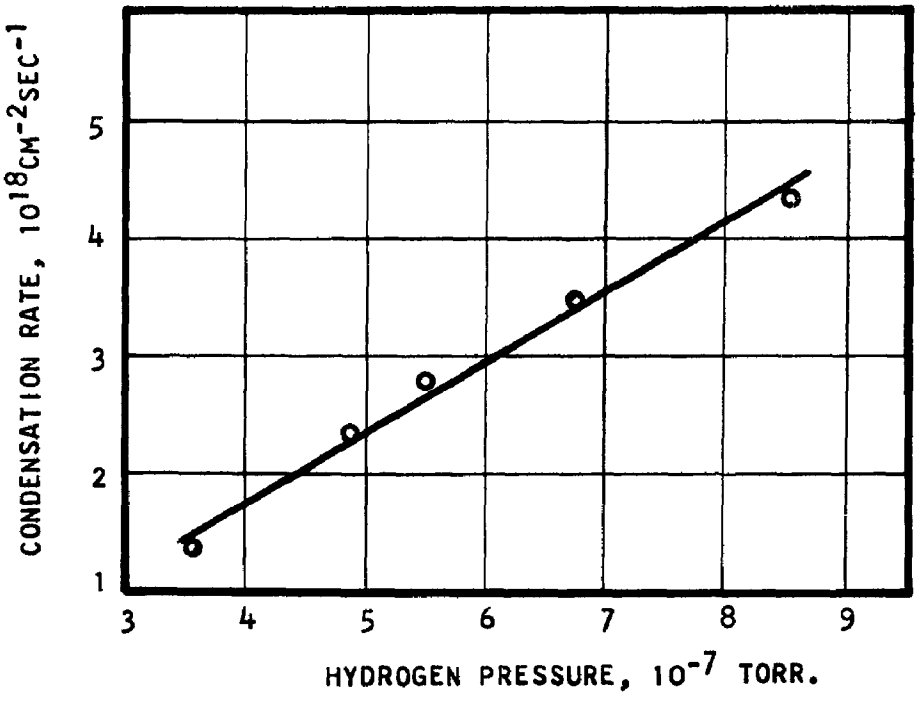

Fig. 20 Hydrogen Pressure as a Function of Carbon Dioxide Condensation Rate (CO_2+ 1.04% H_2).

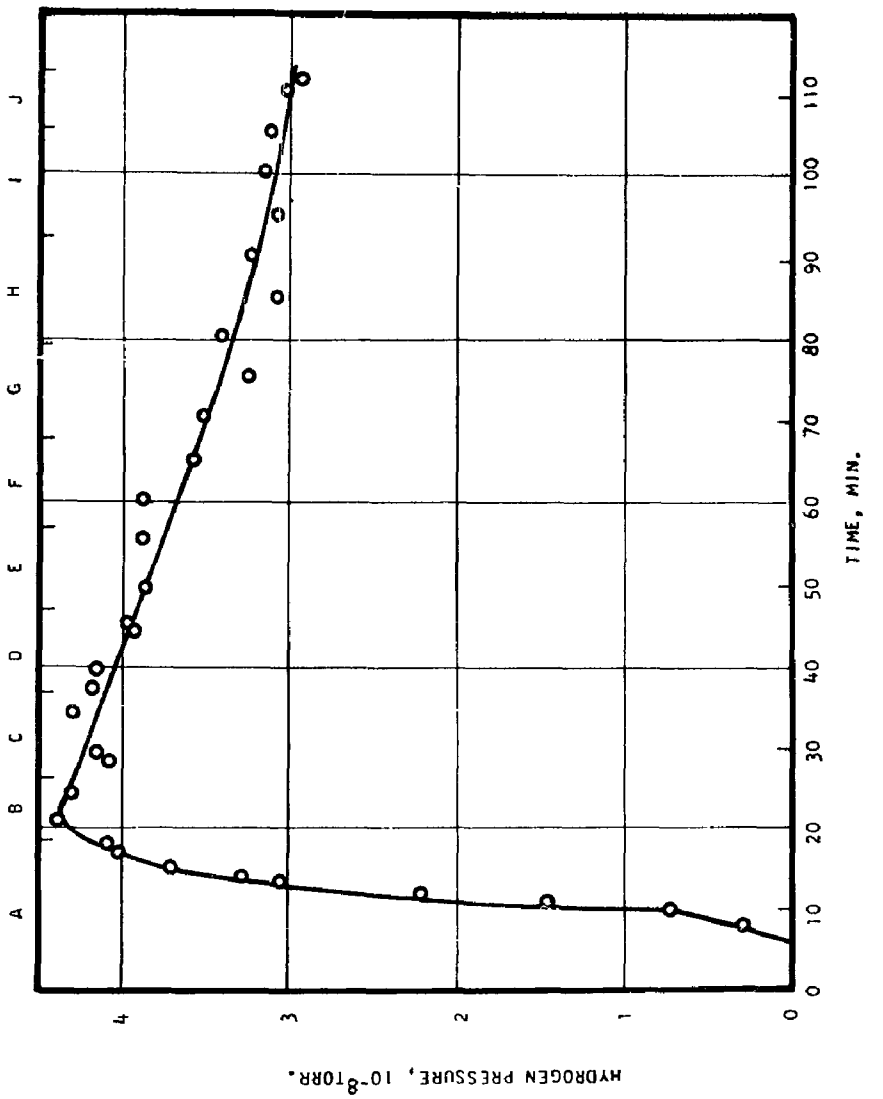

Fig. 21 Hydrogen Pressure During Condensation of Carbon Dioxide Containing 0.89% Hydrogen. Condensation Rates: A-3.80 x 10^{17} $cm^{-2}sec^{-1}$, B-2.32 x 10^{17} $cm^{-2}sec^{-1}$, C-2.03 x 10^{17} $cm^{-2}sec^{-1}$, D-1.94 x 10^{17} $cm^{-2}sec^{-1}$, E-2.14 x 10^{17} $cm^{-2}sec^{-1}$, F-1.85 x 10^{17} $cm^{-2}sec^{-1}$, G-1.85 x 10^{17} $cm^{-2}sec^{-1}$, H-1.59 x 10^{17} $cm^{-2}sec^{-1}$, I-1.64 x 10^{17} $cm^{-2}sec^{-1}$, J-1.68 x 10^{17} $cm^{-2}sec^{-1}$.

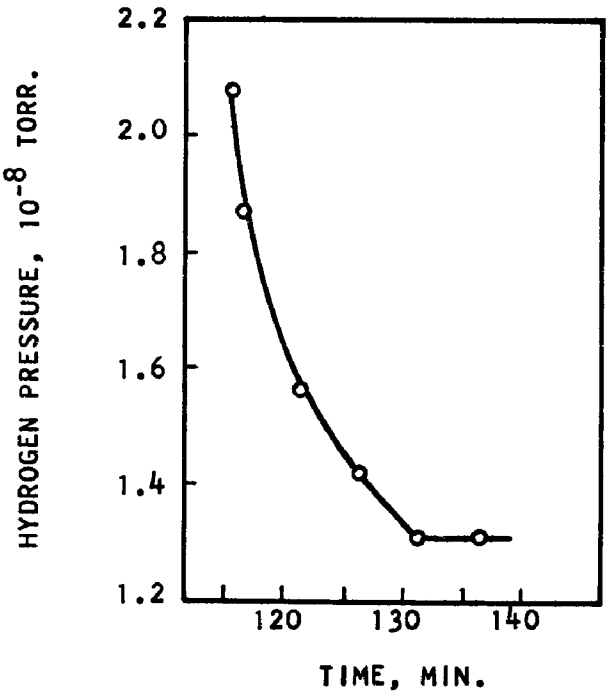

Fig. 22 Hydrogen Pressure After Termination of Carbon Dioxide Condensation. (See Fig. 21).

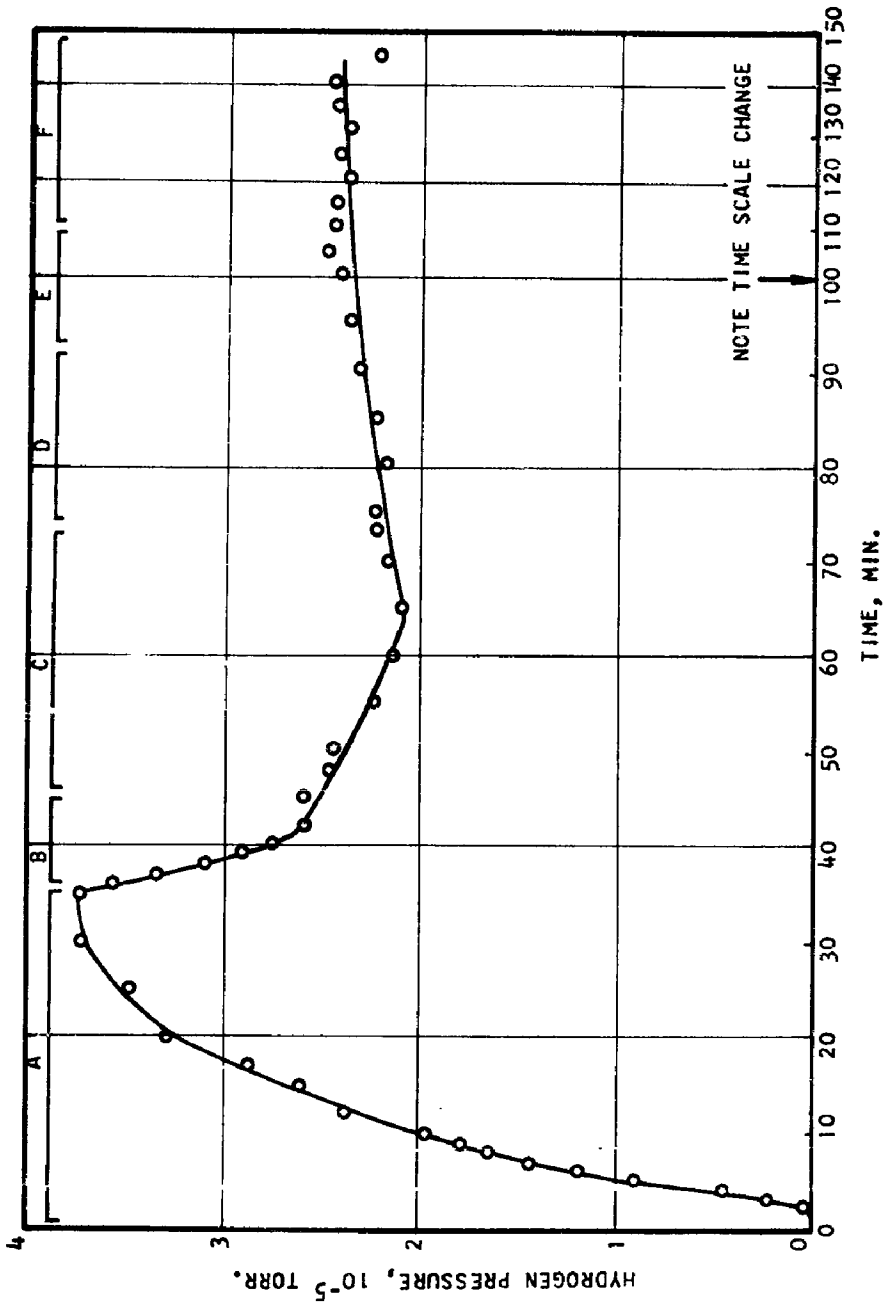

Figure 23 - Hydrogen Pressure During Condensation of Carbon Dioxide Containing 5.39% Hydrogen. Condensation Rates: A-9.44 x $10^{16}cm^{-2}sec^{-1}$, B-7.70 x $10^{16}cm^{-2}sec^{-1}$, C-7.04 x $10^{16}cm^{-2}sec^{-1}$, D-6.64 x $10^{16}cm^{-2}sec^{-1}$, E-6.40 x $10^{16}cm^{-2}sec^{-1}$, F-7.70 x $10^{16}cm^{-2}sec^{-1}$.

Arnold Engineering Development Center
Arnold Air Force Station, Tennessee
Rpt. No. AEDC-TDR-63-127. RESEARCH STUDY OF THE CRYOTRAPPING OF HELIUM AND HYDROGEN DURING 20°K CONDENSATION OF GASES: PHASES I AND II. May 1963, 112 p. incl 21 refs., illus., tables.

Unclassified Report

Phase I: A study of the variables affecting cryotrapping of helium and hydrogen during 20°K condensation of oxygen and nitrogen is presented. The mechanism of helium trapping appears to involve burying helium atoms in the solid oxygen or nitrogen. The process is most efficient at high condensation rates, but is not likely to find application for the removal of helium in a large space chamber. Experimental results indicate that hydrogen trapping occurs by adsorption of hydrogen molecules on the surface of the solid oxygen or nitrogen and is most efficient at low condensation rates and low heat flux to the solid surface.

These conditions indicate that hydrogen trapping may be applicable for hydrogen removal in a large space chamber. Attempts to improve helium trapping by ionizing the atoms and collecting them on a charged 20°K surface were unsuccessful. Phase II: The trapping of hydrogen by nitrogen condensed on a 20°K surface has been studied under conditions where the surface was shielded from ambient temperature radiation. The process is shown to be an inefficient means for hydrogen pumping and is likely to have value only as a bonus in the operation of a large space chamber. *Hydrogen trapping by methane, some simple fluorocarbons,* and carbon dioxide condensed on a 20°K surface not shielded from ambient temperature radintion has been studied. CCl_2F_2 and carbon dioxide show rather large capacities for hydrogen and may be useful for the pumping of hydrogen in a space chamber and in special applications.

1. Cryogenics
2. Adsorption
3. Condensation
4. Oxygen
5. Nitrogen
6. Low temperature research
7. Space environmental conditions
8. Test facilities
9. Diffusion pumps
10. Vacuum pumps
- I. AFSC Program Area 850E, Project 7778, Task 777801
- II. Contract AF 40(600)-945
- III. Linde Company, Tonawanda, New York
- IV. R. A. Hemstreet, D. J. Webster, D. M. Ruttenbur,
- V. Available from OTS
- VI. In ASTIA Collection

Arnold Engineering Development Center
Arnold Air Force Station, Tennessee
Rpt. No. AEDC-TDR-63-127. RESEARCH STUDY OF THE CRYOTRAPPING OF HELIUM AND HYDROGEN DURING 20°K CONDENSATION OF GASES: PHASES I AND II. May 1963, 112 p. incl 21 refs., illus., tables.

Unclassified Report

Phase I: A study of the variables affecting cryotrapping of helium and hydrogen during 20°K condensation of oxygen and nitrogen is presented. The mechanism of helium trapping appears to involve burying helium atoms in the solid oxygen or nitrogen. The process is most efficient at high condensation rates, but is not likely to find application for the removal of helium in a large space chamber. Experimental results indicate that hydrogen trapping occurs by adsorption of hydrogen molecules on the surface of the solid oxygen or nitrogen and is most efficient at low condensation rates and low heat flux to the solid surface.

These conditions indicate that hydrogen trapping may be applicable for hydrogen removal in a large space chamber. Attempts to improve helium trapping by ionizing the atoms and collecting them on a charged 20°K surface were unsuccessful. Phase II: The trapping of hydrogen by nitrogen condensed on a 20°K surface has been studied under conditions where the surface was shielded from ambient temperature radiation. The process is shown to be an inefficient means for hydrogen pumping and is likely to have value only as a bonus in the operation of a large space chamber. *Hydrogen trapping by methane, some simple fluorocarbons,* and carbon dioxide condensed on a 20°K surface not shielded from ambient temperature radiation has been studied. CCl_2F_2 and carbon dioxide show rather large capacities for hydrogen and may be useful for the pumping of hydrogen in a space chamber and in special applications.

1. Cryogenics
2. Adsorption
3. Condensation
4. Oxygen
5. Nitrogen
6. Low temperature research
7. Space environmental conditions
8. Test facilities
9. Diffusion pumps
10. Vacuum pumps
- I. AFSC Program Area 850E, Project 7778, Task 777801
- II. Contract AF 40(600)-945
- III. Linde Company, Tonawanda, New York
- IV. R. A. Hemstreet, D. J. Webster, D. M. Ruttenbur,
- V. Available from OTS
- VI. In ASTIA Collection

UNCLASSIFIED